

# Stimulus perception and signal transduction in the KdpD/KdpE two-component system

Dissertation der Fakultät für Biologie  
der Ludwig-Maximilians-Universität München



vorgelegt von

**Hannah Schramke**

am 28.04.2016

1. Gutachter: Prof. Dr. Kirsten Jung, LMU München
2. Gutachter: Prof. Dr. Marc Bramkamp, LMU München

Tag der mündlichen Prüfung: 18.7.2016

„Ein Abend, an dem sich alle einig sind, ist ein verlorener Abend.“

Albert Einstein

Für meine Familie

## **Eidesstattliche Erklärung**

Ich versichere hiermit an Eides statt, dass die vorgelegte Dissertation von mir selbstständig und ohne unerlaubte Hilfe angefertigt wurde. Des Weiteren erkläre ich, dass ich nicht anderweitig ohne Erfolg versucht habe, eine Dissertation einzureichen oder mich der Doktorprüfung zu unterziehen. Die folgende Dissertation liegt weder ganz, noch in wesentlichen Teilen einer anderen Prüfungskommission vor.

München, 28.04.2016

## **Statutory Declaration**

I declare that I have authored this thesis independently, that I have not used other than the declared sources/references. As well I declare that I have not submitted a dissertation without success and not passed the oral exam. The present dissertation (neither the entire dissertation nor parts) has not been presented to another examination board.

Munich, 28.04.2016

## Contents

Eidesstattliche Erklärung.....	IV
Statutory Declaration.....	IV
Contents.....	V
Nomenclature.....	VIII
Abbreviations.....	IX
Publications and Manuscripts presented in this thesis.....	XI
Contributions to publications and manuscripts presented in this thesis.....	XII
Summary.....	XIV
Zusammenfassung.....	XVI
1 Introduction.....	1
1.1 Importance of intracellular potassium for bacteria.....	1
1.2 Potassium transport systems in <i>Escherichia coli</i> .....	2
1.3 Two-component signal transduction.....	3
1.4 The KdpD/KdpE two-component system of <i>Escherichia coli</i> .....	7
1.5 The histidine kinase KdpD.....	9
1.6 Nature of the stimulus sensed by KdpD.....	11
1.7 Scope of this thesis.....	12
2 Results.....	13
2.1 Perception of the K <sup>+</sup> stimulus by the histidine kinase KdpD in <i>Escherichia coli</i> .....	13
2.1.1 Extracellular K <sup>+</sup> inhibits the autokinase activity and intracellular K <sup>+</sup> stimulates the phosphatase activity of KdpD.....	13
2.1.2 Regulation of both enzymatic activities is essential for a controlled stress response.....	19
2.1.3 A mathematical model describes the <i>in vivo</i> response dynamics.....	20
2.1.4 Dual sensing by a bifunctional histidine kinase ensures robust homeostasis in fluctuating environments.....	22
2.2.....Functional analysis of the GAF domain within the histidine kinase KdpD of <i>Escherichia coli</i> .....	26
2.2.1 The replacement of the GAF domain with the GAF domain of 3E0Y results in deregulated enzyme activities.....	26
2.2.2 The replacement of the GAF domain with GAF domains from different KdpD proteins influences KdpD activity.....	29
2.2.3 The deletion of the GAF domain results in an inverted response.....	30
2.2.4 The third helix of the GAF domain is important for signalling.....	32

## Contents

2.2.5	Amino acids within the extended transmembrane helix interact with the GAF domain to transmit the K <sup>+</sup> signal across the membrane. ....	35
2.3	Cross-talk regulation between the KdpD/KdpE and PhoR/PhoB two-components systems in <i>Escherichia coli</i> .....	39
2.3.1	<i>E. coli</i> requires the KdpFABC system to grow under K <sup>+</sup> limitation .....	39
2.3.2	KdpE mediated induction of <i>kdpFABC</i> expression rescues the growth arrest in the absence of KdpD .....	40
2.3.3	Only a very small subpopulation is able to survive under K <sup>+</sup> limitation.....	42
2.3.4	Mutations in the phosphate transporter <i>pst</i> result in <i>kdpFABC</i> expression.....	43
2.3.5	The histidine kinase PhoR is responsible for <i>kdpFABC</i> expression in the absence of KdpD .....	45
2.3.6	BACTH experiments indicate interactions between the KdpDE and PhoRB two-component systems.....	47
2.3.7	Phosphate starvation enhances <i>kdpFABC</i> expression .....	49
2.3.8	K <sup>+</sup> limitation enhances <i>pstS</i> expression.....	50
2.4	Binding of cyclic Di-AMP to the <i>Staphylococcus aureus</i> sensor kinase KdpD occurs via the universal stress protein domain and downregulates the expression of the Kdp potassium transporter .....	52
2.4.1	c-di-AMP binds to the USP domain of <i>Staphylococcus aureus</i> KdpD.....	52
2.4.2	A conserved SxS-X <sub>20</sub> -FTAxY motif in KdpD <sup>Sa</sup> (USP) is involved in c-di-AMP binding. ....	55
2.4.3	High levels of c-di-AMP inhibit the up-regulation of <i>kdpA</i> under salt stress. ...	57
2.4.4	Influence of c-di-AMP on KdpD <sup>Sa</sup> activity <i>in vitro</i> .....	58
3	Discussion .....	60
3.1	K <sup>+</sup> sensing and signal transduction in the histidine kinase KdpD .....	60
3.2	Interconnection of Kdp mediated K <sup>+</sup> homeostasis with cellular processes .....	65
4	Materials and Methods .....	69
4.1	Materials .....	69
4.2	Strains, plasmids, oligonucleotides used in this study.....	69
4.3	Molecular biological techniques .....	71
4.4	Random mutagenesis .....	72
4.5	Growth conditions .....	72
4.6	β-galactosidase activity assays (determination of <i>kdpFABC</i> expression <i>in vivo</i> ) .....	72
4.7	P <sub><i>pstS</i></sub> promoter activity assays .....	73
4.8	RNA isolation, cDNA synthesis and qRT-PCR .....	73
4.9	Cell fractionation and preparation of membrane vesicles .....	73
4.10	Overproduction and purification of soluble proteins .....	74

## Contents

4.11	Phosphorylation and dephosphorylation assays .....	74
4.12	Determination of extracellular and intracellular K <sup>+</sup> concentrations .....	75
4.13	Determination of KdpFABC production by quantitative Western blot analysis. ....	76
4.14	Synthesis of radiolabelled acetyl phosphate .....	76
4.15	Analytical Procedures .....	77
4.16	Bacterial adenylate cyclase two-hybrid assay (BACTH) .....	77
4.17	Structural modelling .....	77
4.18	Fitting of autokinase and phosphatase K <sup>+</sup> dependency .....	78
4.19	Mathematical model – KdpD switching dynamics .....	78
5	References .....	86
6	Supplemental Material .....	95
6.1	Supplemental Figures .....	95
6.2	Supplemental tables .....	96
	Danksagung .....	103
	Curriculum vitae .....	104

## **Nomenclature**

Gene products are numbered in a way that the first methionine/valine of the wild-type protein is designated “1” in the amino acid sequence (if present: independently of the N-terminal affinity tag). N-terminal and C-terminal affinity tags are marked in genes and proteins corresponding to their position (e.g. 6His-KdpE or KdpE-6His).

Amino acid substitutions in proteins are termed as follows: The native amino acid is designated in three-letter code, followed by the respective amino acid position in the protein. The amino acid introduced by (site-directed) mutagenesis is terminally added in one-letter code unless otherwise stated (Example: KdpE-D52E). Deletions of genes are marked by “Δ”. Unless otherwise noted, nucleotide positions indicate the distance from the transcriptional start site (+1).

## Abbreviations

aa	<u>a</u> mino <u>a</u> cid
ATP	adenosine-5'-triphosphate
bp	<u>b</u> ase <u>p</u> airs
CA	<u>c</u> atalytic and <u>A</u> TP binding domain
cAMP	<u>c</u> yclic <u>a</u> denosine-5'- <u>m</u> ono <u>p</u> hosphate
c-di-AMP	bis-(3'-5')- <u>c</u> yclic <u>d</u> imeric <u>a</u> denosine <u>m</u> ono <u>p</u> hosphate
c-di-GMP	bis-(3'-5')- <u>c</u> yclic <u>d</u> imeric <u>g</u> uanosine <u>m</u> ono <u>p</u> hosphate
CM	<u>c</u> ytoplasmic <u>m</u> embrane
CP	<u>c</u> ytoplasm
DBD	<u>D</u> NA <u>b</u> inding <u>d</u> omain
DHp	<u>d</u> imerization and <u>h</u> istidine <u>p</u> hosphotransfer domain
DNA	<u>d</u> eoxyribo <u>n</u> ucleic <u>a</u> cid
DNase	deoxyribonuclease
DTT	1,4- <u>d</u> ithio <u>t</u> hreit <u>o</u> l
GAF	protein domain present in c <u>G</u> MP-specific phosphodiesterases, <u>a</u> denylyl cyclases and <u>F</u> hlA
HAMP	protein domain present in histidine kinases, adenlyl cyclases, methylaccepting chemotaxis proteins, and some phosphatases
HK	<u>h</u> istidine <u>k</u> inase
n-His tag	affinity tag composed of n histidine residues
HPt	<u>H</u> is-containing <u>p</u> hospho <u>t</u> ransfer protein
LB	lysogeny <u>b</u> roth
RR	<u>r</u> esponse <u>r</u> egulator
PAGE	poly <u>a</u> crylamide gel <u>e</u> lectro <u>p</u> horesis
PAS	protein domain present in <u>P</u> er, <u>A</u> mnt, <u>S</u> im proteins
PP	<u>p</u> eriplasm
RD	<u>r</u> eceiver <u>d</u> omain

## Abbreviations

RNase	ribonuclease
TM	transmembrane domain
Usp	universal stress protein

## **Publications and Manuscripts presented in this thesis**

### **Chapter 1.3, 1.4, 1.5 and 1.6:**

Schramke H, Wang Y, Heermann R, Jung K: **Stimulus perception by histidine kinases**. In de Bruijn, F.J. (Editor) *Stress and environmental control of gene expression in bacteria*, Wiley-Blackwell Publishers. (accepted)

### **Chapter 2.1 and 3.1:**

Schramke H, Tostevin F, Heermann R, Gerland U, Jung K: **A dual-sensing receptor confers robust cellular homeostasis**. (Cell Reports, under review)

### **Chapter 2.2 and 3.1:**

Schramke H, Gabriel G, Wang Y, Pfaffinger V, Heermann R, Jung K: **Functional analysis of the GAF domain within the histidine kinase KdpD of *Escherichia coli***. (In preparation)

### **Chapter 2.3 and 3.2:**

Schramke H, Laermann V, Tegetmeyer H, Brachmann A, Jung K, Altendorf K: **Cross-talk between the Kdp and Pho two-component systems interconnects K<sup>+</sup> and PO<sub>4</sub><sup>3-</sup> homeostasis in *Escherichia coli***. (In preparation)

### **Chapter 2.4 and 3.2:**

Moscoso JA, Schramke H, Zhang Y, Tosi T, Debhi A, Jung K, Gründling A: **Binding of c-di-AMP to the *Staphylococcus aureus* sensor kinase KdpD occurs via the USP domain and down-regulates the expression of the Kdp potassium transporter**. *J. Bacteriol.* 2015 Jul 20. pii: JB.00480-15.

## **Contributions to publications and manuscripts presented in this thesis**

### **Chapter 1: Introduction**

Parts of Chapter 1.3, 1.4, 1.5 and 1.6 are already published in the book chapter “Stimulus perception by histidine kinases” written by Hannah Schramke, Yang Wang, Ralf Heermann and Kirsten Jung (In: Stress and environmental control of gene expression in bacteria, Wiley-Blackwell Publishers, de Bruijn, F.J. (Editor), accepted.)

### **Chapter 2.1 and 3.1: Perception of the K<sup>+</sup> stimulus by the histidine kinase KdpD**

Hannah Schramke, Ralf Heermann and Kirsten Jung designed the experiments. Hannah Schramke performed all *in vivo* and *in vitro* experiments. Filipe Tostevin and Ulrich Gerland developed the mathematical model and Filipe Tostevin performed simulations. Hannah Schramke, Filipe Tostevin, Ralf Heermann, Ulrich Gerland and Kirsten Jung wrote the manuscript.

### **Chapter 2.2 and 3.1: Functional analysis of the GAF domain within the histidine kinase KdpD**

Hannah Schramke, Ralf Heermann, Günther Gabriel and Kirsten Jung designed the experiments. Hannah Schramke performed all *in vivo* and *in vitro* experiments. *In vivo* and *in vitro* analysis of KdpD-GAF 3e0Y and KdpD variants in chapter 2.2.5 were performed by Hannah Schramke during her diploma thesis (Schramke, 2011). Plasmids constructed by Günther Gabriel and Verena Pfaffinger are indicated in Table S2. Hannah Schramke, Ralf Heermann and Kirsten Jung wrote the manuscript.

### **Chapter 2.3 and 3.2: Cross-talk between the KdpD/KdpE and PhoR/PhoB two component systems**

Hannah Schramke, Vera Laermann, Kirsten Jung and Karlheinz Altendorf designed the experiments. Vera Laermann performed experiments presented in Chapter 2.3.1, 2.3.2 and 2.3.3 (Laermann, 2014). Hannah Schramke performed experiments presented in Chapter 2.3.4, 2.3.5, 2.3.6, 2.3.7 and 2.3.8. Halina Tegetmeyer and Andreas Brachmann performed and analysed genome sequencing. Hannah Schramke, Vera Laermann, Kirsten Jung and Karlheinz Altendorf wrote the manuscript.

**Chapter 2.4 and 3.2: Binding of cyclic Di-AMP to the *Staphylococcus aureus* sensor kinase KdpD occurs via the universal stress protein domain and downregulates the expression of the Kdp potassium transporter**

Figures and text in Chapter 2.4.1-2.4.3 are already published (Moscoso *et al.*, 2015) and were partially modified. Joana Moscoso and Angelika Gründling designed experiments presented in chapter 2.4.1-2.4.3. Joana Moscoso, Yong Zhang, Tommaso Tosi and Amina Debhi performed experiments presented in chapter 2.4.1-2.4.3. Joana Moscoso, Hannah Schramke, Kirsten Jung and Angelika Gründling designed experiments presented in chapter 2.4.4. Hannah Schramke established an overproduction protocol for *S. aureus* KdpD and together with Joana Moscoso performed *in vitro* phosphorylation experiments and measurements of intracellular K<sup>+</sup> concentrations (not presented here), which were not included in the publication. Joana Moscoso and Angelika Gründling wrote the manuscript. The discussion part about c-di-AMP in chapter 3.2 was taken from Moscoso *et al.*, 2015, which was written by Joana Moscoso and Angelika Gründling, in a shortened and partially modified form.

We hereby confirm the above statements:

Hannah Schramke

Prof. Dr. Kirsten Jung

## Summary

The perception of environmental stimuli is a matter of survival for all organisms. Two-component systems consisting of a histidine kinase and a response regulator display the predominant strategy of bacteria to sense and adapt to environmental changes. Among these the widespread KdpD/KdpE two-component system is essential for adaptation to  $K^+$  limitation and osmotic stress. Even though the histidine kinase KdpD of *Escherichia coli* has been studied in detail *in vivo* and *in vitro*, the exact mechanism of stimulus perception is not clear so far. The main purpose of this thesis was to elucidate how the bifunctional histidine kinase KdpD perceives different cellular and environmental stimuli and accordingly regulates its kinase and phosphatase activities. By using bioinformatic, genetic and biochemical approaches combined with mathematic modelling new insights into stimulus perception and signal transduction by the KdpD/KdpE two-component system and its contribution to the maintenance of robust intracellular  $K^+$  homeostasis were obtained.

In the first part of the work the perception of the  $K^+$  stimulus by the histidine kinase KdpD of *E. coli* was investigated in detail ([chapter 2.1](#)). *In vitro* analysis revealed an inhibitory effect of  $K^+$  on the kinase activity and a stimulative effect on the phosphatase activity, respectively. Using site-directed mutagenesis an extracellular  $K^+$  recognition site was identified, which is responsible for the regulation of the kinase activity. Moreover, the phosphatase activity was shown to be stimulated by intracellular  $K^+$  recognition within the C-terminal cytoplasmic domain. Consequently KdpD regulates its kinase and phosphatase activities by monitoring both, the intra- and extracellular  $K^+$  concentration. A mathematical model based on *in vivo* and *in vitro* data was developed and enabled a comparison between different regulation strategies. Simulated competition experiments revealed that dual sensing and dual regulation within the bifunctional histidine kinase is superior to simpler strategies and ensures robust intracellular  $K^+$  homeostasis.

In [chapter 2.2](#) the function of the so far uncharacterised GAF domain within *E. coli* KdpD was analysed. Hybrid proteins, in which the GAF domain of KdpD was replaced with other GAF domains were characterised by altered signalling properties, highlighting its importance for signal transduction to the output domain. Furthermore first evidence was obtained that the GAF domain of KdpD might be important for dimerization and signal transduction across the membrane.

## Summary

The study presented in chapter 2.3 identified a link between  $K^+$  and  $PO_4^{3-}$  homeostasis in *E. coli*. A strain lacking the constitutively produced  $K^+$  uptake systems Trk and Kup and the histidine kinase KdpD could not grow under  $K^+$  limitation. This growth defect was rescued by suppressor mutations in the *pst* phosphate transporter, which acts as a phosphate sensor for the histidine kinase PhoR and negatively influences its activity. *In vivo* and *in vitro* analysis revealed cross-talk regulation between the KdpD/KdpE and PhoR/PhoB two-component systems in both directions, which could also be observed in the wild-type strain. This regulation strategy displays a fine-tuned mechanism to balance the ratio between positively and negatively charged ions in the cell.

Chapter 2.4 focusses on the influence of the second messenger c-di-AMP on KdpD activity in *Staphylococcus aureus*. Ligand binding assays revealed that c-di-AMP binds within the USP domain of *S. aureus* KdpD. Furthermore it was shown that high levels of c-di-AMP negatively influence *kdpA* expression. Moreover an overproduction and purification protocol for KdpD and KdpE of *S. aureus* was established to analyse the influence of c-di-AMP on *S. aureus* KdpD activity *in vitro*.

## Zusammenfassung

Die Wahrnehmung von externen Umweltreizen ist lebensnotwendig für alle Organismen. Bakterien nutzen Zweikomponentensysteme bestehend aus einer Histidinkinase und einem Antwortregulator als Hauptstrategie, um ändernde Umweltbedingungen wahrzunehmen und sich entsprechend anzupassen. Das weitverbreitete KdpD/KdpE Zweikomponentensystem ist von großer Bedeutung für die Anpassung an  $K^+$ -Limitation und osmotischen Stress. Obwohl die Histidinkinase KdpD von *Escherichia coli* bereits intensiv *in vivo* und *in vitro* untersucht wurde, ist der genaue Mechanismus der Reizwahrnehmung noch immer unbekannt. In dieser Arbeit sollte untersucht werden, wie KdpD verschiedene zelluläre und externe Stimuli wahrnimmt und abhängig davon die Kinase- und Phosphataseaktivität reguliert. Mit Hilfe bioinformatischer, genetischer und biochemischer Methoden in Kombination mit mathematischer Modellierung konnten neue Erkenntnisse in Signalwahrnehmung und -weiterleitung innerhalb des KdpD/KdpE Zweikomponentensystems und dessen Beitrag zur robusten Aufrechterhaltung der intrazellulären Kaliumhomöostase erzielt werden.

Im ersten Teil der Arbeit wurde detailliert die Wahrnehmung von  $K^+$  durch die Histidinkinase KdpD von *E. coli* untersucht (Kapitel 2.1). Durch *in vitro* Experimente konnte gezeigt werden, dass  $K^+$  einen inhibitorischen Effekt auf die Kinaseaktivität und einen stimulierenden Effekt auf die Phosphataseaktivität hat. Mit Hilfe von gerichteten Mutagenesestudien wurde eine extrazelluläre Kaliumerkennungsstelle identifiziert, welche für die Regulation der Kinaseaktivität verantwortlich ist. Weiterhin wurde gezeigt, dass die Phosphataseaktivität durch Erkennung von intrazellulärem  $K^+$  innerhalb der C-terminalen cytoplasmatischen Domäne stimuliert wird. Somit kann KdpD die Kinase- und Phosphataseaktivität abhängig von der intra- und extrazellulären  $K^+$  Konzentration regulieren. Die Entwicklung eines mathematischen Modells – basierend auf *in vivo* und *in vitro* Daten – ermöglichte den Vergleich unterschiedliche Regulationsstrategien. Durch Simulation von Wettbewerbsexperimenten konnte gezeigt werden, dass der duale Sensor- und Regulationsmechanismus einfacheren Strategien überlegen ist und die robuste Aufrechterhaltung der intrazellulären  $K^+$  Konzentration sicherstellt.

In Kapitel 2.2 wurde die Funktion der bisher uncharakterisierten GAF-Domäne von *E. coli* KdpD untersucht. Hybridproteine, in welchem die GAF-Domäne von *E. coli* KdpD durch andere GAF-Domänen ersetzt wurde, zeichneten sich durch veränderte Signaltransduktioneigenschaften aus, was deren wichtige Rolle bei der Signalweiterleitung unterstreicht. Weiterhin wurden erste Hinweise dafür gefunden, dass die GAF-Domäne von

KdpD eine wichtige Rolle bei der Dimerisierung und der Signalweiterleitung über die Membran spielen könnte.

In der in Kapitel 2.3 dargestellten Studie konnte eine Schnittstelle zwischen  $K^+$  und  $PO_4^{3-}$  Homöostase in *E. coli* identifiziert werden. Eine *E. coli* Mutante, welcher die konstitutiv produzierten  $K^+$  Aufnahmesysteme Trk und Kup und die Histidinkinase KdpD fehlen, kann unter  $K^+$  limitierten Bedingungen nicht wachsen. Dieser Wachstumsdefekt kann durch Supressormutationen in dem *pst* Phosphattransporter aufgehoben werden, der als Phosphatsensor für die Histidinkinase PhoR dient und dessen Aktivität negativ reguliert. *In vivo* und *in vitro* Studien zeigten „Crosstalk“ zwischen dem KdpD/KdpE und PhoR/PhoB Zweikomponentensystem, der ebenso im Wildtyp Stamm nachgewiesen wurde. Diese Regulationsstrategie stellt einen feinabgestimmten Mechanismus dar, welcher die Balance zwischen positiv und negativ geladenen Ionen in der Zelle aufrechterhält.

Kapitel 2.4 beschäftigt sich mit dem Einfluss des „second messengers“ c-di-AMP auf die Aktivität von KdpD in *Staphylococcus aureus*. Durch Ligandenbindestudien wurde gezeigt, dass c-di-AMP innerhalb der USP-Domäne von *S. aureus* KdpD bindet. Des Weiteren wurde nachgewiesen, dass hohe Konzentrationen von c-di-AMP die *kdpA* Expression negativ beeinflussen. Zusätzlich wurde ein Protokoll zur Überproduktion und Reinigung von *S. aureus* KdpD und KdpE etabliert, um den Einfluss von c-di-AMP auf die KdpD Aktivität *in vitro* zu untersuchen.

# 1 Introduction

## 1.1 Importance of intracellular potassium for bacteria

$K^+$  is the most abundant cation in bacterial cells and is crucial for several cellular processes like the maintenance of cell turgor (Epstein, 2003), the regulation of the cytoplasmic pH (Booth, 1985), the activity of some cytoplasmic enzymes (Suelter, 1970), as well as for protein translation by binding to the active site of the ribosome (Nissen *et al.*, 2000). Even though the  $K^+$  concentration is low in many environments (0.1-10 mM) bacteria accumulate high intracellular  $K^+$  levels ranging from 18 mM in *Thermoplasma acidophilum* (Searcy, 1976) to 4 M in *Halobacterium halobium* (Walderhaug *et al.*, 1987). The Gram-negative enterobacterium *Escherichia coli* maintains intracellular  $K^+$  concentrations between 150-600 mM  $K^+$  (Epstein & Schultz, 1965). However, some species – for instance *Corynebacterium glutamicum* – do not require  $K^+$  under optimal growth conditions, but accumulate high  $K^+$  levels under acidic stress conditions. It has been shown that this is essential for the maintenance of internal pH and membrane potential and therefore contributes to survival under certain stress conditions (Ochrombel *et al.*, 2011).  $K^+$  also plays a crucial role during the osmotic stress response. Changes in the external osmotic pressure cause water influx and lysis (hyperosmotic stress) or dehydration (hypoosmotic stress), respectively. To counteract these scenarios bacteria have developed diverse adaptation mechanisms in order to survive (Wood, 2006, Wood, 2011, Wood, 2015). Generally the first response towards an osmotic upshift is the accumulation of  $K^+$  as counter ion for glutamate (McLaggan *et al.*, 1994, Epstein, 2003). Subsequently osmoprotectants like glycine, betaine or proline are either taken up or synthesised to replace the  $K^+$ /glutamate complex, because a high intracellular ionic strength negatively affects activity of some cytoplasmic enzymes.

Recently it has been reported that  $K^+$  plays an important role in cell-cell communication. In this regard Prindle *et al.* revealed that bacteria use electrical communication via  $K^+$  ion-channel-mediated signalling within biofilms (Prindle *et al.*, 2015, Liu *et al.*, 2015). A metabolic trigger causes the wavelike release of intracellular  $K^+$ , which results in depolarization of neighbouring cells and therefore acts as a long-range signal in cellular communities (Prindle *et al.*, 2015, Liu *et al.*, 2015).

## 1.2 Potassium transport systems in *Escherichia coli*

The cytoplasmic membrane consists of a phospholipid bilayer and acts as a permeability barrier for many molecules including ions. Thus integral membrane proteins are required to accomplish  $K^+$  uptake from the environment. *E. coli* has two constitutively produced  $K^+$  low-affinity transporters, namely Trk and Kup, and one high-affinity  $K^+$  transporter KdpFABC, that is synthesised under  $K^+$  limitation (Epstein, 2003). The Trk transporter consists of the integral membrane proteins TrkG/TrkH and the NAD(H) binding peripheral membrane protein TrkA (Schlösser *et al.*, 1993, Schlösser *et al.*, 1995). It has been shown that  $K^+$  transport via Trk requires the proton motive force and ATP. However Trk is not an ATPase hypothesising rather a regulatory than energetically role for ATP in Trk mediated  $K^+$  uptake (Stewart *et al.*, 1985). The Trk and Kup  $K^+$  transporter are the main  $K^+$  uptake systems in *E. coli* albeit both have low affinity for  $K^+$  ( $\sim 1$  mM) (Rhoads *et al.*, 1976). Accordingly under  $K^+$  limitation ( $< 5$  mM  $K^+$ ) these transporters are not sufficient for the maintenance of high intracellular  $K^+$  levels and the high affinity transporter KdpFABC needs to be synthesised. The KdpFABC protein complex belongs to the superfamily of P-type ATPases and uses energy of ATP hydrolysis to transport  $K^+$  across the cytoplasmic membrane. P-type ATPases are characterised by a catalytic cycle with two conformational states E1 and E2 (Møller *et al.*, 1996). The conformational alteration is triggered by the formation of a phospho-intermediate at a conserved aspartate residue, which in turn changes binding affinity for ATP and the transport substrate (Møller *et al.*, 1996). Within KdpFABC the catalytic and ion transport domains are located in the two different subunits KdpB (72 kDa) and KdpA (59 kDa), respectively (Bramkamp *et al.*, 2007). The  $K^+$  translocating KdpA subunit shows similarities to KcsA-like  $K^+$  channel proteins (Van der Laan *et al.*, 2002, Durell *et al.*, 2000). The small KdpF (3 kDa) subunit consists of one transmembrane helix and seems to have a stabilising effect on the transporter complex (Gabel *et al.*, 1999, Bramkamp *et al.*, 2007). KdpC (20 kDa) is anchored in the cytoplasmic membrane with one transmembrane helix, whereas the C-terminal portion is located in the cytoplasm. This part of the protein contains an ATP binding site and is supposed to act as a catalytic chaperone by enhancing ATP binding affinity within the phosphorylation site of KdpB (Ahnert *et al.*, 2006, Gabel & Altendorf, 2001, Greie & Altendorf, 2007). KdpFABC functions as a dimer (Heitkamp *et al.*, 2008) and transports  $K^+$  with high affinity ( $K_m \sim 0,002$  mM) (Rhoads *et al.*, 1976). As high affinity transport is only needed under  $K^+$  limitation, KdpFABC synthesis is regulated via the KdpD/KdpE two-component system.

### 1.3 Two-component signal transduction

Bacteria live in environments, where surrounding parameters like nutrient availability, osmolarity, pH, temperature, or cell density can suddenly change. Therefore, monitoring and adequate adaptation to these changing conditions is a prerequisite to survive. For that reason, bacteria are equipped with specific signal transduction systems that mediate the response to varying environmental stimuli. The most widely distributed type of signal transduction system is the histidine kinase/response regulator system, also known as sensor kinase/response regulator system. The prototype of this system consists of a histidine kinase that detects the stimulus and a response regulator that mediates the output response (Figure 1.3-1). Signalling is initiated when the histidine kinase autophosphorylates at a conserved histidine upon stimulus perception. Subsequently, the phosphoryl group is transferred to an aspartate within the response regulator resulting in modulation of its activity, and ultimately in the adaption of the cell to the changed environment (Figure 1.3-1) (see (Stock *et al.*, 2000, Gao & Stock, 2009) for review).

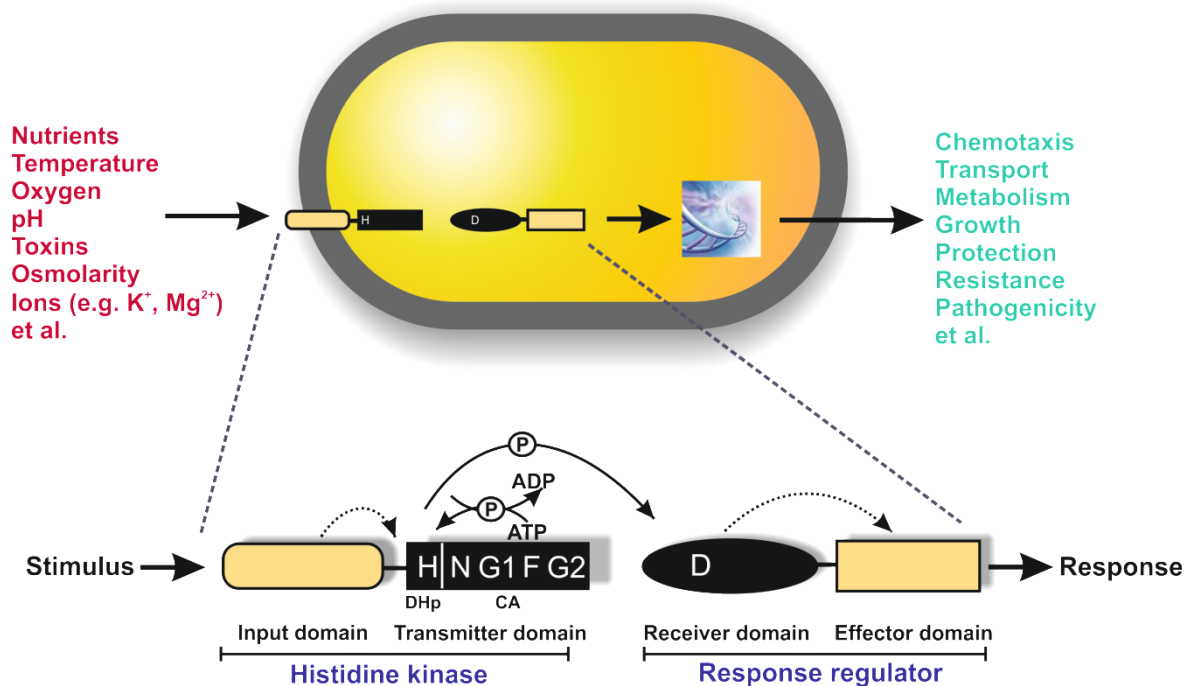


**Figure 1.3-1: Scheme of a prototypical two-component system.** Bacteria use two-component systems to sense different environmental stimuli like the availability of nutrients, changes in temperature, pH, osmolarity or ion concentrations. Upon stimulus perception the histidine kinase autophosphorylates and transfers the phosphoryl group to an aspartate within the response regulator. The response regulator in turn modulates the output response, resulting in changes of motility, production of transporters, metabolic changes or protection and resistance mechanisms. The figure was provided by Ralf Heermann.

## Introduction

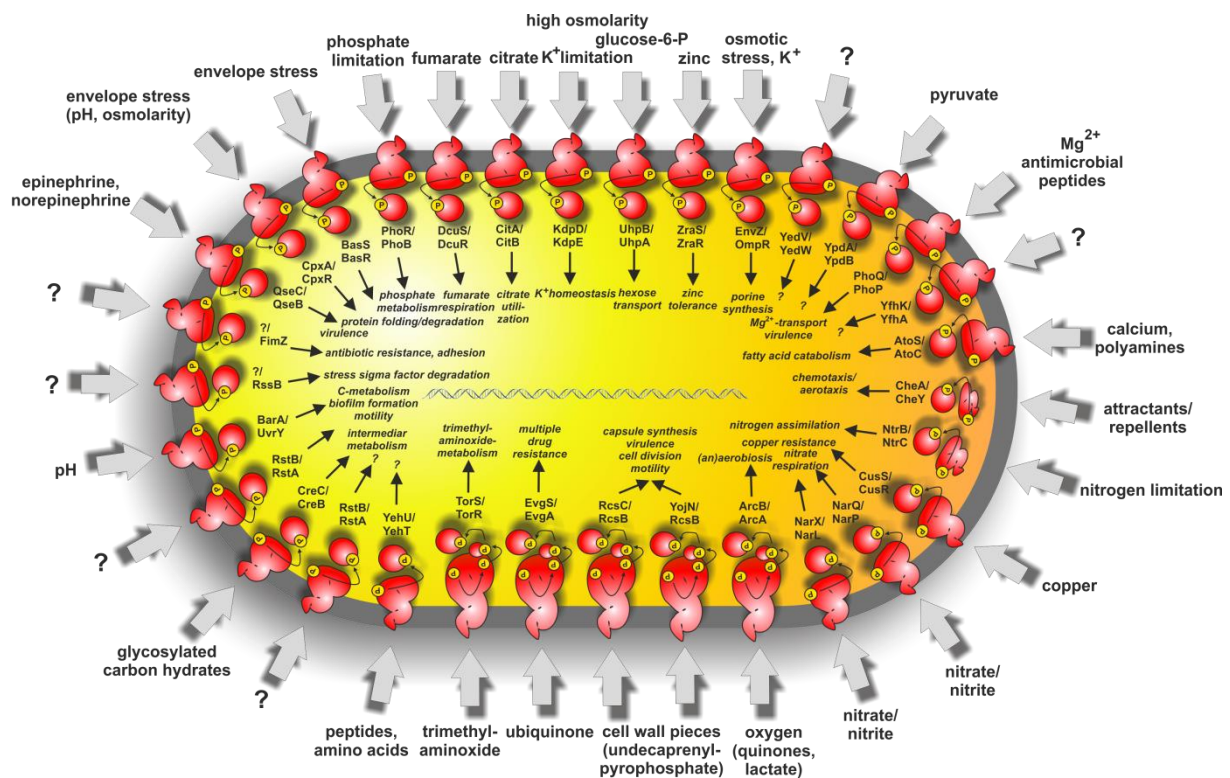


**Figure 1.3-2: Scheme of two-component systems of *E. coli*.** Histidine kinases can be either membrane integrated or soluble in the cytoplasm. The corresponding response regulators are located in the cytoplasm. Known stimuli of histidine kinases are indicated. The figure was provided by Ralf Heermann and modified.

The number of histidine kinase/response regulator systems differs enormously between bacterial species. It is assumed that the overall number correlates with the variety of environmental cues the bacteria are exposed to. It ranges from zero in *Mycoplasma genitalium*, over 30/32 in *E. coli* (Figure 1.3-2), 36/34 in *Bacillus subtilis*, to 131/80 in *Anabaena* sp. strain PCC7120, and 132/119 in *Myxococcus xanthus* (Heermann & Jung, 2009).

Histidine kinase/response regulator systems have a modular domain organization (Parkinson & Kofoid, 1992, Swanson *et al.*, 1994). They all share homology within the transmitter domain of the histidine kinase and the receiver domain of the response regulator. Transmitter and receiver domains contain the conserved H (histidine) and D (aspartate) boxes, respectively, and communicate via phosphorylation and dephosphorylation reactions (Figure 1.3-1). These modules are associated with various domains that function as input and output elements and are specific for each system. The input domain of a histidine kinase modulates the activity of the transmitter domain. Receiver domains activate or inhibit the corresponding output domains. Besides two-component systems with a single phosphotransfer step, phosphorelays exist that allow multiple phosphotransfer reactions. The histidine kinases in those systems are so-called hybrid-histidine kinases that contain a transmitter domain, which is fused to a receiver domain. The phosphoryl group is transferred from the H-box to the D-box within the respective histidine

kinase. Then, the phosphoryl group goes to a histidine within a histidine-containing phosphotransfer domain (HPt), which is either located within the hybrid histidine kinase or forms a separate protein. The HPt domain then transfers the phosphoryl group to the receiver domain of the response regulator (see (Heermann & Jung, 2009, Jung *et al.*, 2012) for review). Histidine kinases are key players in bacterial signal transduction. They sense specific stimuli, and transduce this information into an intracellular signal by initiating the phosphorylation cascade. Three general mechanisms how histidine kinases perceive stimuli are known (Figure 1.3-3) (Mascher *et al.*, 2006). The majority of histidine kinases senses extracellular stimuli and is membrane-integrated by at least two transmembrane helices that frame the external sensing or input domain (Figure 1.3-3, left panel). The corresponding transmitter domain is located in the cytoplasm. In these histidine kinases input and transmitter domains are located in two different cellular compartments, which make a signal transduction via the membrane indispensable. A second group of histidine kinases senses the stimuli by the transmembrane domain alone or by a combination of the membrane helices and an N-terminal cytoplasmic domain (Figure 1.3-3, middle panel). These histidine kinases perceive stimuli that have their origin in the membrane interface or the cytoplasm. Histidine kinases that are either membrane associated or soluble realize a third mechanism of stimulus perception (Figure 1.3-3, right panel). The stimulus sensed by this group is exclusively of intracellular nature. However, all groups of histidine kinases share a basic mechanism of signal transduction, independent how they perceive the stimulus. Upon stimulus perception, the histidine kinase is activated, which results in autophosphorylation at the H-box with the  $\gamma$ -phosphoryl group originating from ATP. However, phosphorylation of one histidine kinase in *Bacillus anthracis* involved in induction of sporulation was found to be strictly dependent on GTP (Scaramozzino *et al.*, 2009). Histidine kinases are homodimers, and mostly autophosphorylation occurs *in trans*, implying that one monomer binds ATP and phosphorylates the conserved H-box of the other monomer (Filippou *et al.*, 2008, Heermann *et al.*, 1998). Furthermore, many histidine kinases also function as phosphatases, meaning that they dephosphorylate the response regulator, and thereby switch off the signalling cascade (see (Stock *et al.*, 2000) for review). All histidine kinases share unique sequence motifs in their transmitter domains, designated as H, N, G1, F, and G2 boxes (Figure 1.3-3). The transmitter domain can be further dissected into two parts: the H-box containing dimerization and histidine phosphotransfer domain (DHp), and the HK-type ATPase catalytic (HATPase\_c) domain, better known as catalytic and ATP-binding (CA) domain (Figure 1.3-3) (Dutta *et al.*, 1999).

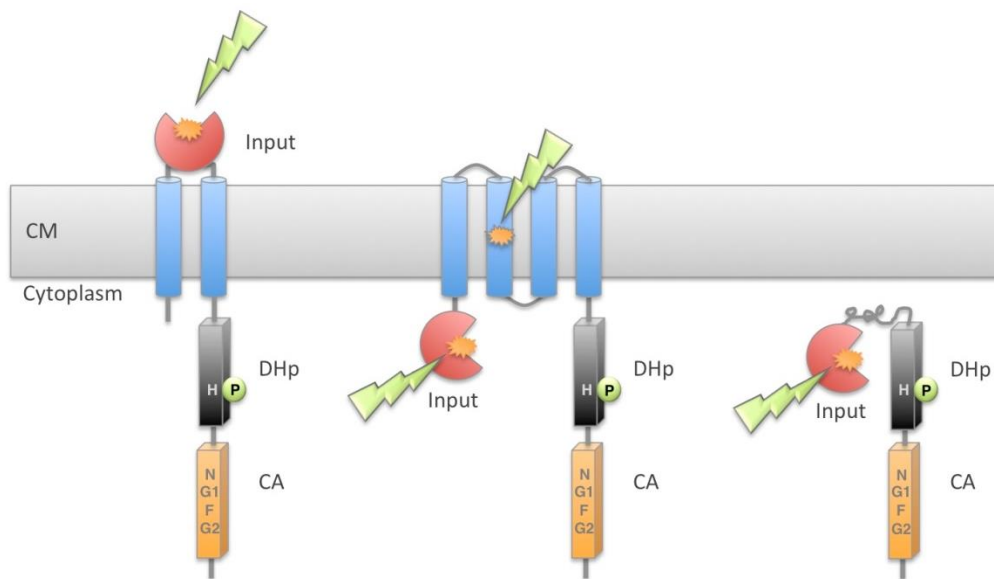


**Figure 1.3-3: Different mechanisms of stimulus perception by histidine kinases.** The sensor kinase perceives extracellular (left panel), transmembrane (middle panel) or intracellular (right panel) stimuli. Upon stimulus perception (represented by the orange star) the signal is transduced to the transmitter domain, which consists of the DhP subdomain (grey) and the CA subdomain (orange). For autophosphorylation, ATP is bound by the CA domain and the  $\gamma$ -phosphoryl group is then transferred to the conserved H motif within the DHp domain. Then, the phosphoryl group is further transferred to the D motif within the response regulator (not shown) activating the cellular response. CM: cytoplasmic membrane. The figure was created by Ralf Heermann.

Although the basic biochemistry of histidine kinase/response regulator systems is quite well understood, several important issues are less clear, particularly the nature of the environmental stimulus sensed by the histidine kinase. For a few examples it is known that the activity of the histidine kinase can be attenuated by a so-called accessory protein that transmits a specific signal or that directly influences the enzymatic activities of the sensor (see (Jung *et al.*, 2012) for review). However, the main activation mechanism of a histidine kinase is mediated by perception of a direct stimulus from the environment. Compared to the overall known number of different histidine kinases, the corresponding stimuli have been experimentally verified only in a few cases. Among the various stimuli that histidine kinases are known to detect are chemical and physical parameters such as different ions, temperature, pH, oxygen pressure, osmolarity, autoinducers, the redox state of electron carriers, and the contact with host cells (Figure 1.3-2) (see (Calva & Oropeza, 2006) for review). For many pathogens, two-component systems have been found to be important or even essential for virulence, what makes them interesting as potential specific targets for antimicrobial drugs (see (Beier & Gross, 2006) for review). However, it is obvious that the virulence-attenuated phenotype of many histidine kinase/response regulator mutants is caused by interference with the cells' metabolic requirements rather than with changes in the production of specific virulence factors. The

general understanding of how histidine kinases work and how they are integrated into networks as well as the number known stimuli that activate specific systems is constantly increasing.

#### 1.4 The KdpD/KdpE two-component system of *Escherichia coli*

The histidine kinase KdpD together with the response regulator KdpE regulates synthesis of KdpFABC, a high affinity  $K^+$  uptake system. Under  $K^+$  limitation or osmotic stress imposed by a salt, KdpD autophosphorylates at a conserved histidine (H673) and transfers the phosphoryl group to an aspartate (D52) within KdpE (Figure 1.4-1) (Nakashima *et al.*, 1993, Jung *et al.*, 1997).

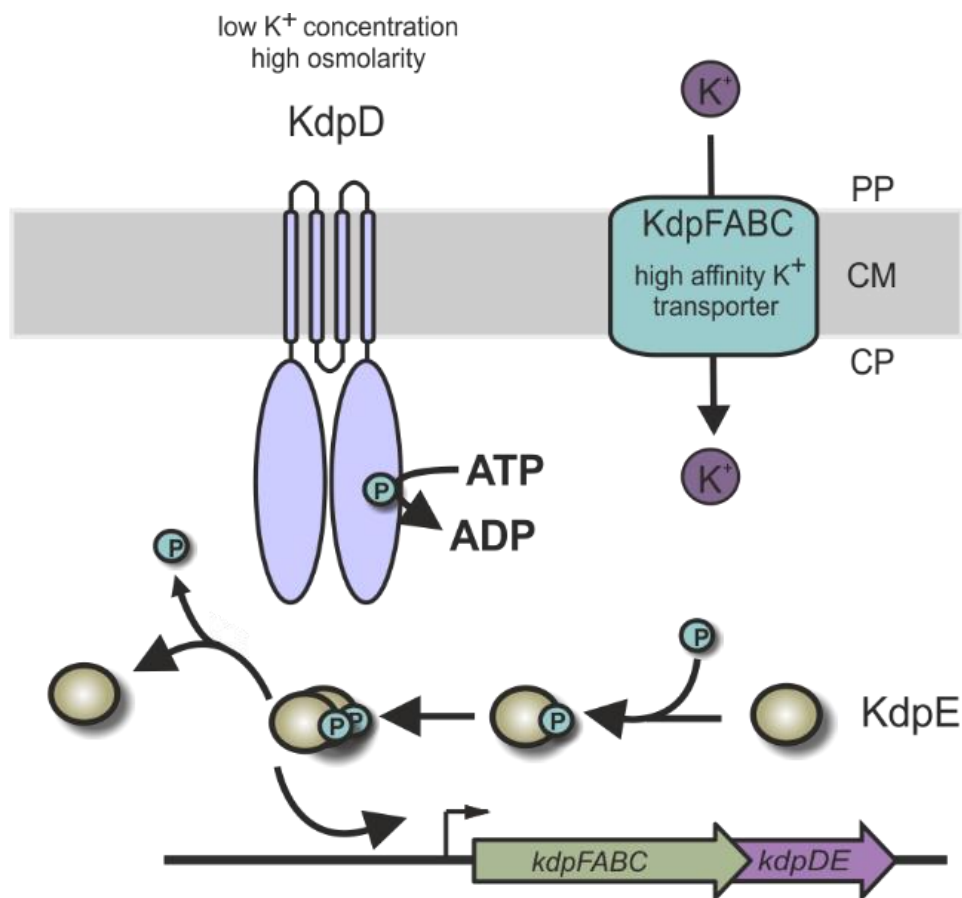


**Figure 1.4-1: Scheme of KdpD/KdpE signalling.** Under  $K^+$  limitation or high osmolarity the histidine kinase KdpD autophosphorylates and transfers the phosphoryl group to the response regulator KdpE. KdpE dimerizes in the phosphorylated state and activates expression of *kdpFABC*, encoding a high affinity  $K^+$  uptake system. In the presence of  $K^+$  KdpD acts as a phosphatase and terminates transcription of *kdpFABC*. PP: periplasm, CM: cytoplasmic membrane, CP: cytoplasm.

It has been shown earlier that KdpE can be phosphorylated *in vitro* via acetyl phosphate (Heermann *et al.*, 2003a), thus KdpE is supposed to catalyse the phosphotransfer reaction itself. KdpE dimerizes in the phosphorylated state, binds 20 bp upstream of the *kdpFABC* promoter and activates transcription (Sugiura *et al.*, 1992). Binding of each KdpE monomer to the target DNA occurs via a helix-turn-helix motif in the effector domain. The crystal structure of the

response regulator KdpE bound to its target DNA has been solved recently (Figure 1.4-2) (Narayanan *et al.*, 2014). It revealed that KdpE binds as an asymmetric dimer, one subunit (KdpE<sub>A</sub>) in a compact form and one subunit (KdpE<sub>B</sub>) in an extended form, respectively. Each KdpE protomer consists of a receiver domain (RD, residues 129-225) and a DNA binding domain (DBD, residues 129-225) connected by a linker (Figure 1.4-2) (Narayanan *et al.*, 2014).

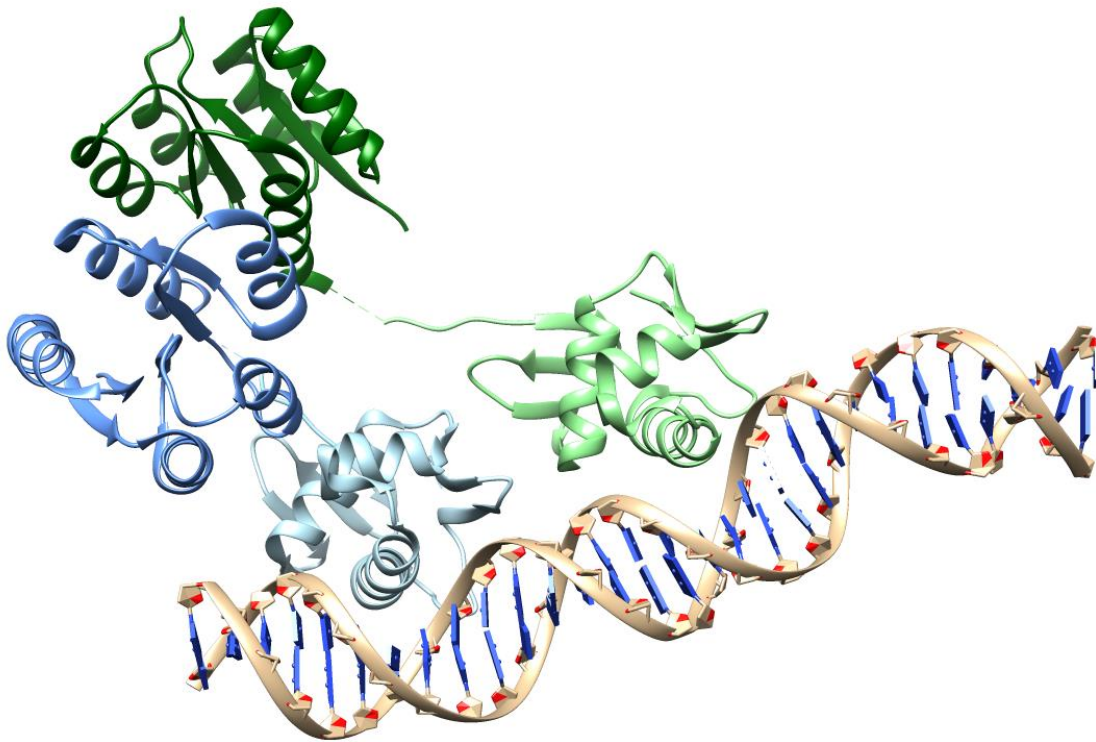


**Figure 1.4-2: Crystal structure of the KdpE-DNA complex.** KdpE binds as an asymmetric dimer composed of a compact (KdpE<sub>A</sub>, blue ribbons) and an extended (KdpE<sub>B</sub>, green ribbons) form. Each protomer of KdpE<sub>A</sub> and KdpE<sub>B</sub> consists of a receiver domain (dark blue for KdpE<sub>A</sub> and dark green for KdpE<sub>B</sub>) and a DNA binding domain (light blue for KdpE<sub>A</sub> and light green for KdpE<sub>B</sub>). Structural information (pdb file) was received from the protein data bank (pdb: 4KFC) and visualized using the UCSF Chimera program (Pettersen *et al.*, 2004).

Directly downstream and overlapping with *kdpFABC* operon the *kdpDE* operon is located (Figure 1.4-1) (Polarek *et al.*, 1992, Walderhaug *et al.*, 1992). Even though the *kdpDE* operon has its own constitutive promoter (Polarek *et al.*, 1992), an upregulation of both components is observed under K<sup>+</sup> limitation (Surmann *et al.*, 2014). The open reading frames of *kdpD* and *kdpC* overlap with eight nucleotides and it has been proposed that upregulation of *kdpFABC* under inducing conditions results in an additional upregulation of *kdpDE* via readthrough effects (Polarek *et al.*, 1992, Voelkner *et al.*, 1993).

## 1.5 The histidine kinase KdpD

The histidine kinase KdpD comprises 894 amino acids and is anchored in the cytoplasmic membrane via four transmembrane helices (Figure 1.5-1). The input domain of KdpD consists of the large N-terminal cytoplasmic domain, four transmembrane helices, and about 150 amino acids at the C-terminal cytoplasmic side (Figure 1.5-1) (Zimmann *et al.*, 1995, Heermann & Jung, 2010, Heermann & Jung, 2012). The N-terminal cytoplasmic domain comprises a highly conserved KdpD domain (Heermann *et al.*, 2000, Heermann *et al.*, 2003a) and an Usp domain that has similarities to the universal stress protein family (Heermann *et al.*, 2009a, Heermann *et al.*, 2009b) (Figure 1.5-1). A truncated KdpD variant composed of these two domains (KdpD/1-395) causes constitutive *kdpFABC* expression by stabilizing the interaction of phosphorylated KdpE with the corresponding DNA binding site (Heermann *et al.*, 2000, Heermann *et al.*, 2003a). The KdpD domain contains a “Walker-type” ATP binding site, that is important for the regulation of the phosphatase activity (Jung & Altendorf, 1998b). Furthermore it has been shown that the first 50 amino acids of KdpD are responsible for membrane localization via the signal recognition particle (Maier *et al.*, 2008). The Usp domain is important for KdpD activation under osmotic stress by interaction with the universal stress protein UspC (Heermann *et al.*, 2009a, Heermann *et al.*, 2009b).



**Figure 1.5-1: Domain arrangement within the histidine kinase KdpD of *E. coli*.** It consists of a large N-terminal cytoplasmic domain (KdpD and Usp domains), four transmembrane helices (TM 1 - TM 4) and a C-terminal cytoplasmic domain (GAF, DHp and CA domains). Amino acid (aa) positions are indicated.

The transmembrane domains form a four-helix bundle (Maslennikov *et al.*, 2010) and seem to be essential for the positioning of the large N- and C-terminal cytoplasmic domain to each other (Heermann *et al.*, 2003b). The fourth transmembrane helix extends into the cytoplasm and contains a cluster of positively charged arginines that has been shown to be involved in the modulation of kinase and phosphatase activities (Jung & Altendorf, 1998a, Zimmann *et al.*, 2007). The C-terminal cytoplasmic domain includes a so-called GAF domain (cGMP-specific phosphodiesterases, adenylyl cyclases and FhlA) (Figure 1.5-1) (Aravind & Ponting, 1997). GAF domains are widely distributed and form a three layer structure: a basal layer of two or more  $\alpha$ -helices, a middle layer of four or more  $\beta$ -strands, and

a distal layer of more variable structure (Levdikov *et al.*, 2009). Besides roles in signal transduction and transcriptional regulation GAF domains were shown to bind a variety of different ligands like cyclic nucleotides, ions and heme (Cann, 2007b, Heikaus *et al.*, 2009, Martinez *et al.*, 2002, Ho *et al.*, 2000, Podust *et al.*, 2008). Initial studies regarding the function of the GAF domain within KdpD indicate a role in signal transduction processes (Günther Gabriel, unpublished data; (Schramke, 2011)).

The transmitter domain of KdpD harbours the typical motifs of histidine kinase proteins. The DHp domain is essential for dimerization and contains the autophosphorylation site (H673) (Voelkner *et al.*, 1993), whereas the CA domain acts as ATP binding site and has several highly conserved regions (G1, G2, F and N boxes) (Parkinson & Kofoid, 1992). The crystal structure of a chimeric protein encompassing the entire transmitter domain of the *E. coli* histidine kinase EnvZ fused to the HAMP domain of the *Archaeoglobus fulgidus* Af1503 receptor was solved recently. The HAMP and DHp domains form an elongated four-helix bundle and the CA domains a  $\alpha/\beta$ -sandwich fold (Figure 1.5-2) (Ferris *et al.*, 2014). As the DHp and CA domains of KdpD are homologous to EnvZ, a similar structure is expected for the KdpD transmitter domain.

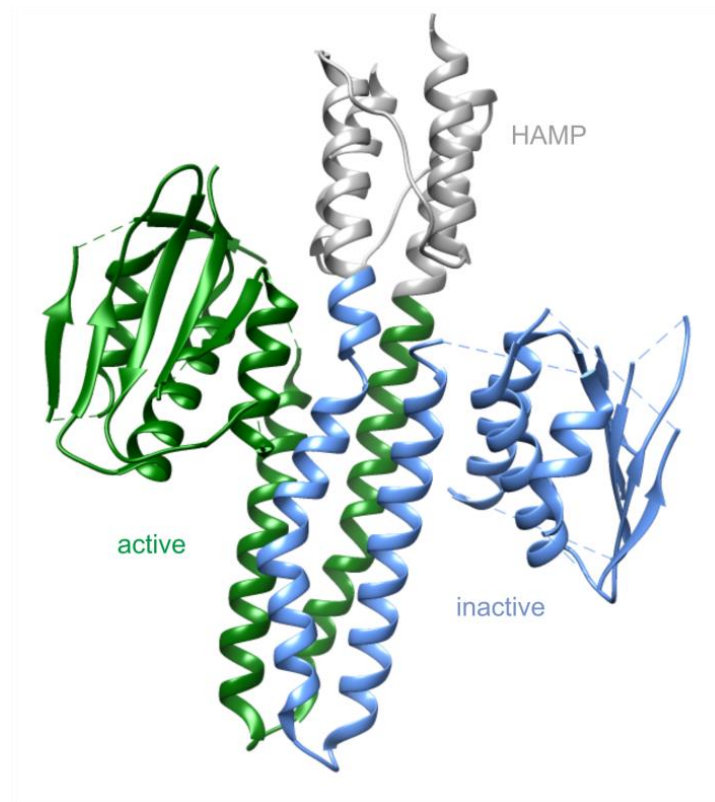


**Figure 1.5-2: The crystal structure of a dimeric Af1503-EnvZ.** The HAMP domain of Af1503 is depicted in grey, the catalytic domain of EnvZ in an active conformation in green and an inactive conformation in blue, respectively. Structural information (pdb file) was received from the protein data bank (pdb: 4CTI) and visualized using the UCSF Chimera program (Pettersen *et al.*, 2004).

Some histidine kinases do not only catalyse autophosphorylation and phosphotransfer, but also the reverse reaction meaning the dephosphorylation of the response regulator. This mechanism might be independent of the phospho-histidine intermediate (Hsing & Silhavy, 1997). Likewise KdpD is a bifunctional enzyme harbouring autokinase and phosphatase activities, respectively. Consequently KdpD dephosphorylates phospho-KdpE under non-inducing conditions and thereby terminates the response (Narayanan *et al.*, 2012). Bifunctional enzymes acting as both autokinase and phosphatase are found in many two-component systems, and were shown to render the response less sensitive to fluctuations in the concentrations of the two components (Batchelor & Goulian, 2003) or other factors such as ATP availability (Shinar *et al.*, 2007). However, how the cell regulates the two enzymatic activities as a function of the sensed stimuli is one question addressed in this study.

## 1.6 Nature of the stimulus sensed by KdpD

Since  $K^+$  plays a major role in maintaining turgor, it was first proposed that a decrease in turgor or some effect thereof activates the Kdp-system (Laimins *et al.*, 1981), a suggestion which could not be confirmed by further studies (Asha & Gowrishankar, 1993, Hamann *et al.*, 2008, Sugiura *et al.*, 1994). Instead, *in vitro* and *in vivo* studies indicate that KdpD senses changes of chemical, intracellular parameters under hyperosmotic stress conditions. Indications for an effect of the ionic strength on KdpD activity are based on experiments with right-side-out membrane vesicles. An increase of the ionic strength in the lumen of the vesicles stimulates KdpD kinase activity (Jung *et al.*, 2000). The loss of water is associated with an increase of the concentration of all dissolved molecules and consequently an increase of the ionic strength (Record *et al.*, 1998). Thus, it is conceivable that KdpD detects alterations of the intracellular ionic strength. ATP, whose concentration is upregulated under hyperosmotic stress (Ohwada & Sagisaka, 1987), is regarded as another stimulus, because KdpD harbours a regulatory ATP-binding site within the input domain, which affects the ratio between kinase and phosphatase activity.  $K^+$  ions have an inhibitory effect on KdpD kinase activity (Jung *et al.*, 2000). The effect of intracellular  $K^+$  on KdpD activation was corroborated by the observation that transcription of *kdpFABC* is also induced when cells are grown in the presence of  $Cs^+$ , an inhibitor of  $K^+$  uptake systems (Jung *et al.*, 2001). A putative  $K^+$ -binding site is suspected within the cytoplasmic extension of transmembrane helix IV (Rothenbücher *et al.*, 2006, Zimmann *et al.*, 2007) and seems to be important for the regulation of the phosphatase activity (Heermann *et al.*, 2014). However, recent studies showed that KdpD also senses changes in the extracellular  $K^+$  concentration (Laermann *et al.*, 2013). Apart from

that KdpD can perceive several other stimuli by interacting with other proteins. For instance the universal stress protein UspC and the enzyme EIIA<sup>Ntr</sup> were shown to bind and modulate KdpD activity. UspC was shown to be important for activation of KdpD under salt stress (Heermann *et al.*, 2009b), whereas enzyme EIIA<sup>Ntr</sup> interconnects KdpD activity with metabolic processes (Lüttmann *et al.*, 2009). These examples show that despite extensive studies the exact mechanism of stimulus perception and signal transduction in KdpD and its crucial role in cellular processes is not yet resolved.

### **1.7 Scope of this thesis**

The K<sup>+</sup> responsive KdpD/KdpE system is one of the best characterised two-component systems in *Escherichia coli*. K<sup>+</sup> is a direct stimulus for the histidine kinase KdpD, however it is still controversially discussed whether KdpD senses the extra- or intracellular K<sup>+</sup> concentration. The main scope of this thesis was to unravel the mechanism of K<sup>+</sup> sensing and regulation of kinase and phosphatase activity within KdpD. The GAF domain of KdpD was proposed to act as a K<sup>+</sup> sensor and its function should be characterised in detail in this study. Moreover, additional regulatory cellular components should be identified that influence the KdpD/KdpE signalling cascade, what might be important to connect K<sup>+</sup> homeostasis with other cellular processes.

## 2 Results

### 2.1 Perception of the K<sup>+</sup> stimulus by the histidine kinase KdpD in *Escherichia coli*

Even though K<sup>+</sup> levels are low in many environments, bacteria manage to maintain high intracellular K<sup>+</sup> concentrations. As illustrated in Figure 2.1-1A, the external availability of K<sup>+</sup> is expected to vary wildly, while the dilution of internal K<sup>+</sup> by cell growth depends on other fluctuating variables like carbon and nitrogen availability. How can a two-component system ensure optimal control of these operations under a wide variety of external and internal conditions? KdpD activity is known to be modulated by K<sup>+</sup>, however, no binding site for K<sup>+</sup> has ever been detected, and it is still unclear whether KdpD senses the extra- or intracellular K<sup>+</sup> concentration (Heermann *et al.*, 2014, Laermann *et al.*, 2013). This chapter focusses on K<sup>+</sup> sensing characteristics of KdpD, the K<sup>+</sup>-dependent regulation of KdpD kinase and phosphatase activities and the importance of the Kdp system for K<sup>+</sup> homeostasis under fluctuating conditions. *In vivo* and *in vitro* experiments were performed by Hannah Schramke. Filipe Tostevin and Ulrich Gerland (Technische Universität München) developed the mathematical model and Filipe Tostevin performed simulations.

#### 2.1.1 Extracellular K<sup>+</sup> inhibits the autokinase activity and intracellular K<sup>+</sup> stimulates the phosphatase activity of KdpD.

To analyse how K<sup>+</sup> affects signal transduction from KdpD to KdpE we sought to understand how K<sup>+</sup> influenced the rates of each of the two enzymatic activities of KdpD (namely autokinase and phosphatase activities). It should be noted that phosphorylated KdpD immediately transfers the phosphoryl group to KdpE (phosphotransferase activity) (Jung *et al.*, 1997). We first tested the influence of K<sup>+</sup> on the autokinase activity of KdpD *in vitro* by examining the phosphorylation of KdpD in the absence of KdpE. For these experiments we used membrane vesicles prepared from disrupted cells. A large proportion of the vesicles produced in this way is ruptured or otherwise not sealed off, such that both the cytoplasmic and periplasmic portions of KdpD are accessible to K<sup>+</sup> (Mevel-Ninio & Yamamoto, 1974, Zeng *et al.*, 1998). The quantitative dependence of the autophosphorylation rate on the K<sup>+</sup> concentration is plotted in Figure 2.1-1C, showing that K<sup>+</sup> inhibits this enzymatic activity with half-maximal inhibition at  $K_{0.5} = 2.7_{-0.7}^{+1.1}$  mM (upper and lower bounds of 68% confidence range).

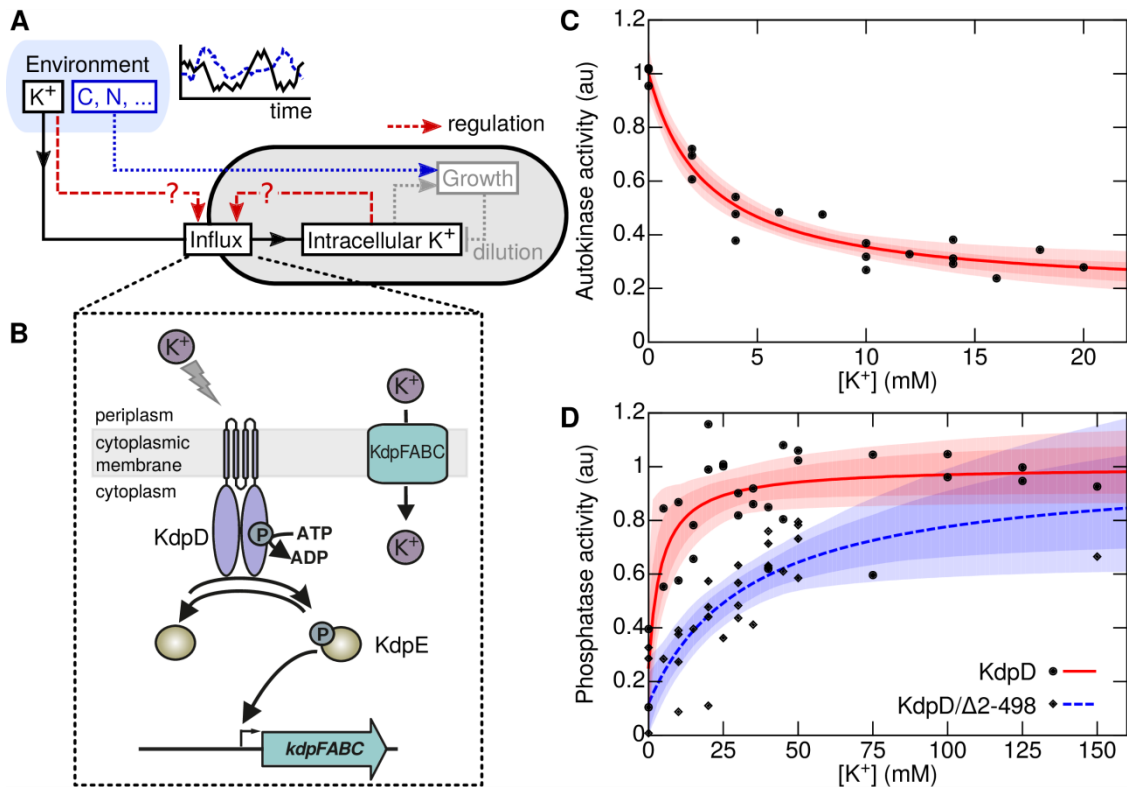


**Figure 2.1-1: Sensing of  $K^+$  by the bifunctional histidine kinase KdpD.** (A) Bacteria in varying environments must regulate their uptake of a limiting resource (here  $K^+$ ). Uptake can be regulated in accordance with the availability of, or the bacteria's need for the resource, or a combination of both. Other environmental factors may non-specifically affect the demand for the resource, for example by altering the growth rate. (B) Schematic of the Kdp regulation system. The bifunctional histidine kinase KdpD acts as both an autokinase (including phosphotransferase) and phosphatase for the response regulator KdpE. Phosphorylated KdpE activates expression of the genes encoding the high-affinity  $K^+$  transporter KdpFABC. (C, D). KdpD autokinase activity (C) and phosphatase activity (D) both depend on  $K^+$  concentration. Autokinase activity was determined from the initial rates of KdpD autophosphorylation; phosphatase activity from the initial rate of KdpE-P dephosphorylation by wild-type KdpD or by KdpD/ $\Delta$ 2-498. Lines show the best-fit Michaelis form; shading denotes regions that contain all activity curves within 68% and 95% confidence limits. The figure was created by Filipe Tostevin.

We next studied the dependence of the KdpD phosphatase activity on  $K^+$  by measuring the rate of dephosphorylation of phospho-KdpE *in vitro* in the absence of KdpD autophosphorylation. The quantitative dependence of the dephosphorylation rate on  $K^+$  concentration is plotted in Figure 2.1-1D, and shows half-maximal activation at  $K_{0.5} = 4.2^{+7.8}_{-3.0}$  mM.  $K^+$  therefore has both an inhibitory effect on the autokinase activity and a stimulating effect on the phosphatase activity of KdpD.

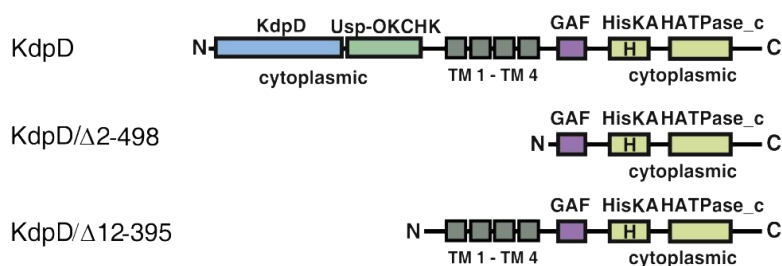
The cytoplasmic C-terminal domain of KdpD (KdpD/ $\Delta$ 2-498) (Figure 2.1-2A), has been proposed to harbor a  $K^+$  sensor (Rothenbücher *et al.*, 2006). Having found that purified KdpD/ $\Delta$ 2-498 showed  $K^+$ -independent autokinase activity (Figure 2.1-2B), we hypothesized that this variant might have a  $K^+$ -dependent phosphatase activity. We therefore tested the effect of  $K^+$  on the phosphatase activity of KdpD/ $\Delta$ 2-498 using phospho-KdpE as substrate. The quantitative dependence of the dephosphorylation rate on  $K^+$  concentration is plotted in Figure 2.1-1D, showing a stimulatory effect with half-maximal activity at  $K_{0.5} = 34^{+52}_{-19}$  mM  $K^+$ . This

## Results

demonstrated that the C-terminal domain is sufficient for regulation of the phosphatase but not the autokinase activity.

To search for a domain bearing a  $K^+$  recognition site, we tested the  $K^+$ -dependent autokinase activity of several truncated KdpD proteins (Figure 2.1-2). Remarkably, the autokinase activity of a truncated KdpD variant that lacked the Kdp and Usp domains but still retained the four transmembrane helices (KdpD/ $\Delta$ 12-395, Figure 2.1-2A) displayed a  $K^+$  sensitivity similar to that of wild-type KdpD (Figure 2.1-2B). Therefore, we focused on a stretch of conserved amino acids in the second periplasmic loop (loop 3) (Figure 2.1-3A), and employed a systematic alanine mutagenesis screen. Using an *E. coli* *P<sub>kdpFABC</sub>-lacZ* reporter strain, we found that KdpD variants with alanine substitutions at amino acid positions P466, T469, L470 and V472 were less  $K^+$ -sensitive, and that these mutations shifted the onset of *kdpFABC* expression to external  $K^+$  concentrations that would normally inhibit expression (Figure 2.1-3B). Replacement of F463, I464, R467 and S473 had minor effects on KdpD activity (Figure 2.1-4).

### A



### B

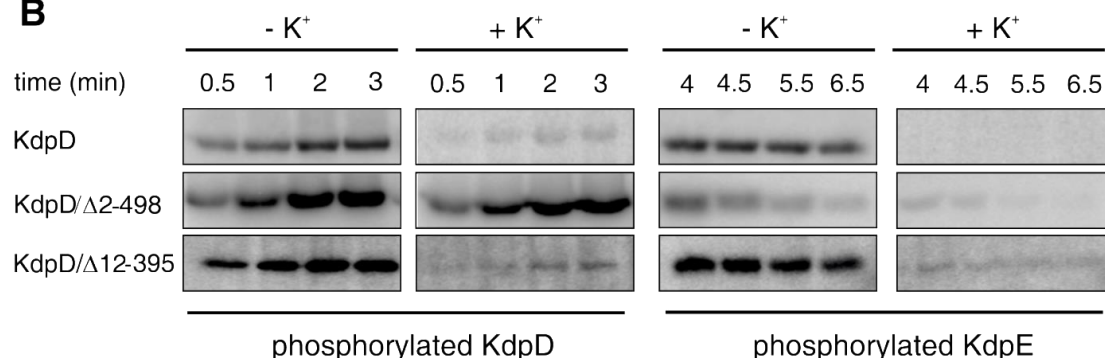


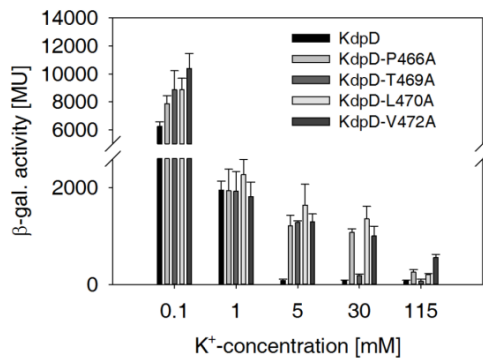
**Figure 2.1-2: *In vitro* activities of truncated KdpD variants.** (A) Schematics of wild-type KdpD in comparison to the truncated variants KdpD/ $\Delta$ 2-498 and KdpD/ $\Delta$ 12-395. TM: transmembrane helix. (B) Time dependent autophosphorylation of KdpD and truncated KdpD variants and dephosphorylation of KdpE in the absence (-) and presence (+) of 250 mM  $K^+$  at constant ionic strength. Shown are representative autoradiographs of three independent experiments.

## Results

**A**

	TM 3	Loop 3	TM 4	
<i>Escherichia coli</i>	GRWPS-VVATVINNVVSFDL	FIAPRGT	LAVSDVQYLLTFAVMLTVGLVIG	492
<i>Yersinia pestis</i>	GRWPS-VLAAVINVASFDL	FVQPHWSLAVT	DVQYLLTFGVMLIVGIVVG	493
<i>Photorhabdus luminescens</i>	GRRPS-IFAAFINVISFDI	FVQPHWSLAVT	DMQYLLTFVSMIVGVVVG	496
<i>Salmonella typhimurium</i>	GRWPS-VVATVINNVASFDL	FIAPRGT	LAVSDVQYLLTFAVMLTVGLVIG	492
<i>Klebsiella pneumoniae</i>	GRWPS-VLATVINVISFDL	FVAPRGT	LAVSDVQYLLTFGVMLTVGLLIG	492
<i>Erwinia amylovora</i>	GRWPS-VVATLLNIAAFDL	FVAPTGMTVVS	DVQYLVTFGVMLAVGVIVG	490
<i>Enterococcus faecalis</i>	GYFWS-SLSSILSVLSFNW	FVEPLYSLTVYKQGY	PFTLLMLLVVALMSS	459
<i>Staphylococcus aureus</i>	RSFIIGFLAAIINVFNVE	FTEPRYTFEVEY	RFDYPITFIVSILTSILTS	481
	.....*	* * * * *	* . * : : . . . . .	

**B**



**C**

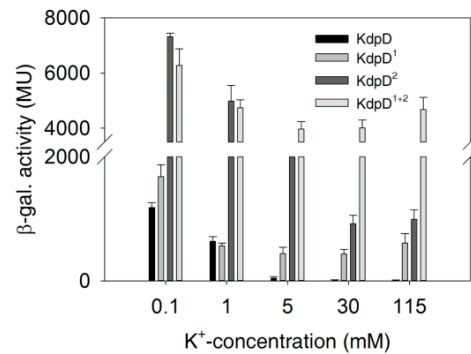


**Figure 2.1-3: The periplasmic loop between transmembrane helix three and four is involved in  $K^+$ -sensing.** (A) Multiple sequence alignment of the periplasmic loop (Loop 3) between transmembrane helix 3 (TM3) and 4 (TM4). The alignment was created using the ClustalW2 program. (B) The  $\beta$ -galactosidase activities of the reporter strain ( $P_{kdpFABC}::lacZ$ ) carrying plasmids encoding KdpD and the variants KdpD-P466A, KdpD-T469A, KdpD-L470A and KdpD-V472A were determined after cultivation of cells in minimal medium at the indicated  $K^+$ -concentrations. (C) The  $\beta$ -galactosidase activities of the reporter strains LF3, HS2, HS3 and HS4 ( $P_{kdpFABC}::lacZ$ ) carrying KdpD and the variants KdpD<sup>1</sup>, KdpD<sup>2</sup> and KdpD<sup>1+2</sup> were determined after cultivation of cells in minimal medium at the indicated  $K^+$ -concentrations.

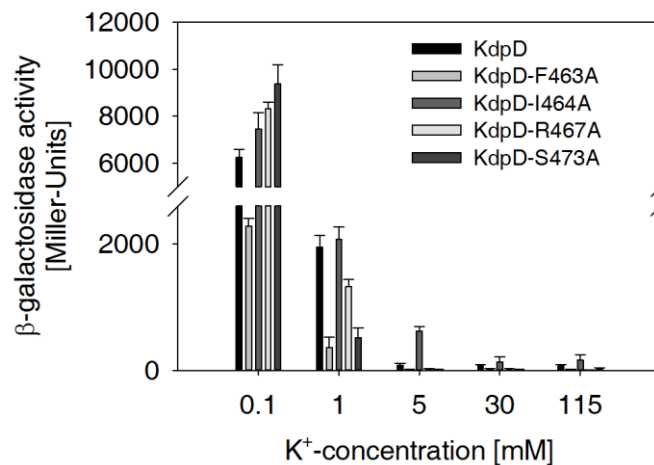


**Figure 2.1-4:  $\beta$ -galactosidase activities of the reporter strain ( $P_{kdpFABC}::lacZ$ ) carrying plasmids encoding KdpD and KdpD variants.**  $\beta$ -galactosidase activities were determined after cultivation of cells in minimal medium at the indicated  $K^+$ -concentration.

## Results

Finally, we generated a KdpD variant in which all four amino acids (P466, T469, L470, V472) were replaced with alanine, and designated this variant as KdpD<sup>1</sup> (Figure 2.1-5A). KdpD<sup>1</sup> was characterized by a K<sup>+</sup>-independent autokinase activity, and a K<sup>+</sup>-sensitive phosphatase activity for KdpE-P *in vitro* (Figure 2.1-5B). The regulation of the phosphatase activity was found to be similar to the C-terminal KdpD/ $\Delta$ 2-498 fragment ( $K_{0.5}=32^{+71}_{-18}$  mM K<sup>+</sup>; Figure 2.1-6).

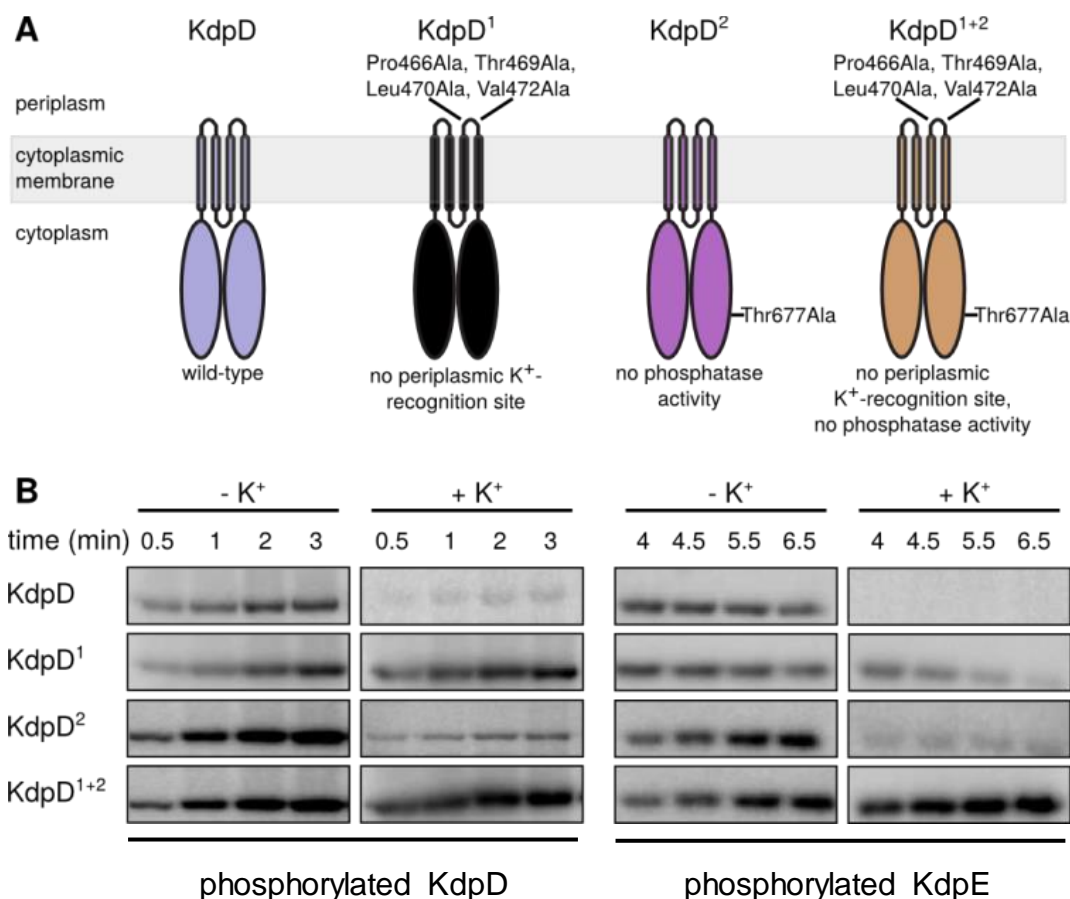


**Figure 2.1-5: *In vitro* activities of different KdpD variants.** (A) Topology model of wild-type KdpD and the locations of amino acid substitutions. Variant KdpD<sup>1</sup> contains four amino acid substitutions (P466A, T469A, L470A and V472A) in the periplasmic loop region. KdpD<sup>2</sup> contains a single substitution (T677A) in the C-terminal domain. KdpD<sup>1+2</sup> combines these five substitutions. (B) Time-dependent autokinase activity of KdpD and KdpD variants in membrane vesicles was monitored by incubation with [ $\gamma$ -<sup>32</sup>P]ATP in the presence and absence of 250 mM K<sup>+</sup> (left side). After 3.5 min, KdpE was added, and time-dependent dephosphorylation was monitored (right side). Phosphorylated KdpD and KdpE were separated by SDS-PAGE and gels were exposed to a phosphoscreen.

Further evidence for K<sup>+</sup> recognition by the second periplasmic loop was provided by variants in which the N- and C-terminal cytoplasmic domains of KdpD were connected by different linkers. When the two domains were connected by a 5Gly/5Ala or a 10Gly linker, *kdpFABC* expression in the reporter strain was no longer repressed at high K<sup>+</sup> concentrations; however, when the domains were linked by the periplasmic loop sequence, repression at high K<sup>+</sup>

## Results

concentrations was restored (Figure 2.1-7). Together, these data suggest that the second periplasmic loop of KdpD contains a specific  $K^+$  recognition site that regulates autokinase activity in response to extracellular  $K^+$ .

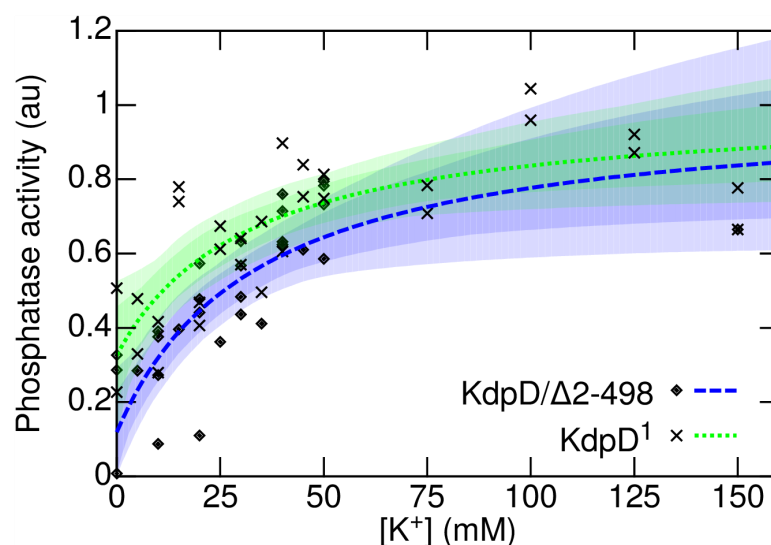


**Figure 2.1-6: *In vitro* phosphatase activity of KdpD<sup>1</sup>.** Full lines show the best-fit Michaelis form; shading denotes regions that contain all activity curves within 68% and 95% confidence regions. Data for KdpD/Δ2-498 is the same as in Figure 2.1-1. The figure was created by Filipe Tostevin.

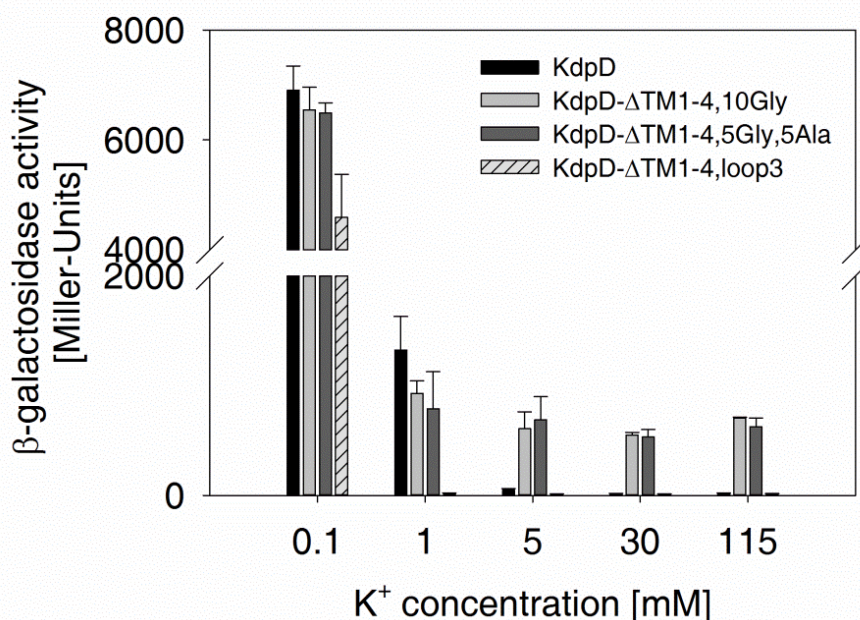


**Figure 2.1-7:  $\beta$ -galactosidase activities of the reporter strain ( $P_{kdpFABC}::lacZ$ ) carrying plasmids encoding KdpD and truncated KdpD variants.** The truncated KdpD variants lack the four transmembrane domains and are linked by a 10 glycine (KdpD-ΔTM1-4,10Gly), 5 glycine 5 alanine (KdpD-ΔTM1-4,5Gly,5Ala) and the periplasmic loop sequence (KdpD-ΔTM1-4,loop3), respectively.  $\beta$ -galactosidase activity was determined after cultivation of cells in minimal medium at the indicated  $K^+$ -concentrations.

We next turned to the K<sup>+</sup>-dependent regulation of the phosphatase activity. As mentioned above, the C-terminal cytoplasmic domain of KdpD has a K<sup>+</sup>-dependent phosphatase activity (Figure 2.1-1D). However, in spite of intensive efforts, we could not localize a K<sup>+</sup> recognition site in this domain (Schramke, 2011) (Chapter 2.2). In an attempt to circumvent this difficulty, we asked whether loss of the phosphatase activity affected the K<sup>+</sup> dependence of the autokinase activity. Amino acid substitutions at position T677 in KdpD are known to eliminate the phosphatase activity (Figure 2.1-5A) (Brandon *et al.*, 2000), as do substitutions of the same conserved threonine residue in many other sensor kinases (Willett & Kirby, 2012). We therefore assayed the activity of the KdpD variant T677A (KdpD<sup>2</sup>) *in vitro*. The data reveal that although KdpD<sup>2</sup> lacked phosphatase activity, it retained K<sup>+</sup>-sensitive autokinase activity (Figure 2.1-5B). Thus, how exactly K<sup>+</sup> modulates the phosphatase activity of KdpD remains unclear; it may act via the cytoplasmic GAF domain (residues 515-655), since GAF domains are well-known ligand binding sites also for ions (Cann, 2007a, Cann, 2007b, Heikaus *et al.*, 2009). However, our data clearly demonstrate that the autokinase and phosphatase activities of KdpD are individually regulated by K<sup>+</sup>.

Next, we combined the mutations of *kdpD*<sup>1</sup> and *kdpD*<sup>2</sup>, and found that the resulting KdpD<sup>1+2</sup> variant had an additive phenotype, displaying a K<sup>+</sup>-independent autokinase activity and no phosphatase activity, such that KdpE remained stably phosphorylated (Figure 2.1-5B). Taken together, these results support the idea that KdpD senses extracellular K<sup>+</sup> via the periplasmic loop to control its autokinase activity, while intracellular K<sup>+</sup> boosts its phosphatase activity.

### **2.1.2 Regulation of both enzymatic activities is essential for a controlled stress response.**

To probe the functional behavior of the Kdp system *in vivo*, we shifted exponentially growing *E. coli* MG1655 cells from K<sup>+</sup>-saturating conditions to media that imposed different degrees of K<sup>+</sup> limitation, and monitored extra- and intracellular K<sup>+</sup> levels and growth over time (Figure 2.1-8B). The cells maintained K<sup>+</sup> homeostasis until extracellular K<sup>+</sup> was completely exhausted, but continued to grow beyond this point, thus progressively diluting their intracellular pool of K<sup>+</sup>. The decrease in intracellular K<sup>+</sup> was in turn accompanied by a gradual reduction in the growth rate of the population. We then probed the response mediated by wild-type KdpD as well as that of variants KdpD<sup>1</sup>, KdpD<sup>2</sup> and KdpD<sup>1+2</sup> by quantifying the production of the high-affinity transporter KdpFABC two hours after shifting cells to media with different K<sup>+</sup> concentrations covering a broad range of K<sup>+</sup> availability (Figure 2.1-8C). Wild-type KdpD mediated a graded KdpFABC response at external K<sup>+</sup> concentrations below 5 mM. The KdpD<sup>1</sup> variant displays this behavior only at very low K<sup>+</sup> concentrations, such that KdpFABC is

produced at a constant rate at  $K^+$  concentration  $> 1$  mM, which is consistent with its  $K^+$ -independent autokinase activity. The KdpD<sup>2</sup> variant is less sensitive to intracellular  $K^+$  than the wild-type, highlighting the importance of the counteracting phosphatase activity in ensuring a tightly controlled stress response. Finally, in cells harboring the KdpD<sup>1+2</sup> variant, KdpFABC production becomes essentially independent of the  $K^+$  concentration. Similar results were obtained on the basis of  $P_{kdpFABC::lacZ}$  promoter activity (Figure 2.1-3C).

### 2.1.3 A mathematical model describes the *in vivo* response dynamics.

To quantitatively explore the consequences of different regulatory strategies, we developed a mathematical model for the relevant aspects of the Kdp system, including the dynamics of KdpD/KdpE phosphorylation, rates of KdpFABC production and turnover, rates of  $K^+$  import by both KdpFABC and constitutive transporters, and  $K^+$ -dependent growth (see Materials and Methods for details). While previous models were forced to make ad hoc assumptions about the regulation of the Kdp response (Heermann *et al.*, 2014), we used the enzymatic activities measured *in vitro* (Figure 2.1-1C, D) to parameterize the effects of both extracellular and intracellular  $K^+$  on KdpD.

Structural data for bifunctional sensor kinases have suggested the existence of distinct conformational states that possess either autokinase or phosphatase activity (Marina *et al.*, 2005, Ferris *et al.*, 2012, Ferris *et al.*, 2014, Huynh & Stewart, 2011). Our observation that KdpD<sup>1</sup> possesses  $K^+$ -independent autokinase activity but retains  $K^+$ -sensitive phosphatase activity is inconsistent with a simple two-state model in which KdpD is always either autokinase- or phosphatase-active, which implies that the two activities must always be anti-correlated. We therefore considered an extension of this model consisting of three distinct conformational states of KdpD, corresponding to autokinase-active, phosphatase-active, and inactive conformations (Figure 2.1-8A). Switching between these states was assumed to obey thermodynamic equilibrium statistics (Bhate *et al.*, 2015), with switching constants that vary depending on the extra- and intracellular concentrations of  $K^+$ . In such a model, the autokinase and phosphatase activities are correlated, and both depend on extra- and intracellular  $K^+$ . The parameters of these switching constants were determined by fitting to the *in vitro* enzymatic activities of wild-type KdpD and the KdpD<sup>1</sup> variant (Figure 2.1-1C, D; Figure 2.1-6), assuming that the observed activity is proportional to the fraction of KdpD molecules in the corresponding conformational state. The resulting parameterized switching model was then used as the input into a coarse-grained description of KdpD/KdpE signaling and response via *kdpFABC* expression. Parameters for this larger model were taken from the literature where possible, or

otherwise fit to experimental data. The model was able to reproduce both the phosphorylation dynamics *in vitro* (Figure 2.1-9) and the *in vivo* response (Figure 2.1-8B, C, lines) for wild-type KdpD and the variants KdpD<sup>1</sup>, KdpD<sup>2</sup>, and KdpD<sup>1+2</sup> showing that our regulation model is able to capture the main features of KdpD/KdpE signal transduction.

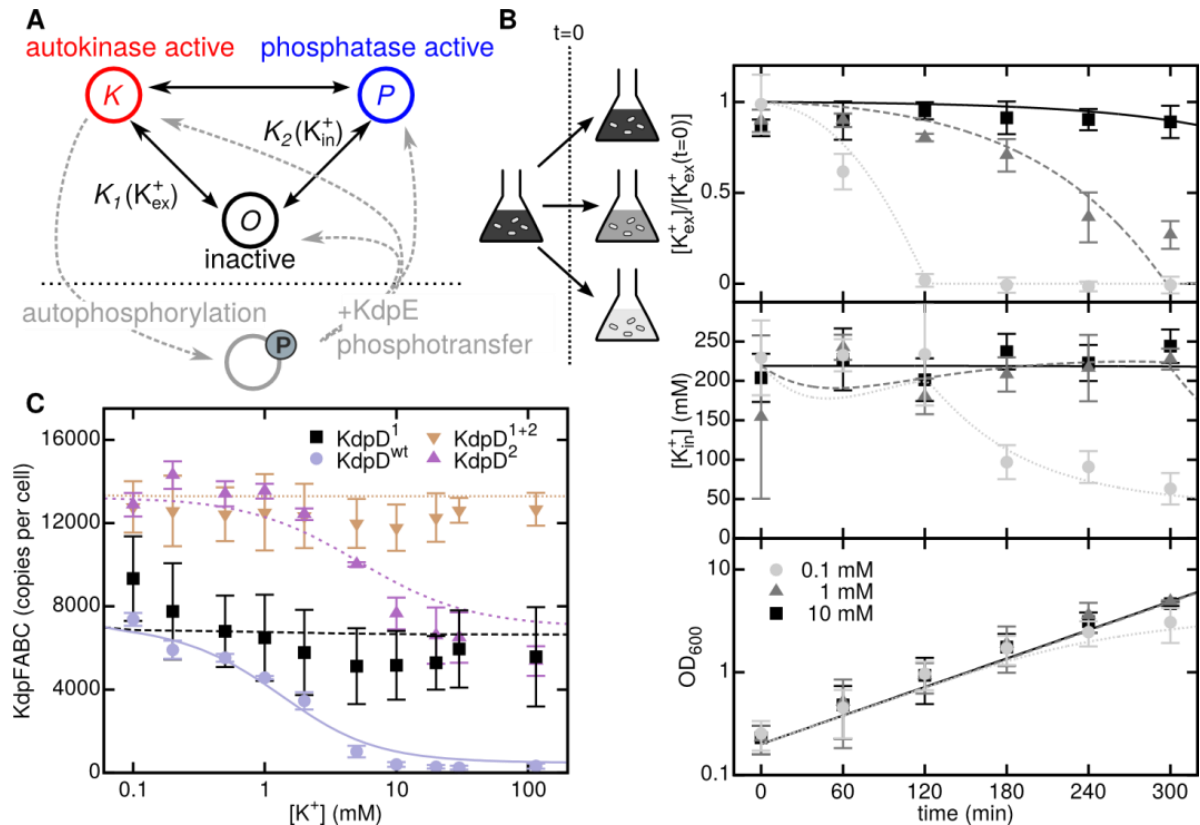


**Figure 2.1-8: Dynamics of Kdp response *in vivo*.** (A) Schematic of switching model of KdpD enzymatic activity. Autokinase and phosphatase activity are assumed to correspond to two distinct molecular conformations, K and P. A third inactive conformation, O, has no enzymatic activity. The equilibrium occupancy of each conformation is biased according to the extracellular and intracellular  $K^+$  concentrations. Molecules in the K state can undergo autophosphorylation. Subsequently, phosphotransfer from phospho-KdpD to KdpE returns KdpD to each state according to their equilibrium occupancies. (B) Dynamics of intracellular and extracellular  $K^+$  concentration for wild-type cells measured by atomic absorption spectroscopy, and optical density at 600 nm. At time  $t=0$ , cells were transferred from medium containing 10 mM  $K^+$  to media with the indicated concentrations. (C) KdpFABC levels were determined by quantitative Western blot analysis, 120 min after transfer of cells to media with the indicated  $K^+$  concentration. Data points are the mean $\pm$ SD of N=3 biological replicates. Lines show results of the mathematical model. The figure was created by Filipe Tostevin.

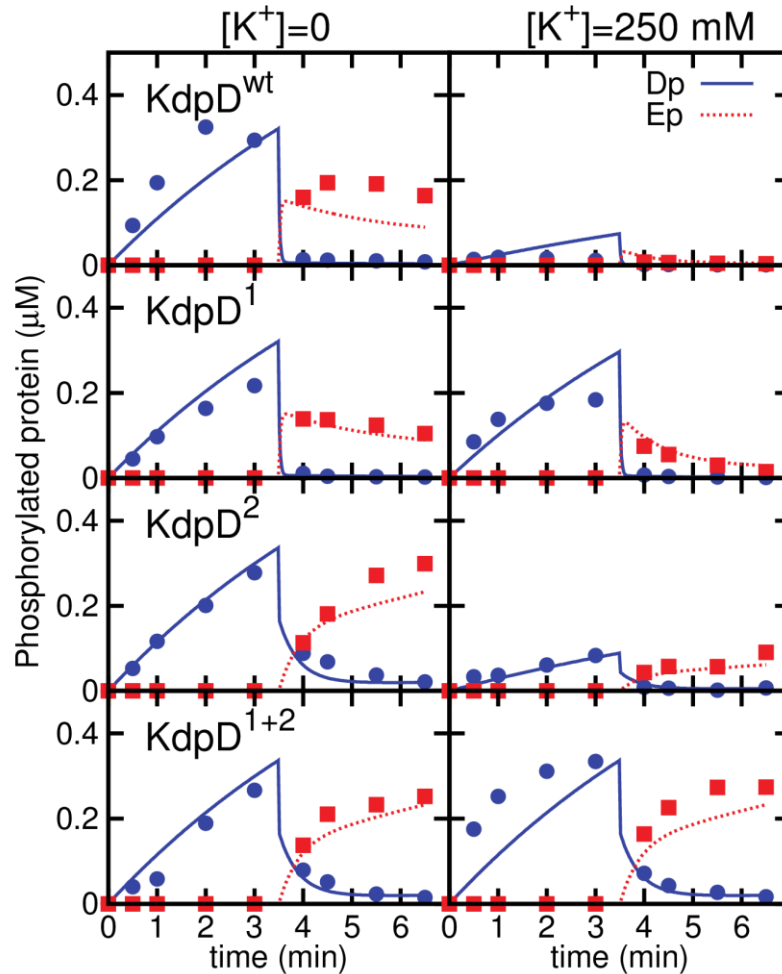


**Figure 2.1-9: Fitting of *in vitro* model to experimental data.** Comparison of the dynamics of the mathematical model (lines) with experimental data (points) for all experimental conditions and strains. The figure was created by Filipe Tostevin.

#### 2.1.4 Dual sensing by a bifunctional histidine kinase ensures robust homeostasis in fluctuating environments.

We next sought to compare the performance of cells employing the dual-sensing strategy to that of mutants with only internal or external sensing under conditions of unpredictable environments (illustrated in Figure 2.1-1A). The strains carrying *kdpD<sup>1</sup>* and *kdpD<sup>2</sup>* mutations were unsuited for this purpose, since these cells constitutively produce high levels of the  $K^+$  transporter. We therefore employed our model to compare three alternative regulation strategies (Figure 2.1-10A): (i) the DUAL strategy of wild-type KdpD featuring dual sensing and bifunctional activities as revealed by our experiments; (ii) external sensing (EX) only, where the enzymatic activities of KdpD are dependent on extracellular  $K^+$  but are insensitive to changes in intracellular  $K^+$ ; and (iii) internal sensing (IN) only, where the enzymatic activities of KdpD are responsive to intracellular but not extracellular  $K^+$ .

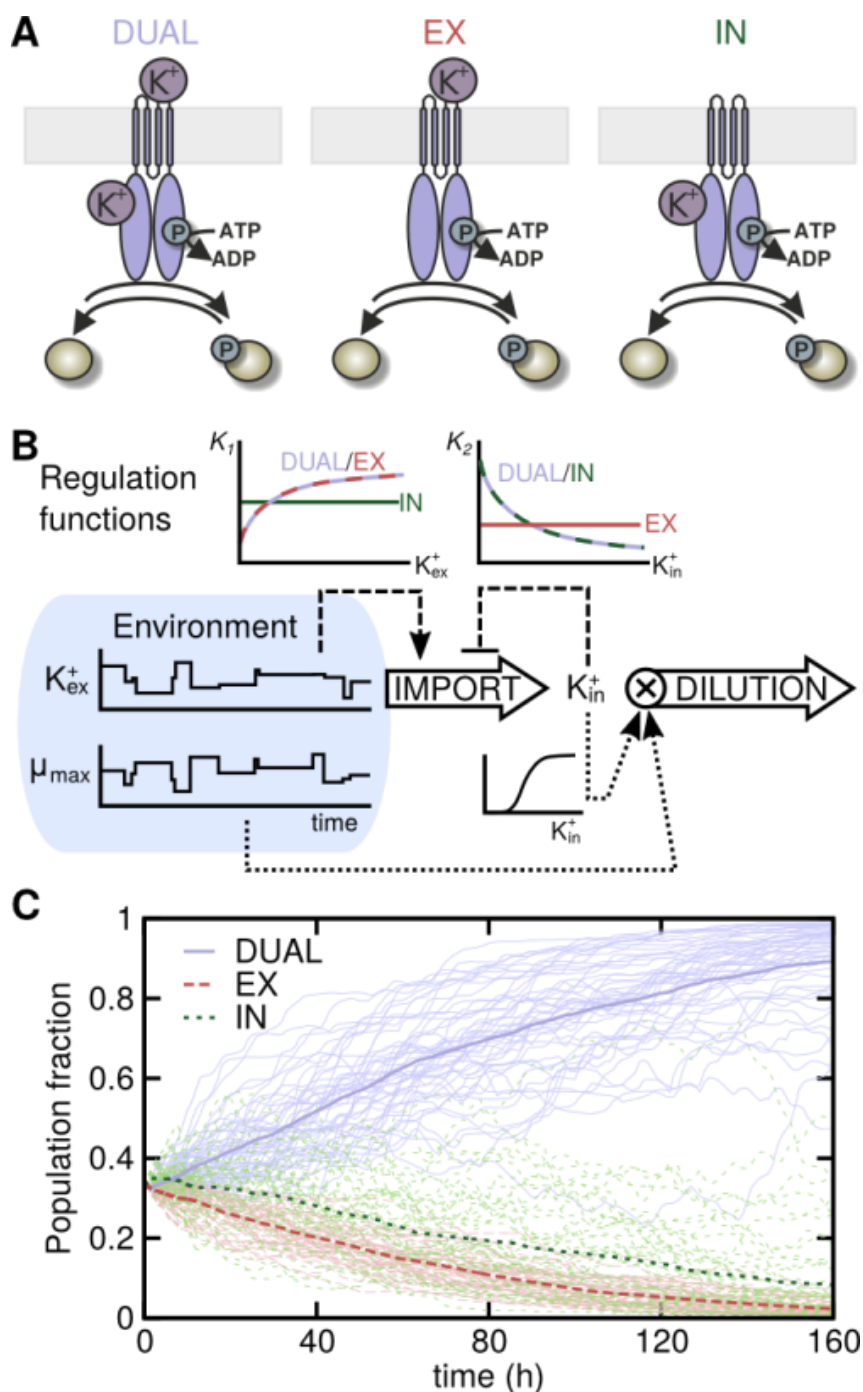


**Figure 2.1-10: Dual sensing and dual regulation provide robust control of intracellular  $K^+$ .** (A) Illustration of different regulation strategies. DUAL strategy: KdpD autokinase activity and phosphatase activity are regulated by extracellular and intracellular  $K^+$ , respectively. EX strategy: both activities are regulated by extracellular  $K^+$  independently of intracellular  $K^+$ ; IN strategy: both activities are regulated by intracellular  $K^+$ , independently of extracellular  $K^+$ . (B) Each strategy is characterized by the regulation functions that determine the enzymatic activities of KdpD as a function of the intra- and extracellular  $K^+$ . These control, via *kdpFABC* expression, the  $K^+$  import rate. The rate of dilution of intracellular  $K^+$  is the instantaneous growth rate, which is taken to be the product of the environmentally determined maximal growth rate,  $\mu_{max}$ , and a factor that depends on the intracellular  $K^+$  level. Both  $\mu_{max}$  and the environmental  $K^+$  level are subject to fluctuations over time. (C) Simulations of the outcome of competition between the three strategies. Starting from initially equal numbers of cells implementing each strategy, the plots depict the evolutionary trajectories of the subpopulations in environments in which both the extracellular  $K^+$  supply and the maximal growth rate vary. Light lines show results for individual environmental realisations; thick lines show the mean over 50 realizations. The figure was created by Filipe Tostevin.

## Results

We first asked how accurately each strategy was able to regulate the  $K^+$  uptake flux in response to varying  $K^+$  supply by comparing steady-state intracellular  $K^+$  levels across a range of extracellular  $K^+$  concentrations (Figure 2.1-11A). The DUAL strategy showed less variability than the IN strategy, which can trigger  $K^+$  uptake only after intracellular  $K^+$  has changed. However, the differences between the DUAL and EX strategies were small, indicating that the additional feedback from intracellular  $K^+$  to uptake plays little role under constant conditions.

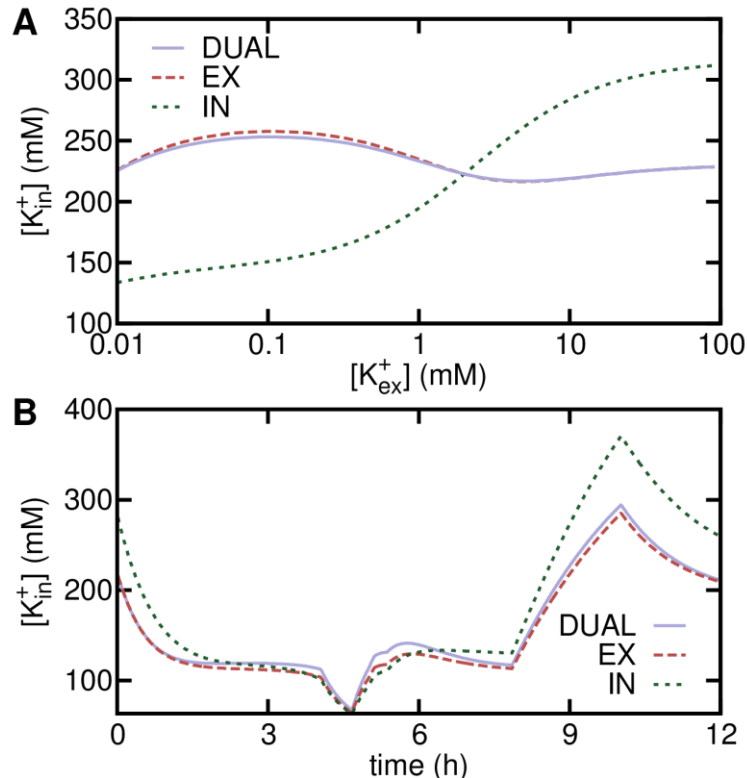


**Figure 2.1-11: Intracellular  $K^+$  for different regulation strategies.** (A) Steady-state intracellular  $K^+$  concentration as a function of extracellular  $K^+$  for different KdpD regulation strategies. (B) An example of the dynamic response of intracellular  $K^+$  in a random environment. The figure was created by Filipe Tostevin.

We reasoned that internal sensing could be beneficial if the intracellular  $K^+$  level were to change independently of the extracellular environment. Crucially, the intracellular  $K^+$  concentration depends on both the uptake rate and the rate of dilution due to growth (Figure 2.1-10B). If cells were exposed to environmental fluctuations that affected growth in a  $K^+$ -independent manner (e.g., changing carbon or nitrogen availability), the intracellular  $K^+$  concentration would be altered even though the environmental  $K^+$  level was unchanged. We therefore simulated direct competition among the strategies, which differ only in the regulation of KdpD activity as a function of  $K^+$  level, under conditions of fluctuating  $K^+$  supply and fluctuations in the maximal growth rate (Figure 2.1-10B). In our model the instantaneous growth rate is taken to be a monotonic, saturating function of the intracellular  $K^+$  concentration, with a prefactor

## Results

determined by the environment; thus differences in the growth rate between strategies reflect differences in intracellular  $K^+$  depletion. We found that both the EX and IN strategies were out-competed by the DUAL strategy, which ultimately came to dominate the population (Figure 2.1-10C). The poor performance of the EX strategy in this competition is primarily due to its inability to respond to the increasing demand for  $K^+$  under conditions of rapid growth. This dominance of dual sensing over internal sensing is due to its ability to achieve  $K^+$  homeostasis more reliably (Figure 2.1-11B), as also observed in the constant environments. The advantage of the DUAL strategy may in fact be greater than estimated here, as our model does not include any penalty for the superfluous overproduction of KdpFABC at high extracellular  $K^+$  concentrations.

## 2.2 Functional analysis of the GAF domain within the histidine kinase KdpD of *Escherichia coli*

The C-terminal cytoplasmic domain is responsible for K<sup>+</sup>-dependent regulation of the phosphatase activity (see chapter 2.1) (Heermann *et al.*, 2014). It comprises a GAF domain as well as the conserved DHp and CA domains (Figure 2.2-1A). This chapter reveals first insights into the function of the GAF domain within the histidine kinase KdpD of *E. coli*.

### 2.2.1 The replacement of the GAF domain with the GAF domain of 3E0Y results in deregulated enzyme activities.

The GAF domain of KdpD is a structural homologue to the GAF domain of the conserved protein 3E0Y from *Geobacter sulfurreducens* (Günther Gabriel, unpublished; (Schramke, 2011) (Figure 2.2-1B)). The crystal structure of the GAF domain of 3E0Y was solved with a bound Na<sup>+</sup> ion coordinated via amino acids N115, Y117, N200 and N202, which are located on  $\beta$ -sheet structures (source: protein data base 3E0Y; Figure 2.2-1B & C). Even though the sequence identity between the GAF domain of 3E0Y and the KdpD GAF domain is low (Figure 2.2-1D), the overall structure is supposed to be similar (Figure 2.2-1C). Therefore we suspected that corresponding amino acids in the GAF domain of KdpD could be involved in K<sup>+</sup> binding (Figure 2.2-1C, Günther Gabriel, unpublished).

To analyse the role of amino acids Q548, L550, V613 and E615 for K<sup>+</sup> recognition we substituted them with alanines (KdpD/Q548A,L550A,V613A,E615A) and with analogous amino acids of 3E0Y (KdpD/ Q548N,L550Y,V613N,E615N), respectively. Activity of KdpD variants was tested *in vivo* in the reporter strain HAK006 after cultivation in minimal medium containing different K<sup>+</sup> concentrations (Figure 2.2-2A). As intracellular K<sup>+</sup> binding results in stimulation of the phosphatase activity (see Chapter 2.1), we expected higher  $\beta$ -galactosidase activities for a KdpD variant, in which the K<sup>+</sup> binding site has been removed or modified. However, variants KdpD/Q548A,L550A,V613A,E615A and KdpD/Q548N,L550Y,V613N,E615N caused lower *kdpFABC* expression than wild-type KdpD (Figure 2.2-2A). Therefore, amino acids Q548, L550, V613 and E615 of KdpD are probably of minor importance for K<sup>+</sup> binding.

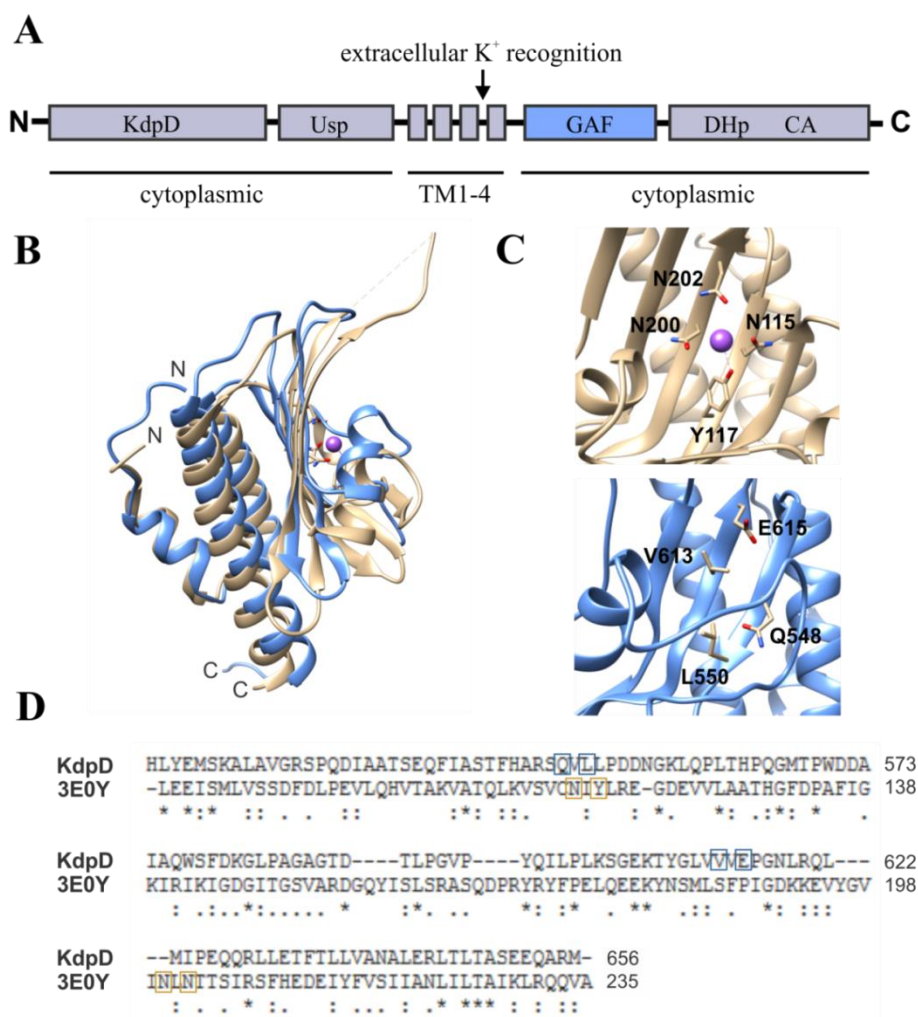


**Figure 2.2-1: Structural and sequence comparison of the GAF domain of *E. coli* KdpD and 3E0Y from *G. sulfurreducens*.** (A) Schematic representation of *E. coli* KdpD. The so far uncharacterized GAF domain is depicted in blue. Extracellular  $K^+$  is sensed in the periplasmic loop between TM3 and TM4. (B) The modeled structure of the GAF domain of *E. coli* KdpD (blue) is overlaid with the crystal structure of the GAF domain of 3E0Y from *G. sulfurreducens* (gold). A  $Na^+$  bound by 3E0Y is shown in purple. The structural model was created using the HHPred (Söding *et al.*, 2005) server and visualized using UCSF Chimera (Pettersen *et al.*, 2004) (C) Detailed view of the  $Na^+$  binding site within 3E0Y (top) and the corresponding amino acids within the GAF domain of KdpD (bottom). (D) Sequence comparison between the GAF domain of *E. coli* KdpD and 3E0Y.

We next constructed a hybrid protein, in which the GAF domain of *E. coli* KdpD (amino acid 515-655) was replaced with the GAF domain of 3e0Y from *G. sulfurreducens* (KdpD-GAF3E0Y). We found that this KdpD variant caused a semi-constitutive *kdpFABC* expression in the reporter strain HAK006. Albeit there was an increase under  $K^+$  limitation we observed a basal activity of around 500 Miller-Units (Figure 2.2-2B). To investigate enzymatic activities of this hybrid protein in more detail we analysed time dependent autophosphorylation and dephosphorylation of phospho-KdpE *in vitro* (Figure 2.2-2C,D).

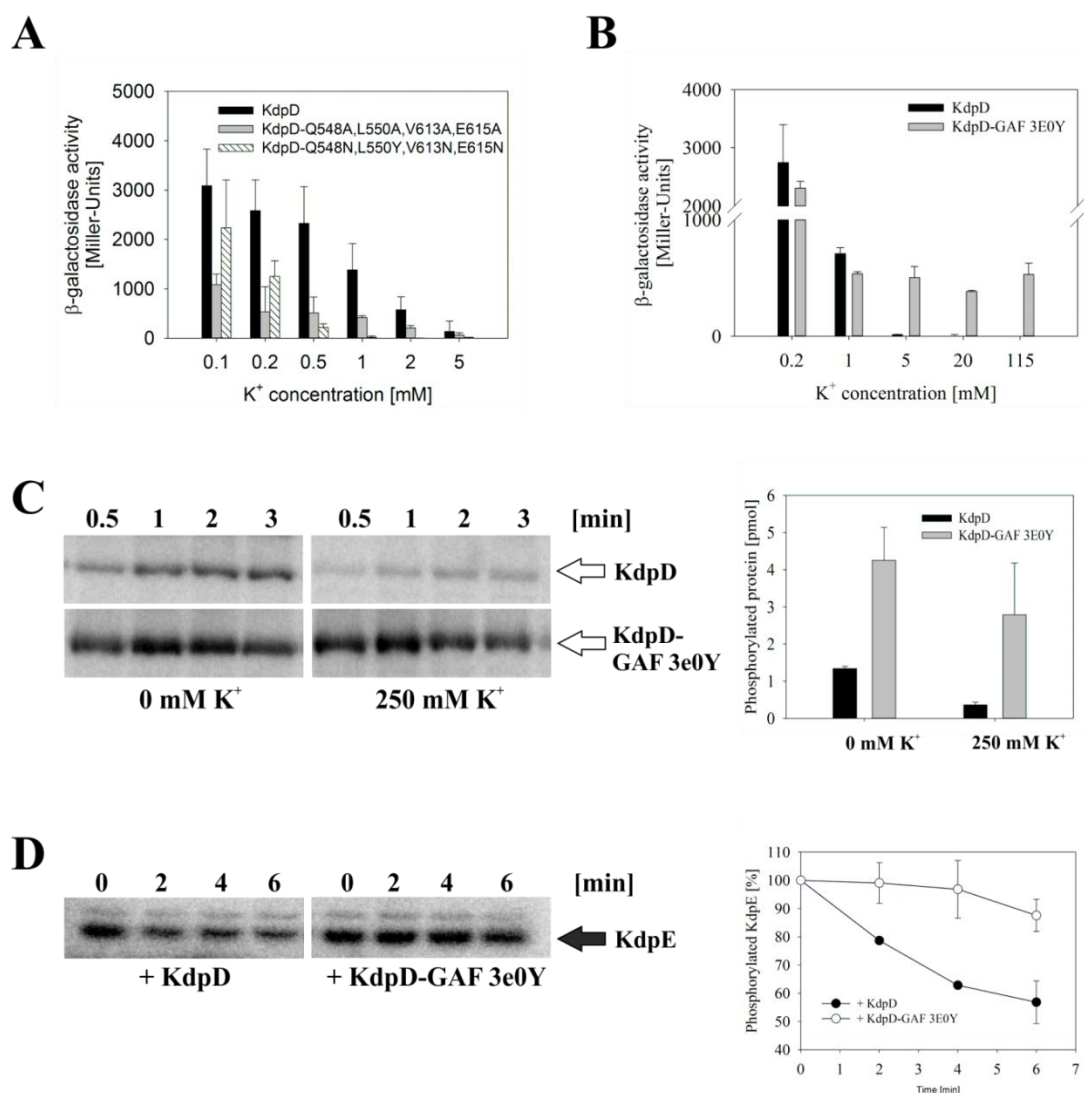


**Figure 2.2-2: *In vivo* and *in vitro* activities of the hybrid protein KdpD-GAF 3E0Y compared to the wild-type.** (A,B)  $\beta$ -galactosidase activities of the reporter strain ( $P_{kdpFABC}::lacZ$ ) carrying plasmids encoding KdpD and the variants KdpD-Q548A,L550A,V613A,E615A, KdpD-Q548N,L550Y,V613N,E615N (A) and KdpD-GAF 3E0Y (B) were determined after cultivation of cells in minimal medium at the indicated  $K^+$  concentrations. Shown are average values and standard deviations from at least three independent experiments. (C) Time-dependent autophosphorylation of wild-type KdpD in comparison to KdpD-GAF3E0Y in the absence and presence of 250 mM  $K^+$  at constant ionic strength. Shown are representative autoradiographs of three independent experiments. Amounts of phosphorylated KdpD and KdpD-GAF 3E0Y after three minutes of autophosphorylation in the presence and absence of 250 mM  $K^+$  (right) Shown is the average and standard deviation of three independent experiments. (D) Time-dependent dephosphorylation of phospho-KdpE by KdpD and KdpD-GAF3E0Y. Shown are representative radiographs of three independent experiments. Quantification of time-dependent dephosphorylation is shown in the right panel. Shown is the average and standard deviation of three independent experiments.

Autophosphorylation of KdpD is inhibited in the presence of  $K^+$  (Heermann *et al.*, 2009b, Lüttmann *et al.*, 2009)(Figure 2.2-2C), whereas the variant KdpD-3E0Y showed an increased  $K^+$ -independent autophosphorylation (Figure 2.2-2C). To analyse phosphatase activity of the hybrid protein, KdpE was phosphorylated *in vitro* and subsequently purified as described in Material and Methods. Consecutively KdpD or KdpD-GAF 3E0Y were added and dephosphorylation of phospho-KdpE was monitored over time. In contrast to wild-type KdpD

the hybrid protein was not able to dephosphorylate phospho-KdpE within the tested time frame (Figure 2.2-2D). Taken together, these results show that the GAF domain of KdpD is essential for the  $K^+$ -dependent regulation of both kinase and phosphatase activities.

### 2.2.2 The replacement of the GAF domain with GAF domains from different KdpD proteins influences KdpD activity

The GAF domain within KdpD proteins is less conserved and varies greatly in amino acid sequence and length (Figure 2.2-3A). Potentially the GAF domain fulfils diverse functions in different organisms and does not always act as a  $K^+$  sensor. Therefore we next sought to find a KdpD variant that is insensitive to intracellular  $K^+$  by replacing the GAF domain with KdpD GAF domains from different organisms (*Staphylococcus aureus*, *Proteus mirabilis*, *Vibrio cholerae*) (Figure 2.2-3A). We found similar *in vivo* activities for wild-type KdpD and the hybrid proteins containing the GAF domains from *S. aureus* (KdpD-SaGAF) and *V. cholerae* (KdpD-VcGAF) KdpD (Figure 2.2-3B). However, *kdpFABC* expression was not induced by the KdpD variant carrying the GAF domain from *P. mirabilis* (KdpD-PmGAF) (Figure 2.2-3B). Curiously the sequence identity of the KdpD GAF domain from *P. mirabilis* is more similar to the one from *E. coli* compared to the *S. aureus* and *V. cholerae* GAF domain. Western Blot analysis confirmed that all hybrid proteins were produced in equal amounts as wild-type KdpD (data not shown). Thus, despite low sequence identity and similarity, the overall structure of the GAF domain from different KdpD proteins might be similar and functional related.

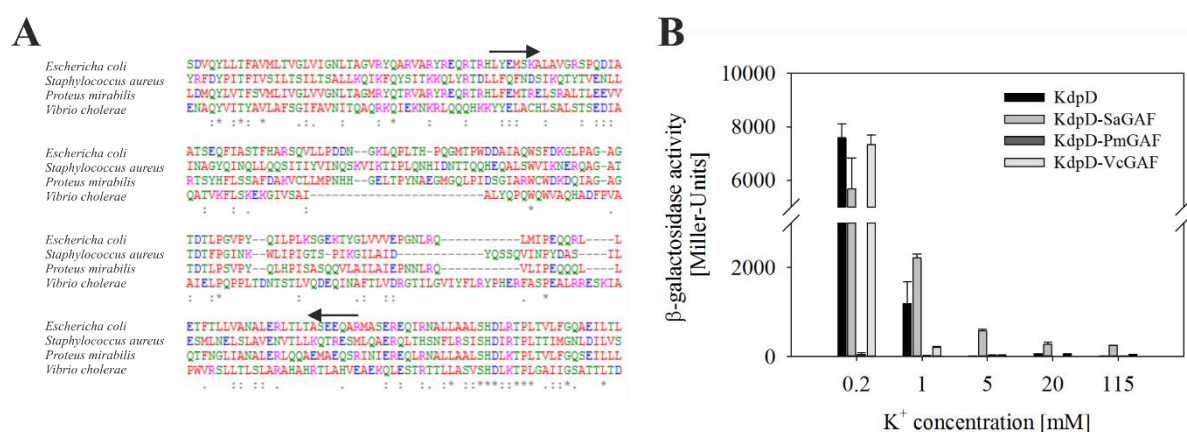


**Figure 2.2-3: Replacement of the GAF domain with GAF domains from different organisms.** (A) Sequence comparison of the GAF domain within KdpD proteins from *E. coli*, *S. aureus*, *P. mirabilis* and *V. cholerae*. Black arrows indicate beginning and end of the GAF domain, respectively. (B)  $\beta$ -galactosidase activities of the reporter strain ( $P_{kdpFABC}::lacZ$ ) carrying plasmids encoding KdpD and KdpD variants. Sa: *S. aureus*, Pm: *P. mirabilis*, Vc: *V. cholerae*.  $\beta$ -galactosidase activity was determined after cultivation of cells in minimal medium at the indicated  $K^+$  concentrations

### 2.2.3 The deletion of the GAF domain results in an inverted response.

By replacing the GAF domain of KdpD with the GAF domain of 3E0Y of *G. sulfurreducens* and GAF domains from different KdpD proteins we could not determine the location of an intracellular  $K^+$  binding site. We next tried to find amino acids involved in  $K^+$  binding via random mutagenesis as described in Materials and Methods. To screen for less  $K^+$  sensitive KdpD variants, we transformed the reporter strain with mutagenized plasmids and plated them on KML+ X-Gal + ampicillin agar plates. Colonies producing wild-type KdpD remain white under these conditions, whereas colonies producing less  $K^+$  sensitive KdpD variants are supposed to turn blue. Plasmids from blue colonies were isolated and mutations identified by sequencing analysis. Most of the mutations resulted in amino acid replacements located in regions predicted to form  $\alpha$ -helices. In many cases amino acids were exchanged by prolines, an amino acid known to be a “helix breaker” (Table S4, Figure 2.2-4, Figure 2.2-5). Therefore we concluded that these KdpD variants have rather structural than  $K^+$  sensing defects. Curiously we identified one KdpD variant in which the GAF domain was deleted (KdpD- $\Delta$ 514-655). This variant caused low, but constitutive activity *in vivo* (Figure 2.2-6A). *In vitro* autophosphorylation and phosphotransfer to KdpE revealed an inverted response. The truncated variant showed a very weak autophosphorylation but a clear phosphotransfer to the response regulator KdpE only in the presence of  $K^+$  (Figure 2.2-6B).

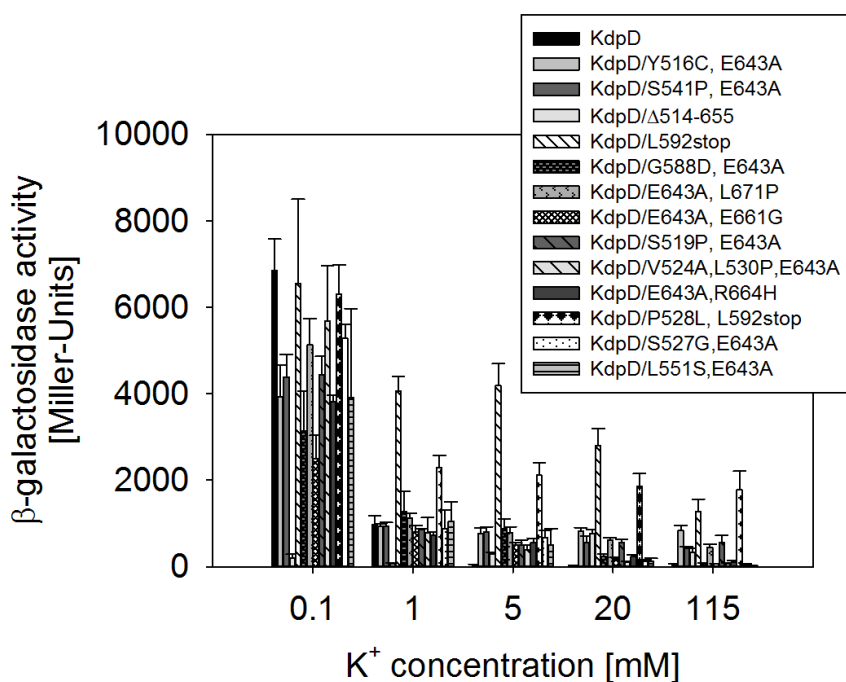


**Figure 2.2-4:  $\beta$ -galactosidase activities of the reporter strain ( $P_{kdpFABC}::lacZ$ ) carrying plasmids encoding KdpD and KdpD variants.**  $\beta$ -galactosidase activity was determined after cultivation of cells in minimal medium at the indicated  $K^+$  concentrations.

## Results

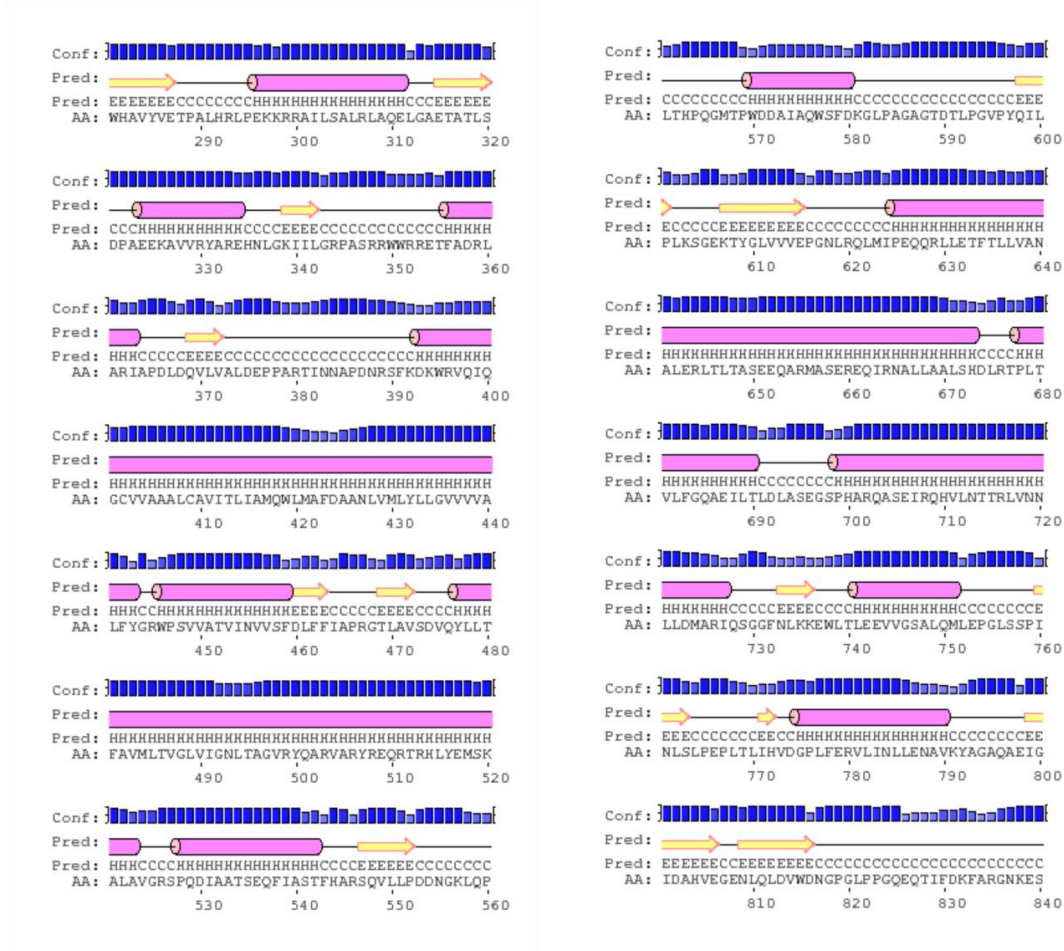


**Figure 2.2-5: Secondary structure prediction of KdpD (amino acids 280-840).** The secondary structure was predicted using the Pspred program (UCL Department of Computer Science).

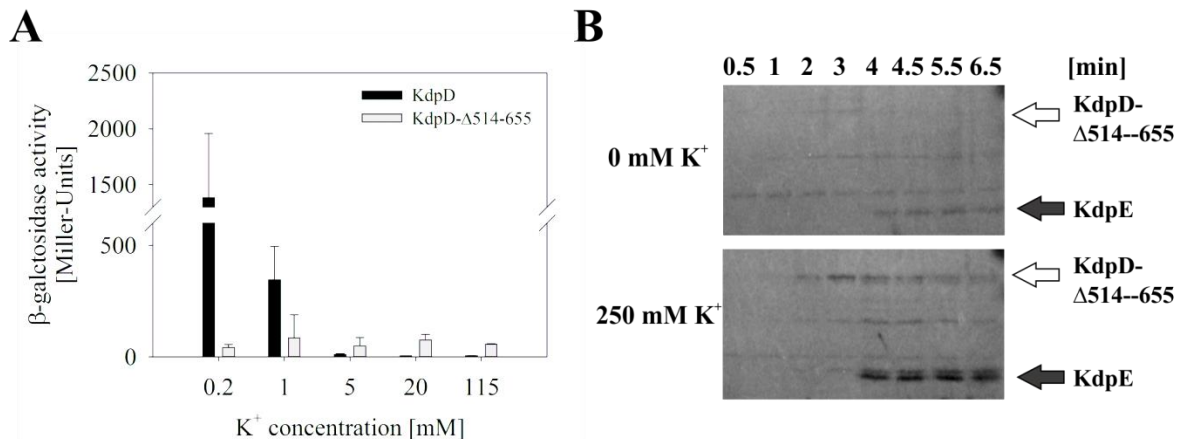


**Figure 2.2-6: The deletion of the GAF domain in KdpD results in an inverted response.** (A)  $\beta$ -galactosidase activities of the reporter strain ( $P_{kdpFABC}::lacZ$ ) carrying plasmids encoding KdpD and the truncated variant KdpD- $\Delta$ 514-655 were determined after cultivation of cells in minimal medium at the indicated K<sup>+</sup> concentrations. Shown are average values and standard deviations from three independent experiments. (B) Time-dependent autophosphorylation of KdpD- $\Delta$ 514-655 and phosphotransfer to KdpE in the absence and presence of 250 mM K<sup>+</sup> at constant ionic strength. KdpE was added after 3.5 minutes. Shown are representative autoradiographs of three independent experiments.

### 2.2.4 The third helix of the GAF domain is important for signalling.

The phenomenon of an inverted response has been described for insertions or truncations within signalling helices (S-helices) (Winkler *et al.*, 2012). S-helices are found in many signalling proteins, are supposed to form parallel coiled-coil elements and usually connect receiver and output domains (Anantharaman *et al.*, 2006). As we observed an inverted response for KdpD/ $\Delta$ 514-655 we considered that the GAF domain could end in an S-helix. S-helices can vary in length and typically contain a highly conserved ‘ERT’ motif (Anantharaman *et al.*, 2006), which is not present in the KdpD GAF domain.

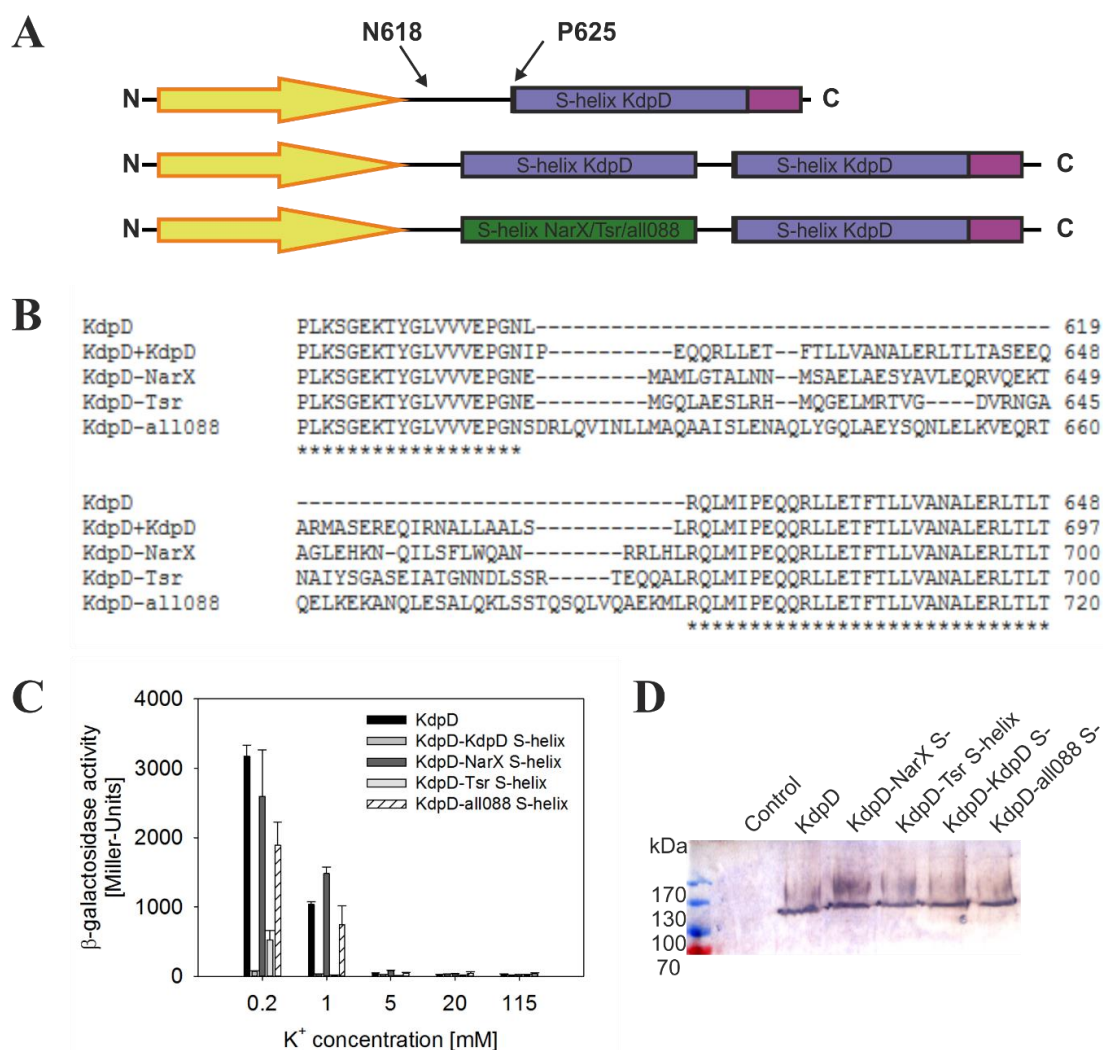


**Figure 2.2-7: Insertion of S-helices in the GAF domain of KdpD.** (A) Scheme of KdpD and variants. The putative S-helix of KdpD (blue) was duplicated by insertion in an unstructured region between a  $\beta$ -sheet (yellow arrow) and the third helix of the GAF domain (pink). In the other variants known S-helices from either NarX, Tsr or all0888 (shown in green) were inserted at the same position. (B) Sequence alignment of constructed hybrid proteins. (C)  $\beta$ -galactosidase activities of the reporter strain ( $P_{kdpFABC}::lacZ$ ) carrying plasmids encoding KdpD and KdpD variants were determined after cultivation of cells in minimal medium at the indicated  $K^+$  concentrations. Shown are average values and standard deviations from three independent experiments. (D) Western blot of whole cell extracts. Equal amounts of cells were mixed with SDS loading dye and analysed by SDS-PAGE and Western Blot analyses as described in Material and Methods.

## Results

We wondered if truncation or insertions in this helix would change signalling properties of KdpD. Initially we inserted known S-helices from the chemoreceptor Tsr, the nitrate sensor protein NarX and from a serine/threonine kinase of *Nostoc* sp (gene *all0886*) as well as another copy of the putative KdpD S-helix in an unstructured region just in front of the last helix of the GAF domain (Figure 2.2-7A,B). The insertion of the NarX and All0888 S-helix did not significantly change signalling *in vivo*, whereas the hybrid protein with an inserted S-helix from Tsr showed lower activity compared to wild-type KdpD (Figure 2.2-7C). Surprisingly the duplication of the KdpD S-helix resulted in a complete loss of the output response (Figure 2.2-7C), even though protein levels were comparable to wild-type KdpD (Figure 2.2-7D). Consistent with the results obtained *in vivo*, the variant KdpD-KdpD S-helix did not show any kinase activity *in vitro* (data not shown).

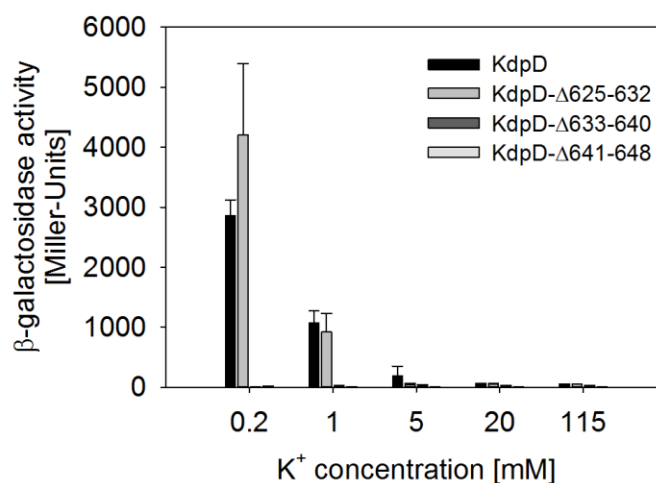


**Figure 2.2-8:  $\beta$ -galactosidase activities of the reporter strain ( $P_{kdpFABC}::lacZ$ ) carrying plasmids encoding KdpD and truncated KdpD variants.**  $\beta$ -galactosidase activity was determined after cultivation of cells in minimal medium at the indicated K<sup>+</sup> concentrations.

We next tested the consequence of different truncations within the third helix of the GAF domain on KdpD activity *in vivo*. Whereas truncations of amino acids 633-640 and 641-648 resulted in a loss of activity, removal of amino acids 625-632 did not affect signalling (Figure 2.2-8). All parts of this helix contain several hydrophobic amino acids, particularly leucines (Figure 2.2-9A), which could be important for dimerization via coiled-coil formation. To analyse this possibility, we tested *in vivo* activity of KdpD variants, in which these leucines were replaced with alanines (Figure 2.2-9B). KdpD-L636A,L637A,V638A and KdpD-L645A,L647A were less active compared to wild-type KdpD, whereas the replacement at position L642 had no significant effect on *in vivo* activity. The variant KdpD-L630A,L631A did not induce *kdpFABC* expression, however Western blot analysis revealed that this KdpD



T25-KdpD could be observed indicating that the hybrid proteins were suitable to detect dimerization of wild-type KdpD. However there was no difference in interaction strength if amino acids L636, L637 and V638 were replaced with alanines (Figure 2.2-9D). Accordingly from these data it is not possible to judge whether KdpD/L636A,L637A,V638A variant dimerizes like wild-type KdpD or if it is an artificial effect due to protein overproduction.

In summary we found that the third helix of the GAF domain plays a crucial role in signalling in KdpD. Insertions and truncations of this helix did not cause an inverted response but resulted in wild-type-like, decreased or loss in protein activity. Furthermore hydrophobic amino acids located on the helix could be involved in KdpD dimerization, even though further biochemical proof is necessary.

### **2.2.5 Amino acids within the extended transmembrane helix interact with the GAF domain to transmit the K<sup>+</sup> signal across the membrane.**

The availability of external K<sup>+</sup> is recognized by the periplasmic loop between transmembrane domain 3 and 4 (Chapter 2.1). According to secondary structure predictions (Figure 2.2-10A) the fourth transmembrane helix extends into the cytoplasm and merges into the GAF domain. A cluster of conserved arginines (R503, R506, R508, R511) located within this helix has been shown to be important for regulation of the kinase and phosphatase activities (Jung & Altendorf, 1998a). Therefore, we were interested to know if the GAF domain could be involved in signalling across the membrane. Homology modelling revealed that the GAF domain of KdpD consists of two  $\alpha$ -helices followed by a bundle of  $\beta$ -sheets and ends in another  $\alpha$ -helix (Figure 2.2-10B). The predicted structure showed that the negatively charged amino acid E626 on the third helix is in close proximity to the cluster of the positive charged arginines. To find out if potential electrostatic interactions between amino acid side chains could be essential for signal transduction, we replaced the negatively charged glutamate with an arginine (KdpD-E626R) and tested the activity of this KdpD variant in the reporter strain HAK006 *in vivo*. Surprisingly we could not detect any *kdpFABC* expression in the reporter strain complemented with the variant KdpD/E626R (Figure 2.2-10C), highlighting the importance of this negatively charged amino acid for KdpD activity. However, wild-type activity could be restored by additionally reversing the charge at position 508 (R508E) resulting in variant KdpD/R508E,E626R, pointing out that electrostatic interactions between these two  $\alpha$ -helices are important for proper signalling. The single charge reversal R508E resulted in wild-type like activity as well. However we found an additional positively charged amino acid (R629) in close proximity to E626, which could compensate electrostatic interactions in the KdpD/R508E variant. Indeed we observed that the double reversal R508E and R629E in turn resulted in an



## Results

activities *in vitro* we reinserted cysteines at positions C852 and C874, which are present in native KdpD and have been shown to be essential for *in vitro* activity (Jung *et al.*, 1998). *In vivo* activity of the resulting variant KdpD-C-less-R508C,E626C,C852,C874 was comparable to KdpD-C-less-R508C,E626C (Figure 2.2-11A). To verify the existence of an “open” and “closed” conformation we tested autophosphorylation and phosphotransfer in the presence and absence of the reducing agent 1,4-dithiothreitol (DTT), which prevents oxidation of sulfhydryl groups to disulfide bridges. Therefore, we expected an “open” and kinase “off” conformation in the presence of DTT and a “closed” and kinase “on” conformation in the absence of DTT, respectively. However we found that autophosphorylation and phosphotransfer was independent of the absence or presence of DTT and the K<sup>+</sup> concentration (Figure 2.2-11B).

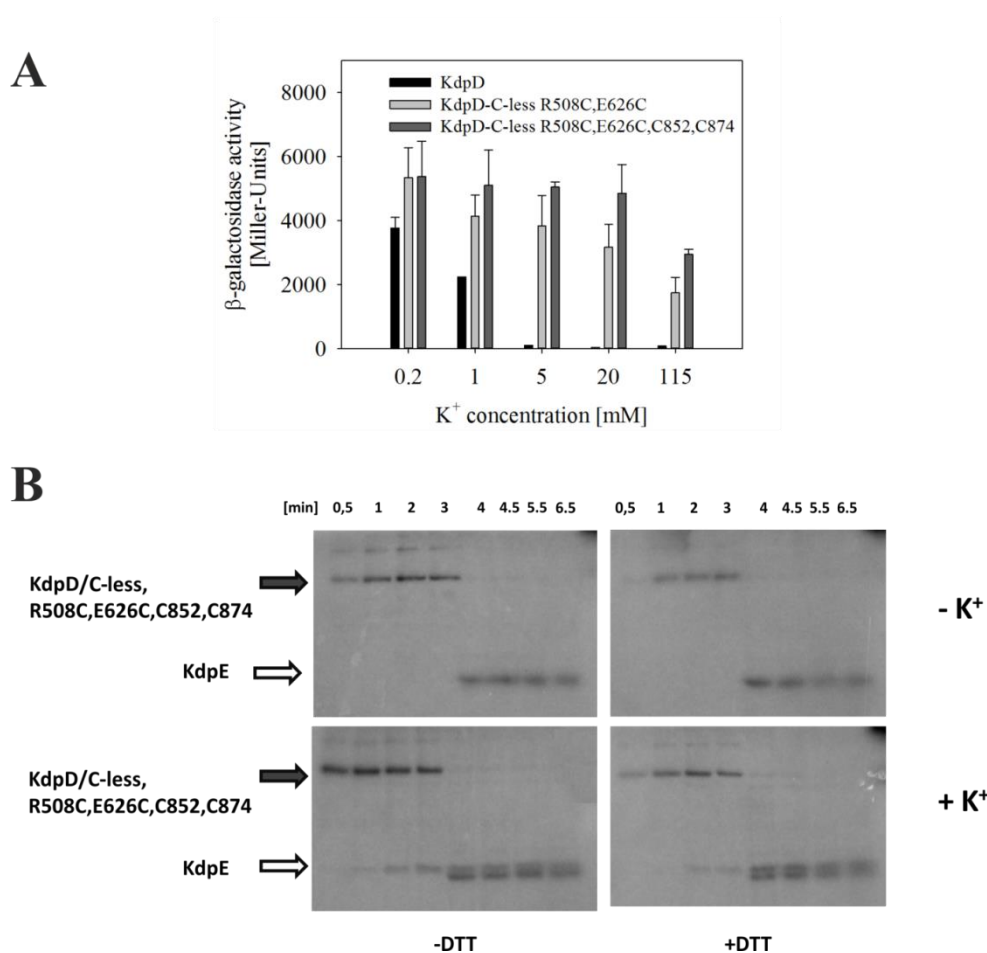


**Figure 2.2-11: Insertion of cysteines at positions R508 and E626 results in a constitutively active KdpD.** (A)  $\beta$ -galactosidase activities of the reporter strain ( $P_{kdpFABC}::lacZ$ ) carrying plasmids encoding KdpD and the variants KdpD-C-less R508C,E626C and KdpD-C-less R508C,E626C,C852,C874 were determined after cultivation of cells in minimal medium at the indicated K<sup>+</sup> concentrations. Shown are average values and standard deviations of three independent experiments. (B) Time-dependent autophosphorylation of KdpD-C-less R508C,E626C,C852,C874 and phosphotransfer to KdpE in the absence and presence of DTT and 250 mM K<sup>+</sup>, respectively. KdpE was added after 3.5 minutes. Shown are representative autoradiographs of two independent experiments.

## Results

Possibly the side chains of the cysteines are oriented in different directions and formation of a disulfide bridge was not possible. The kinase activity of KdpD is regulated by  $K^+$  sensing in the second periplasmic loop (see Chapter 2.1). The fact that we did not observe a difference in the kinase activity in the absence and presence of  $K^+$  confirms that interactions between these two amino acids are essential for transferring the signal of external  $K^+$  availability to the output domain.

## 2.3 Cross-talk regulation between the KdpD/KdpE and PhoR/PhoB two-components systems in *Escherichia coli*

It has been reported earlier that  $K^+$  is important for phosphate ( $PO_4^{3-}$ ) uptake (Weiden *et al.*, 1967). Phosphate is crucial for synthesis of cellular components like membrane lipids or nucleic acids and for signal transduction processes (Crépin *et al.*, 2011, Santos-Beneit, 2015). Free intracellular  $PO_4^{3-}$  levels range from 5 to 20 mM in *E. coli* depending on the growth rate and carbon source (Xavier *et al.*, 1995, Ugurbil *et al.*, 1982, Ugurbil *et al.*, 1978, Shulman *et al.*, 1979, Rao *et al.*, 1993). Upon  $PO_4^{3-}$  starvation (extracellular  $< 4 \mu\text{M}$ ) the two-component system PhoR/PhoB regulates expression of more than 30 genes belonging to the Pho regulon (Hsieh & Wanner, 2010). The Pho regulon comprises genes coding for proteins that are important for phosphate assimilation (Hsieh & Wanner, 2010) and their production level and timing are determined by the binding affinity of PhoB to the corresponding promoters (Gao & Stock, 2015). The histidine kinase PhoR does not sense the availability of  $PO_4^{3-}$  itself, but monitors transport activity of the high affinity  $PO_4^{3-}$  transporter PstCAB via PhoU, which interacts with PstB and PhoR and thereby probably modulates PhoR activity (Gardner *et al.*, 2014). In collaboration with the group of Karlheinz Altendorf (Universität Osnabrück) we identified cross-talk regulation between the KdpD/KdpE and PhoR/PhoB two-component systems in *E. coli*, which couples  $K^+$  and  $PO_4^{3-}$  homeostasis and might be essential to balance the ratio of positively and negatively charged ions within the cell. Experiments in chapter 2.3.1-2.3.3 were performed by Vera Laermann (Universität Osnabrück), genome sequencing and analysis was done by Andreas Brachmann (Ludwig-Maximilians Universität München) and Halina Tegetmeyer (Universität Bielefeld). Experiments presented in chapter 2.3.4-2.3.8 were performed by Hannah Schramke.

### 2.3.1 *E. coli* requires the KdpFABC system to grow under $K^+$ limitation

In order to determine the role of the histidine kinase KdpD for  $K^+$  dependent growth we deleted *kdpD* in the *E. coli* strain LB2240, which additionally has deletions in the *trk* and *kup* genes coding for the two constitutively expressed  $K^+$  transporters. This strain still harbours a functional *kdpFABC* operon, whose transcription is dependent on the KdpD/KdpE two-component system. We tested growth of the *kdpD* deletion strain (LB2240 $\Delta$ *kdpD*) in  $K^+$  limited (0.1 mM  $K^+$ ) and  $K^+$  rich (115 mM  $K^+$ ) medium. In comparison we used the strains LB2240 (the parental strain), LB2240 $\Delta$ *kdpD*/pBD5-3 complemented by a plasmid-encoded *kdpD* and TKV2209 (a strain that has an additional deletion in *kdpE*). All strains were able to grow in  $K^+$  rich (115 mM  $K^+$ ) media (Figure 2.3-1A). Under these conditions unspecific  $K^+$ -uptake is

## Results

sufficient for growth and does not require any specific transporters (Laermann *et al.*, 2013). When these strains were exposed to  $K^+$ -limiting growth conditions (0.1 mM  $K^+$ ) only the two strains carrying either chromosomal (LB2240) and plasmid-encoded *kdpD* (LB2240 $\Delta$ *kdpD*/pBD5-3) were able to grow (Figure 2.3-1B). Under these conditions strain TKV2209 lacking the *kdpD* and *kdpE* genes was unable to grow. Importantly, strain LB2240 $\Delta$ *kdpD* was characterised by a long lag phase, but started to grow again after 22 hours and reached the same optical density as the *kdpD*<sup>+</sup> strains thereafter (Figure 2.3-1B).

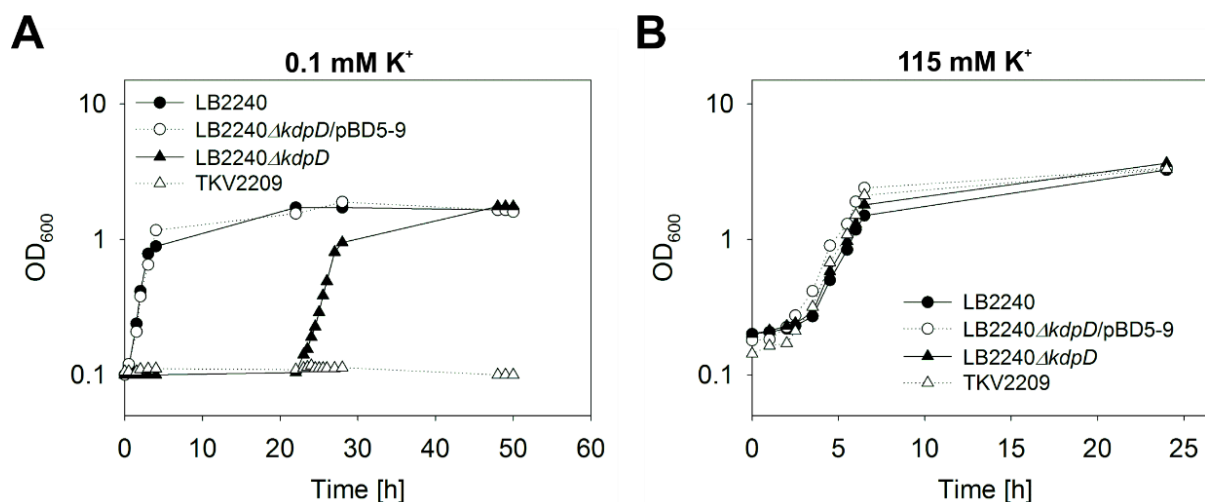


**Figure 2.3-1: Growth curves of different *kdp*<sup>+/-</sup> strains.** LB2240 (*kdpD*<sup>+</sup>), LB2240 $\Delta$ *kdpD*/pBD5-9 (*kdpD*<sup>-</sup>, complemented with plasmid-encoded *kdpD*), LB2240 $\Delta$ *kdpD* and TKV2209 (*kdpD*<sup>-</sup>, *kdpE*<sup>-</sup>) were cultivated in minimal medium containing different  $K^+$  concentrations. (A) Growth curves under  $K^+$  limitation (0.1 mM  $K^+$ ). Cells were cultivated in medium containing 115 mM  $K^+$ , washed with medium without  $K^+$  and inoculated in 0.1 mM  $K^+$  medium to an optical density (OD<sub>600</sub>) of 0.1. Growth was monitored for 52 hours. (B) Growth curves in  $K^+$  rich medium (115 mM  $K^+$ ). Cells were cultivated in medium containing 115 mM  $K^+$  and freshly inoculated to an initial OD<sub>600</sub> of 0.1. Growth was monitored for 24 hours. The curves are representative for at least three biological replicates. Growth studies were performed by Vera Laermann.

### 2.3.2 KdpE mediated induction of *kdpFABC* expression rescues the growth arrest in the absence of KdpD

We concluded that KdpE is required to rescue the growth arrest of strain LB2240 $\Delta$ *kdpD* under  $K^+$  limiting growth conditions, as strain TKV2209 carrying an additional *kdpE* deletion could not grow at all. Therefore, in the next experiment we tested whether KdpE can induce *kdpFABC* expression independently of KdpD. As a measure of *kdpFABC* expression *kdpA* transcripts were quantified by qRT-PCR in exponentially growing cells of strain LB2240 $\Delta$ *kdpD* in  $K^+$  rich media and  $K^+$  limited media (Figure 2.3-2A and B). As expected, no *kdpA* transcripts were detectable in cells cultivated in 115 mM  $K^+$  medium (Figure 2.3-2B). Under  $K^+$  limitation we observed a stepwise increase of *kdpA* transcripts after the 22 hours long lag phase (Figure

2.3-2B). These results revealed that KdpE can activate *kdpFABC* expression in the absence of KdpD under exceptional conditions.

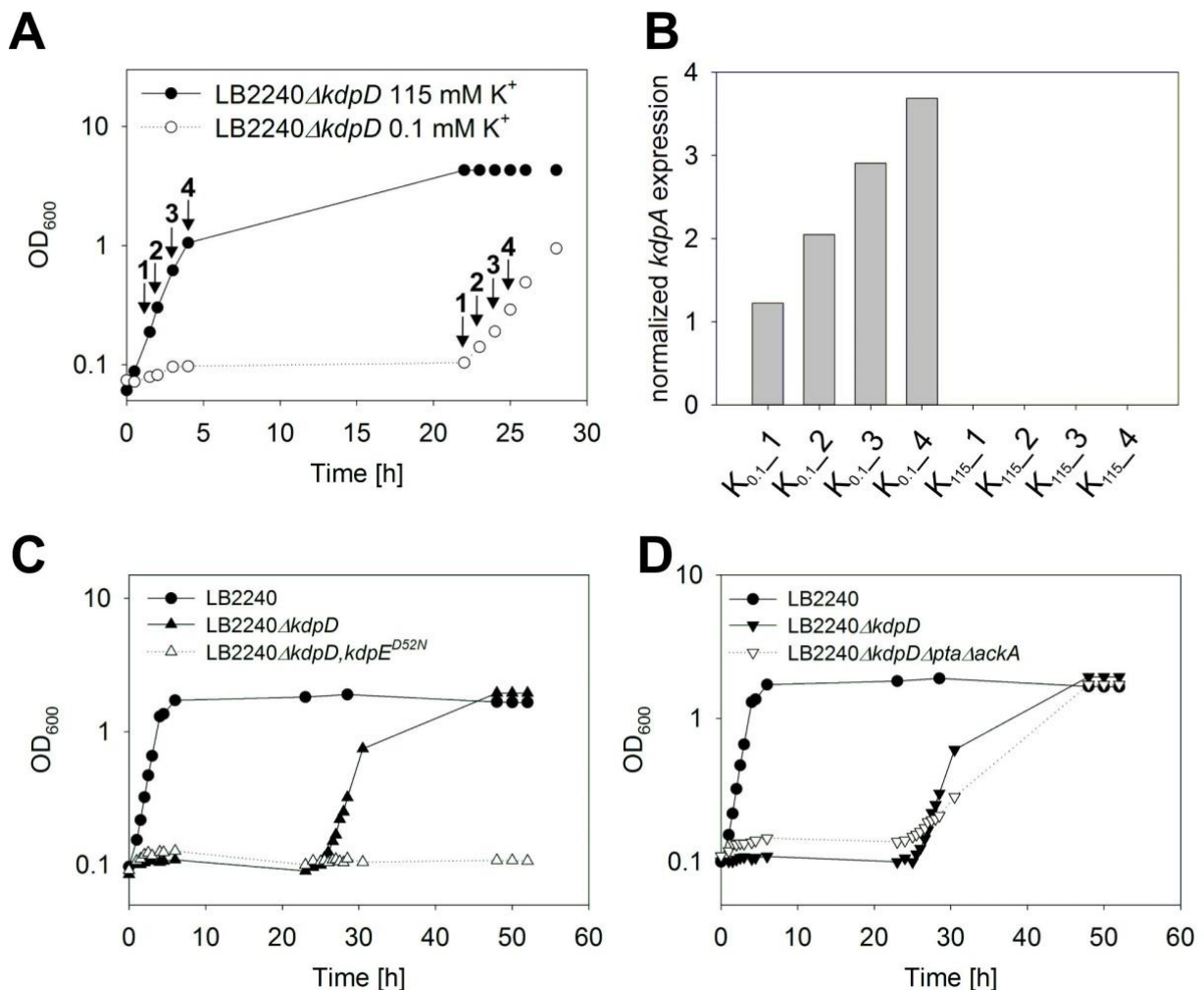


**Figure 2.3-2: Phosphorylation of KdpE leads to induction of *kdpFABC* expression independent of KdpD and acetyl phosphate.** (A) Growth curves under K<sup>+</sup> limitation (0.1 mM K<sup>+</sup>) and K<sup>+</sup> rich medium (115 mM K<sup>+</sup>). Cells were cultivated as described in Figure 2.3-1 and samples were taken at the indicated time points. (B) Samples from the indicated time points (A) were used for q-RT-PCR. RNA was extracted and *kdpA* transcripts were quantified compared to expression of the gap gene. Shown are averages of technical replicates and are representative for biological duplicates. (C) Growth curves of LB2240, LB2240 $\Delta$ *kdpD* and LB2240 $\Delta$ *kdpD*, *kdpE*<sup>D52N</sup> under K<sup>+</sup> limitation (0.1 mM K<sup>+</sup>). Cells were cultivated as described in Figure 2.3-1A. The curves are representative for at least three biological replicates. (D) Growth curves of LB2240, LB2240 $\Delta$ *kdpD* and LB2240 $\Delta$ *kdpD* $\Delta$ *pta* $\Delta$ *ackA*. Cells were cultivated in minimal medium containing 0.1 mM K<sup>+</sup> as described in Figure 2.3-1A and B. The curves show representative results of at least three biological replicates. Experiments were performed by Vera Laermann.

To analyse whether phosphorylation of KdpE is required for activation of *kdpFABC* transcription, the phosphorylation site of KdpE (D52) was inactivated by a chromosomal point mutation causing an amino acid exchange from aspartate to asparagine (D52N). The resulting strain LB2240 $\Delta$ *kdpD*, *kdpE*<sup>D52N</sup> was unable to recover growth arrest within 50 hours, whereas the strain LB2240 $\Delta$ *kdpD* – as described above – started growing again after 22 hours (Figure

2.3-2C). Hence, phosphorylation of KdpE is essential for growth recovery under  $K^+$  limitation in the absence of KdpD.

We then addressed the question, how KdpE can be phosphorylated in the absence of its cognate histidine kinase KdpD. It is known that acetyl phosphate is a phosphodonor for KdpE *in vitro* (Heermann *et al.*, 2003a). In *E. coli* acetyl phosphate is produced as an intermediate of the central metabolism either from the precursors acetyl-CoA and inorganic phosphate by the phosphotransacetylase Pta or from ATP and acetate by the acetate kinase AckA. In order to test if acetyl phosphate is the phosphodonor for KdpE *in vivo* the genes *pta* and *ackA* were deleted in LB2240 $\Delta kdpD$  resulting in strain LB2240 $\Delta kdpD\Delta pta\Delta ackA$ . If acetyl phosphate is responsible for KdpE phosphorylation, this strain should not be able to recover growth arrest under  $K^+$  limitation. However, we observed that this strain likewise started growing after an initial lag phase under  $K^+$  limitation (Figure 2.3-2D). We found that the growth rate of strain LB2240 $\Delta kdpD\Delta pta\Delta ackA$  was lower, however similar effects were observed when this strain was grown in  $K^+$  rich medium (data not shown). Therefore, we concluded that acetyl phosphate does not act as a phosphodonor for KdpE *in vivo* under these conditions.

### 2.3.3 Only a very small subpopulation is able to survive under $K^+$ limitation

Next we were interested to know whether the whole population can survive growth arrest or if only a subpopulation is able to induce *kdpFABC* expression in the absence of KdpD after a certain time. LB2240 $\Delta kdpD$  was cultivated as described before in medium containing 115 mM  $K^+$ . Afterwards about  $10^8$  cells were spread on agar plates containing 0.1 mM  $K^+$  and incubated at 37°C. In average five colonies grew from  $10^8$  cells on the  $K^+$  limited plates, whereas cells of strain LB2240 grew as a bacterial lawn (data not shown). This result provided the first hint that suppressor mutants were generated within the long lag phase of strain LB2240 $\Delta kdpD$ . Indeed, these single clones (from now on called LB2240 $\Delta kdpD^*$ ) were able to grow under  $K^+$  limitation without an extended lag phase (Figure 2.3-3).

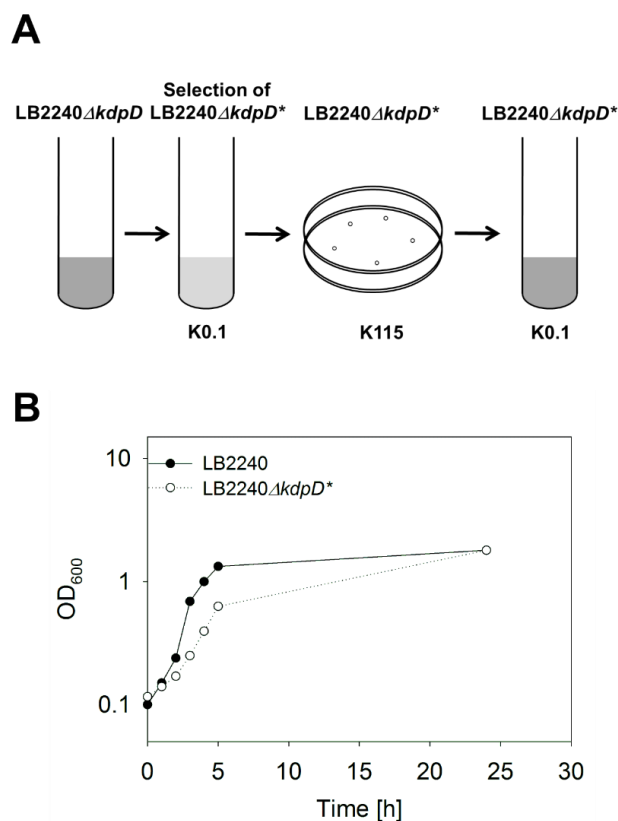


**Figure 2.3-3: Isolation and growth of LB2240 $\Delta kdpD^*$  under K<sup>+</sup> limitation.** (A) Schematics for the isolation procedure of LB2240 $\Delta kdpD^*$ . LB2240 $\Delta kdpD$  was cultivated in medium containing 115 mM K<sup>+</sup>, inoculated in K<sup>+</sup> limited medium (0.1 mM K<sup>+</sup>) and grown until stationary phase. Afterwards dilutions were poured on plates containing 115 mM K<sup>+</sup>. A single clone was inoculated in liquid K<sup>+</sup> limited medium and growth was monitored over time compared to the wild-type LB2240 (B). Growth curves were performed by Vera Laermann

### 2.3.4 Mutations in the phosphate transporter *pst* result in *kdpFABC* expression

As only a tiny proportion of the LB2240 $\Delta kdpD$  population could recover growth under K<sup>+</sup>-limitation and the isolated clones LB2240 $\Delta kdpD^*$  grew in 0.1 mM K<sup>+</sup> medium without a 22 hour lag phase, our next aim was to deduce the suppressor mutation that allows *kdpFABC* expression in the absence of KdpD. On this account we performed whole genome sequencing of LB2240 $\Delta kdpD^*$ . By aligning the sequence to the reference genome LB2240 $\Delta kdpD$  we found a mutation in the *pstC* gene resulting in a shift of the open reading frame. In two other individual clones we found mutations in the *pstB* gene, resulting in a stop codon and a shift in the open reading frame, respectively. *pstC* and *pstB* are part of the *pstSCAB* operon, which codes for the high affinity phosphate transporter PstCAB and the periplasmic phosphate binding protein PstS (Amemura *et al.*, 1985, Rees *et al.*, 2009, Webb *et al.*, 1992). The PstCAB transporter is known to act as a phosphate sensor for the two-component system PhoR/PhoB and forms a signalling complex together with the PhoU protein (Gardner *et al.*, 2014). A deletion in *phoU* or one of the transporter genes *pstCAB* shifts the histidine kinase PhoR in the constitutive kinase “ON” state.

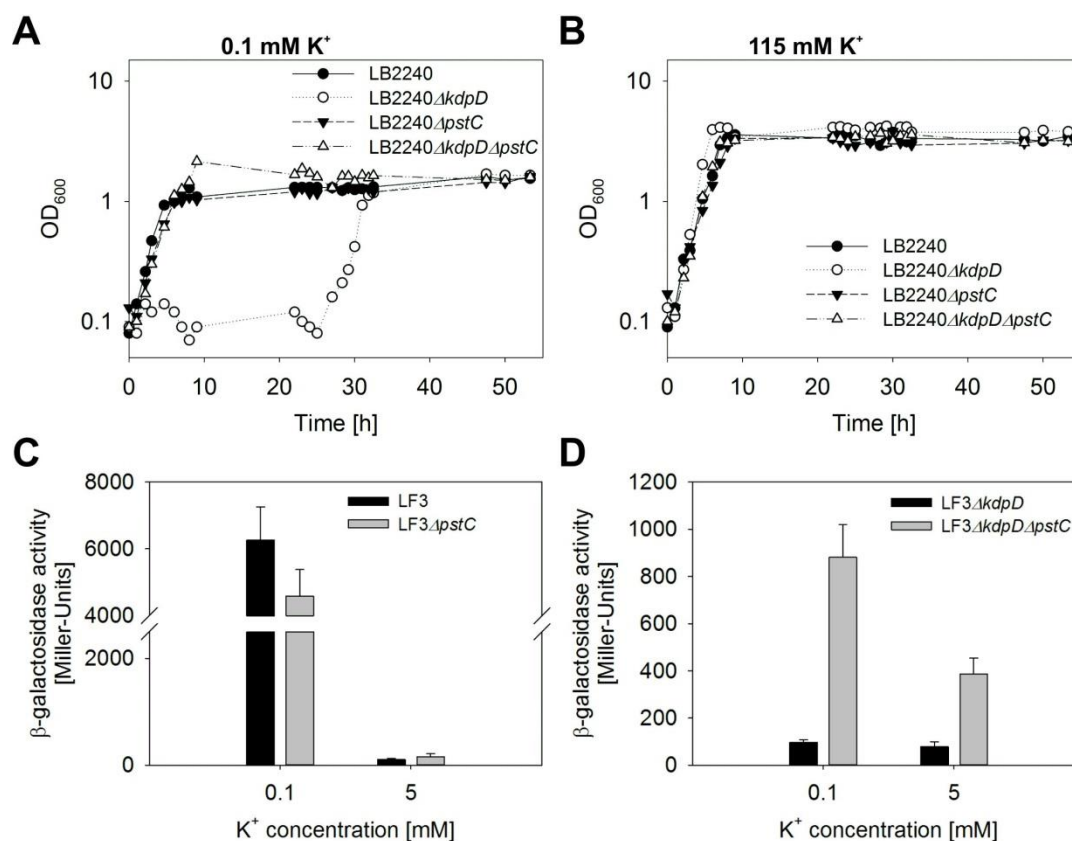


**Figure 2.3-4: Deletion of *pstC* rescues growth defects under K<sup>+</sup>-limitation by inducing *kdpFABC* expression.** (A and B) Growth curves of strains LB2240, LB2240Δ*kdpD*, LB2240Δ*pstC* and LB2240Δ*kdpD*Δ*pstC* under K<sup>+</sup> limitation (A) and K<sup>+</sup> rich medium (B). Cells were cultivated as described in Figure 2.3-1 and growth was monitored for 52 hours. (C and D) The β-galactosidase activities of the reporter strains LF3, LF3Δ*pstC* (C) and the reporter strain LF3 LF3Δ*kdpD*, LF3Δ*kdpD*Δ*pstC* (D). All strains carry a chromosomal P<sub>*kdpFABC*</sub>::*lacZ* fusion and β-galactosidase activities were determined after cultivation of cells in minimal medium at the indicated K<sup>+</sup> concentrations. Shown is the average and standard deviation of at least three biological replicates.

In order to verify the sequencing results we deleted *pstC* in LB2240Δ*kdpD* and tested growth of the resulting mutant under K<sup>+</sup>-limitation (Figure 2.3-4A). Indeed we observed that the strain carrying the double deletion in *kdpD* and *pstC* (LB2240Δ*kdpD*Δ*pstC*) could grow under K<sup>+</sup> limitation directly after inoculation without any lag phase, whereas the single *kdpD* deletion led to a growth arrest as described above (Figure 2.3-4A, Figure 2.3-1A). A single deletion of *pstC* (LB2240Δ*pstC*) did not significantly influence growth compared to the parental strain LB2240. All strains grew well in K<sup>+</sup> rich medium (Figure 2.3-4B).

To further confirm that a deletion in *pstC* would result in *kdpFABC* expression we performed reporter gene assays with the strain LF3, in which the *kdpFABC* promoter is fused to the *lacZ* gene (Fried *et al.*, 2012). This strain harbours functional *kdpFABC* and *kdpDE* operons as well as the two constitutively expressed *trk* and *kup* K<sup>+</sup> transporter genes. In this strain *kdpFABC* expression – measured indirectly via β-galactosidase activity – is induced if the extracellular K<sup>+</sup> concentration falls below 5 mM (Figure 2.3-4C) (Fried *et al.*, 2012). A deletion in *pstC* did

not affect the *kdpFABC* expression pattern after cultivation at the tested  $K^+$  concentrations (0.1 and 5 mM  $K^+$ ; Figure 2.3-4C).

However, in a reporter strain carrying an additional deletion in the *kdpD* gene (LF3 $\Delta$ *kdpD* $\Delta$ *pstC*) *kdpFABC* expression was induced both after cultivation in medium containing 0.1 mM  $K^+$  and 5 mM  $K^+$  (Figure 2.3-4D). In the single *kdpD* deletion mutant (LF3 $\Delta$ *kdpD*) *kdpFABC* expression was not induced under the tested conditions (Figure 2.3-4D). Taken together, these results show that a mutation or deletion in one of the *pst* transporter components rescues growth defects under  $K^+$  limitation by inducing *kdpFABC* expression in the absence of KdpD.

### 2.3.5 The histidine kinase PhoR is responsible for *kdpFABC* expression in the absence of KdpD

The histidine kinase PhoR perceives its stimulus via interaction with the phosphate transporter PstCAB and the negative regulator PhoU (Gardner *et al.*, 2014). As a deletion in *phoU* or *pstCAB* shifts PhoR in a kinase “ON” state we considered PhoR as phosphodonor for KdpE in the absence of KdpD. To test this possibility, we deleted *phoR* in the reporter strain LF3 lacking *kdpD* and *pstC* (resulting in strain LF3 $\Delta$ *kdpD* $\Delta$ *pstC* $\Delta$ *phoR*) and quantified *kdpFABC* expression via  $\beta$ -galactosidase activity after cultivating the cells in minimal medium containing different  $K^+$  concentrations. As expected *kdpFABC* could not be induced in the triple deletion mutant underlining the role of PhoR as phosphodonor for KdpE (Figure 2.3-5A).

Subsequently, we tested the influence of the accessory protein PhoU on the Kdp system. The reporter strain LF3 $\Delta$ *kdpD* carrying a deletion in *phoU* (LF3 $\Delta$ *kdpD* $\Delta$ *phoU*) showed high induction of *kdpFABC* expression independent of the extracellular  $K^+$  concentration. An additional deletion in *phoR* (strain LF3 $\Delta$ *kdpD* $\Delta$ *phoU* $\Delta$ *phoR*) prevented induction (Figure 2.3-5A), strongly supporting the role of PhoR for KdpE phosphorylation in the absence of KdpD. In the presence of KdpD we observed an increase in *kdpFABC* expression under  $K^+$  limitation in the *phoR* and *phoU* mutant strains (LF3 $\Delta$ *phoR* and LF3 $\Delta$ *phoU*) compared to the parental reporter strain LF3 and the *pst* deletion mutant (LF3 $\Delta$ *pstC*). However there was no *kdpFABC* expression at 5 mM  $K^+$  (Figure 2.3-6), probably due to high KdpD phosphatase activity under this condition. Consequently, a *pstC* deletion does not affect *kdpFABC* expression at high  $K^+$  concentrations.

## Results

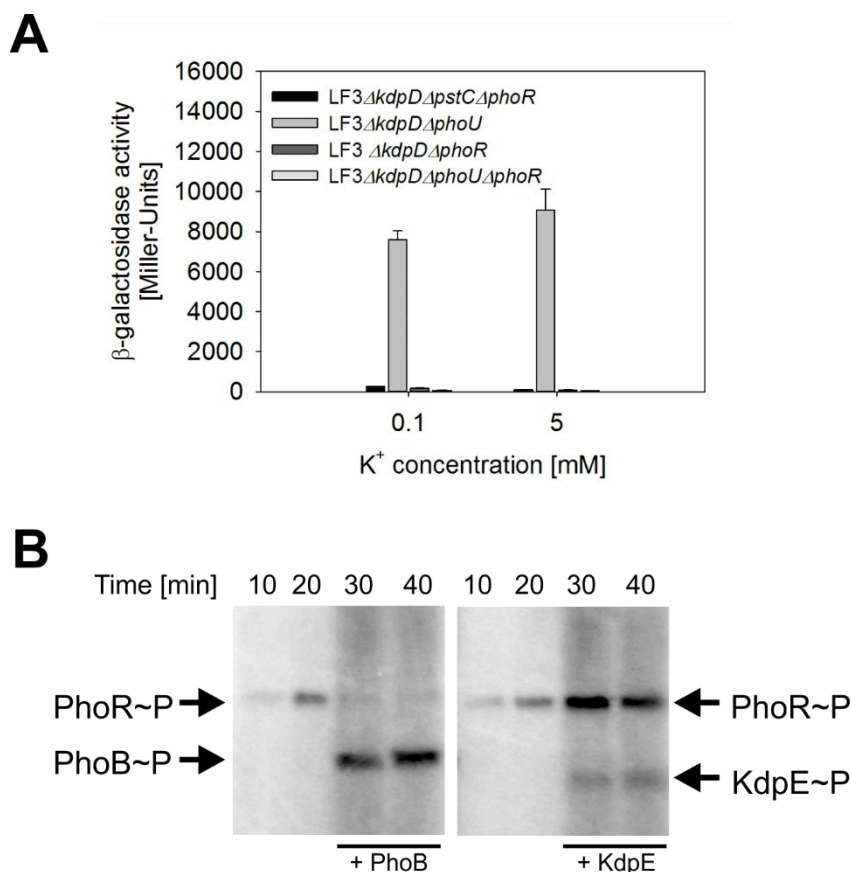


**Figure 2.3-5: The histidine kinase PhoR induces *kdpFABC* expression in the absence of KdpD.** (A) The  $\beta$ -galactosidase activities of the reporter strains LF3 $\Delta$ kdpD $\Delta$ pstC $\Delta$ phoR, LF3 $\Delta$ kdpD $\Delta$ phoU, LF3 $\Delta$ kdpD $\Delta$ phoR and LF3 $\Delta$ kdpD $\Delta$ phoU $\Delta$ phoR. All strains carry a chromosomal  $P_{kdpFABC}::lacZ$  fusion and  $\beta$ -galactosidase activities were determined after cultivation of cells in minimal medium at the indicated K<sup>+</sup> concentrations. Shown is the average and standard deviation of at least three biological replicates. (B) *In vitro* autophosphorylation of PhoR with [ $\gamma$ -<sup>32</sup>P]ATP. After 20.5 min, the partner and non-partner response regulator PhoB and KdpE, respectively, were added and phosphotransfer was monitored. Phosphorylated proteins were separated by SDS-PAGE and gels were exposed to a phosphoscreen. Shown are representative autoradiographs of two independent experiments.

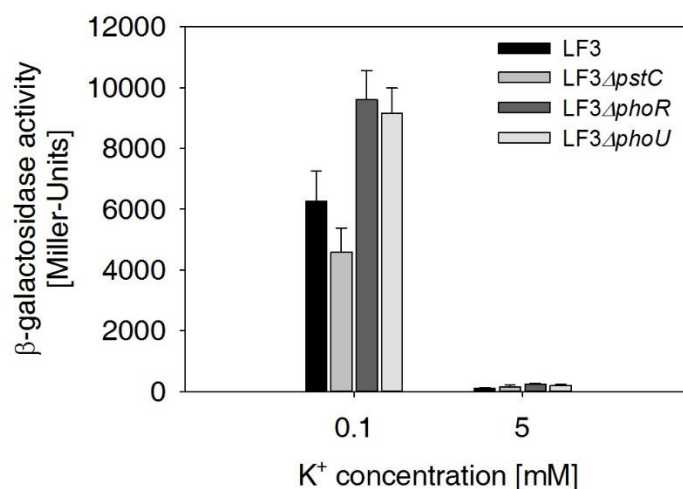


**Figure 2.3-6:  $\beta$ -galactosidase activities of the reporter strains LF3, LF3 $\Delta$ pstC, LF3 $\Delta$ phoR and LF3 $\Delta$ phoU.** All strains carry a chromosomal  $P_{kdpFABC}::lacZ$  fusion and  $\beta$ -galactosidase activities were determined after cultivation of cells in minimal medium at the indicated K<sup>+</sup> concentrations. Shown is the average and standard deviation of at least three biological replicates.

To further confirm that PhoR acts as phosphodonor for KdpE we tested *in vitro* phosphotransfer from PhoR to the partner response regulator PhoB and the non-partner response regulator KdpE. We first tested autophosphorylation of a truncated PhoR lacking the transmembrane domains (Lüttmann *et al.*, 2012) by adding radiolabelled ATP ( $[\gamma\text{-}^{32}\text{P}]\text{ATP}$ ). After 20.5 minutes the response regulators PhoB and KdpE, respectively were added and phosphotransfer was monitored over time. We found that PhoR can phosphorylate its partner response regulator PhoB and – to a lesser extent – its non-partner response regulator KdpE (Figure 2.3-5B). Taken together we conclude that PhoR is responsible for KdpE phosphorylation in the absence of KdpD.

### **2.3.6 BACTH experiments indicate interactions between the KdpDE and PhoRB two-component systems**

Next we were interested whether the components of the two signalling systems directly interact by using the bacterial adenylate cyclase two-hybrid system (BACTH). The *Saccharomyces cerevisiae* yeast leucine zipper fusion constructs zip-T18 and T25-zip was used as a positive control and the T18 and T25 proteins alone as a negative control, respectively. In the first screen we tested interactions on LB plates as well as on plates with a defined Tris-maleic acid (TMA) minimal medium (Weiden *et al.*, 1967) supplemented with different  $\text{K}^+$  and  $\text{PO}_4^{3-}$  concentrations (Figure 2.3-7A). The hybrid protein T18-KdpD showed strong interactions with the cognate response regulator hybrid protein T25-KdpE, T25-PhoR and T25-PhoU on LB plates (Figure 2.3-7A upper column). There was no detectable interaction between T18-KdpD and the non-partner response regulator hybrid protein T25-PhoB. For the hybrid protein T18-PhoR we observed interactions with T25-PhoU, but not with the partner and non-partner response regulators T25-PhoB and T25-KdpE, respectively. Furthermore we found interactions between T25-PhoU and PhoB-T18, but not between PhoU-T18 and T25-KdpE. To verify these results in a quantitative way we performed  $\beta$ -galactosidase assays after cultivating the cells in liquid medium (Figure 2.3-7B). Again we measured high  $\beta$ -galactosidase activities for cells producing T18-KdpD+T25-KdpE and T18-KdpD+T25-PhoR, respectively and moderate to low activities for cells producing T18-KdpD+T25-PhoU and T18-PhoR+T25-PhoU. For all other combinations we could not detect any interactions – in contrast to the cells cultivated on plates, where we found low interactions between PhoB-T18 and T25-PhoU (Figure 2.3-7A and B).

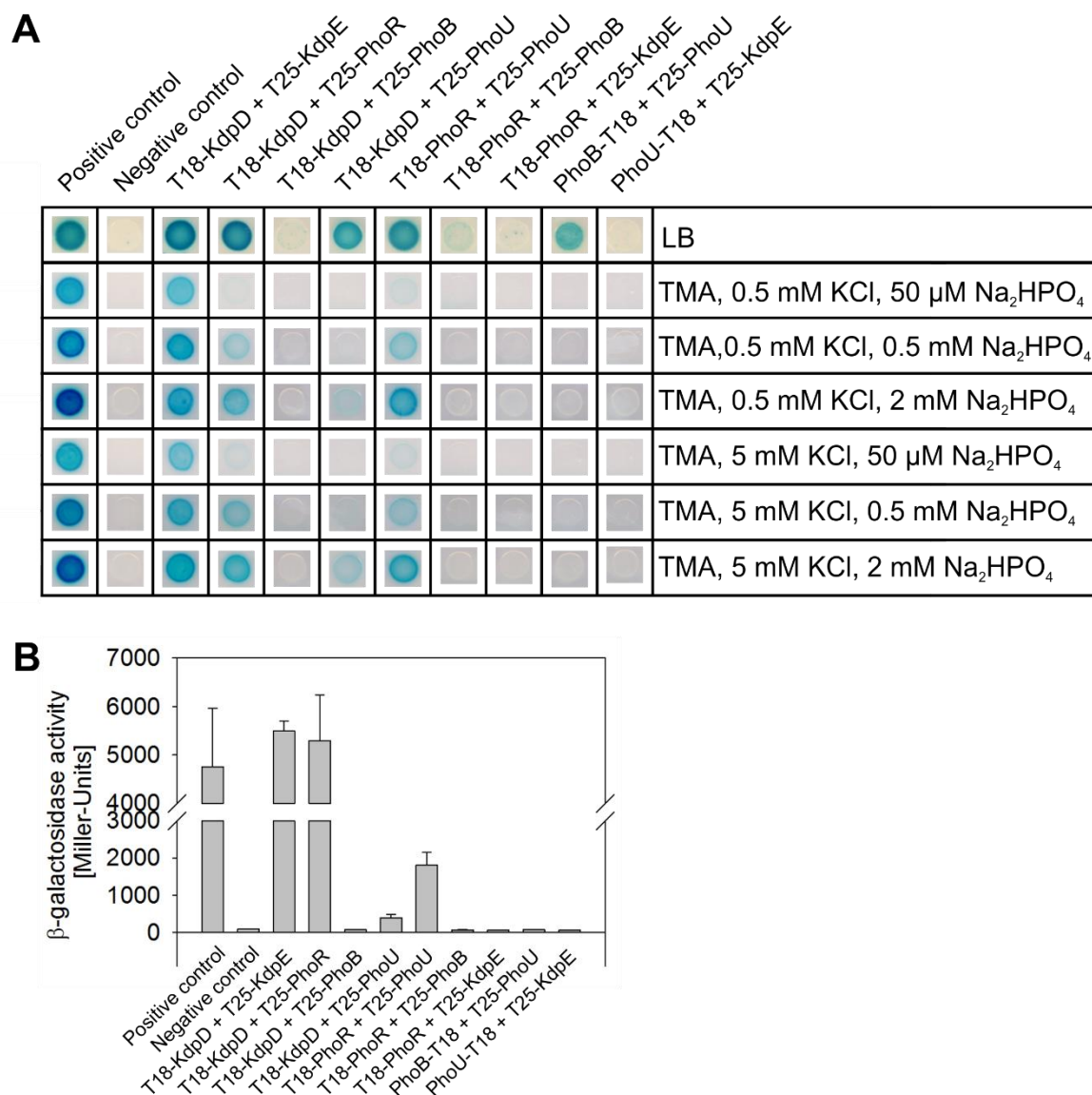


**Figure 2.3-7: Bacterial adenylate cyclase two-hybrid experiments indicate interactions between the KdpD/KdpE and PhoR/PhoB two-component systems.** Fragments T18 and T25 of *Bordetella pertussis* CyaA were fused to proteins of interest as indicated. The fusions to yeast leucine zipper fragments were used as a positive control and the fragments T18 and T25 alone as negative control respectively. *E. coli* BTH101 was cotransformed with plasmid pairs encoding the indicated hybrid proteins and cultivated under aerobic conditions. **(A)** Cells were cultivated in LB medium overnight, washed two times with TMA medium without KCl and  $\text{Na}_2\text{HPO}_4$  and subsequently dropped on plates containing LB and TMA medium containing different  $\text{K}^+$  and  $\text{PO}_4^{3-}$  concentrations as indicated. Plates were incubated at 25°C for 72 hours. All plates were supplemented with ampicillin, kanamycin, IPTG and X-Gal as described in experimental procedures. **(B)** Cells were cultivated in LB medium supplemented with ampicillin, kanamycin, IPTG and X-Gal as described in experimental procedures at 25°C for 48 hours. The activity of the reporter enzyme  $\beta$ -galactosidase was determined and served as a measure of the interaction strength. Shown is the average and standard deviation of at least three biological replicates.

According to our previous results we would have expected interactions between T18-PhoR and T25-KdpE, because we assume that PhoR acts as phosphodonor for KdpE. As we did not detect any interactions, we speculated that these two proteins only interact with each other under special conditions. For this reason we now used plates with a defined Tris-maleic acid (TMA)

minimal medium (Weiden *et al.*, 1967) containing different  $K^+$  and  $PO_4^{3-}$  concentrations. However we found similar patterns as for the LB plates (Figure 2.3-7A). Under extreme  $PO_4^{3-}$  starvation (50  $\mu$ M  $Na_2HPO_4$ ) we observed lower interactions, which is probably due to decreased growth rates and might not display  $K^+$  or  $PO_4^{3-}$  specific effects.

In summary, we found interactions for KdpD with PhoR, KdpD with PhoU and PhoR with PhoU, respectively. There was only a low interaction between PhoR with its partner response regulator PhoB and no interaction with the non-partner response regulator KdpE on LB plates. It cannot be ruled out that in the hybrid protein the T18 fragment disturbs the interaction surface for the response regulator.

### 2.3.7 Phosphate starvation enhances *kdpFABC* expression

Now we were curious if we could find conditions, in which cross-talk between these two systems might be of physiological importance. Again we used the defined TMA medium supplemented with different  $K^+$  and  $PO_4^{3-}$  concentrations to perform reporter gene assay with the strain LF3. As shown before there is no induction of *kdpFABC* expression in  $K^+$  rich (5 mM) medium (Figure 2.3-8A). Under moderate  $K^+$  limitation (0.5 mM  $K^+$ ) *kdpFABC* expression is induced via KdpD. Importantly, we found a threefold higher induction when cells were exposed to phosphate limitation (Figure 2.3-8A).

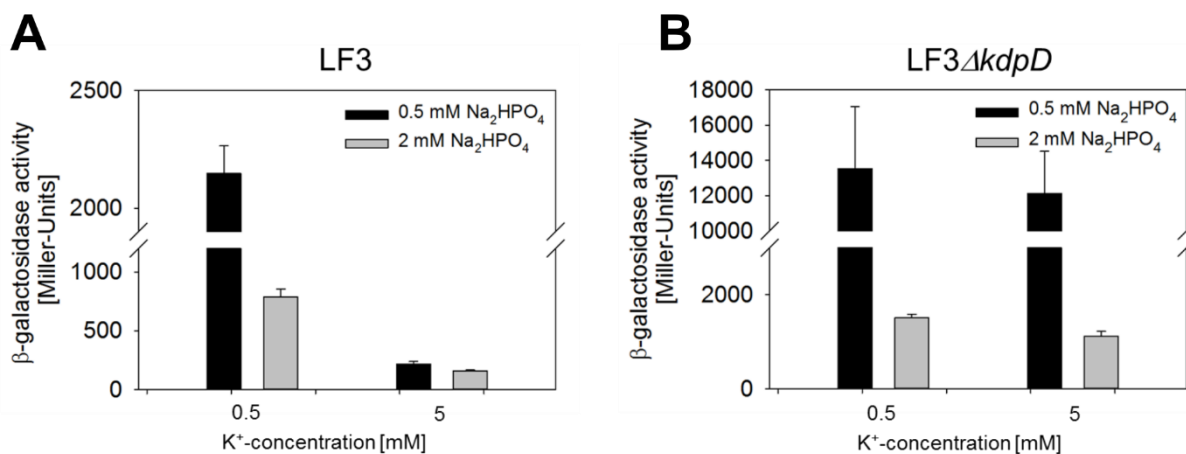


**Figure 2.3-8: Phosphate starvation induces *kdpFABC* expression.** The  $\beta$ -galactosidase activities of the reporter strains LF3 (A) and LF3 $\Delta$ kdpD (B). All strains carry a chromosomal  $P_{kdpFABC}::lacZ$  fusion and  $\beta$ -galactosidase activities were determined after cultivation of cells in TMA minimal medium at the indicated  $K^+$  and  $PO_4^{3-}$  concentrations. Shown is the average and standard deviation of at least three biological replicates.

The *kdpD* deletion mutant (LF3 $\Delta$ kdpD) showed high induction of *kdpFABC* expression, which was independent of the  $K^+$  concentration and gradually increased depending on  $PO_4^{3-}$  starvation level (Figure 2.3-8B). Taken together we conclude that *kdpFABC* expression is stimulated under  $PO_4^{3-}$  starvation and that cross-talk between the KdpD/KdpE and PhoR/PhoB two-component systems is of physiological relevance under certain conditions.

### 2.3.8 K<sup>+</sup> limitation enhances *pstS* expression

So far we revealed cross-regulation from the histidine kinase PhoR to the non-partner response regulator KdpE, if both PO<sub>4</sub><sup>3-</sup> and K<sup>+</sup> are limited. Therefore we were now interested if cross-talk also occurs in the other direction, i.e. from the histidine kinase KdpD to the non-partner response regulator PhoB. PhoB regulates expression of the pho regulon comprising more than 30 target genes, amongst others the *pstSCAB* operon. To analyse PhoB activity we used *E. coli* MG1655 with a plasmid based reporter system, in which the *pstS* promoter is fused to *mcherry*. As above we used the defined TMA medium containing different K<sup>+</sup> and PO<sub>4</sub><sup>3-</sup> concentrations and monitored bacterial growth and fluorescence over time. Promoter activity was calculated by dividing the change in fluorescence by the optical density (Bren *et al.*, 2013).

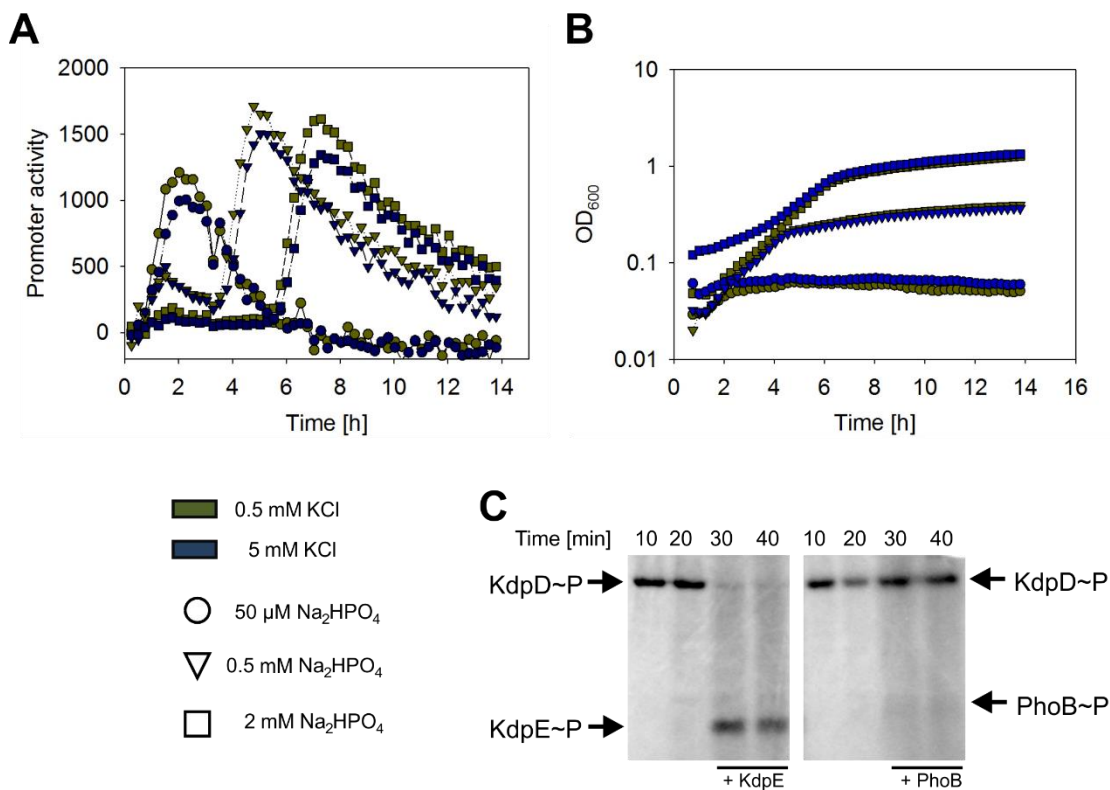


**Figure 2.3-9: K<sup>+</sup> limitation enhances *pstS* expression.** (A) *pstS* promoter activity in *E. coli* MG1655 cells carrying plasmids, in which *mcherry* expression is under the control of the *pstS* promoter. As shown in the legend below green symbols display K<sup>+</sup> limited (0.5 mM) and blue symbols K<sup>+</sup> rich (5 mM) medium. Circles, triangles and squares depict the indicated Na<sub>2</sub>HPO<sub>4</sub> concentration. (B) Corresponding growth curves of strains cultivated in medium with different K<sup>+</sup> and PO<sub>4</sub><sup>3-</sup> concentrations as indicated (A). (C) *In vitro* autophosphorylation of PhoR with [<sup>32</sup>P]ATP. After 20.5 min, the partner and non-partner response regulator PhoB and KdpE, respectively, were added and phosphotransfer was monitored. Phosphorylated proteins were separated by SDS-PAGE and gels were exposed to a phosphoscreen. Shown are representative autoradiographs of two independent experiments.

We observed an early activation of the *pstS* promoter under extreme PO<sub>4</sub><sup>3-</sup> limitation (50 μM Na<sub>2</sub>HPO<sub>4</sub>) and a delayed activation under moderate PO<sub>4</sub><sup>3-</sup> limitation (0.5 mM and 2 mM Na<sub>2</sub>HPO<sub>4</sub>) (Figure 2.3-9A). However *pstS* promoter activity was additionally slightly increased, if K<sup>+</sup> was limited in the medium, indicating cross-phosphorylation from KdpD to

## Results

PhoB (Figure 2.3-9A, green symbols). Bacterial growth was clearly determined by the  $\text{PO}_4^{3-}$  availability, but did not depend on the  $\text{K}^+$  concentration (Figure 2.3-9B). To confirm cross-regulation from KdpD to PhoB we again tested autophosphorylation and phosphotransfer *in vitro*. We observed phosphotransfer to the partner response regulator KdpE and also to the non-partner response regulator PhoB (Figure 2.3-9C), even though it was not that distinct as from PhoR to KdpE (Figure 2.3-5B). To sum up, we identified that cross-phosphorylation between the KdpD/KdpE and PhoR/PhoB two-component systems occurs in both directions *in vitro* and is of physiological importance *in vivo* if both stimuli are limited.

## 2.4 Binding of cyclic Di-AMP to the *Staphylococcus aureus* sensor kinase KdpD occurs via the universal stress protein domain and downregulates the expression of the Kdp potassium transporter

The KdpD/KdpE two-component system is widespread among bacteria and well characterised in *E. coli*. However, the function of this system in other organism is less clear. Previous work identified the *S. aureus* histidine kinase KdpD (from here on out referred to as KdpD<sup>Sa</sup>) as a cyclic diadenosine monophosphate (c-di-AMP) binding protein (Corrigan *et al.*, 2013). c-di-AMP is a recently discovered signalling nucleotide commonly found in Gram-positive bacteria (Corrigan & Gründling, 2013, Römling, 2008). In previous work from the Gründling lab it was reported that depending on the growth phase, *S. aureus* has an intracellular c-di-AMP concentration of 2 to 8  $\mu$ M (Corrigan *et al.*, 2011, Corrigan *et al.*, 2015). A *S. aureus gdpP* mutant strain lacking the c-di-AMP phosphodiesterase has constitutively high levels of c-di-AMP of around 50  $\mu$ M (Corrigan *et al.*, 2011, Corrigan *et al.*, 2015). The *gdpP* mutant is also 20 % reduced in size when compared to the wild-type strain and has an increased resistance to beta-lactam antibiotics (Corrigan *et al.*, 2011). The cyclase DacA and hence c-di-AMP production appears to be essential for the growth of *S. aureus* under standard laboratory conditions, as a *dacA* mutant strain could not be obtained (Corrigan *et al.*, 2015).

In collaboration with the group of Prof. Angelika Gründling from the Imperial College London we have further characterized the role of c-di-AMP in K<sup>+</sup> homeostasis in *S. aureus*. More specifically, the binding and impact of c-di-AMP on the sensor kinase KdpD was investigated. Experiments presented in chapter 2.4.1-2.4.3 were performed by Joana Moscoso, Yong Zhang, Tommaso Tosi and Amina Dehbi (Gründling lab). Experiments in chapter 2.4.4 were performed by Hannah Schranke and Joana Moscoso. Text and Figures presented in chapter 2.4.1-2.4.3 are already published (Moscoso *et al.*, 2015) and were partially modified.

### 2.4.1 c-di-AMP binds to the USP domain of *Staphylococcus aureus* KdpD

Similar to the KdpD protein from *E. coli* (KdpD<sup>Ec</sup>), KdpD<sup>Sa</sup> has a complex modular architecture with an N-terminal cytoplasmic region containing a KdpD domain and a USP domain, which is followed by four transmembrane helices and a C-terminal cytoplasmic region that harbours a putative GAF domain and a histidine kinase domain (Figure 2.4-1A). To investigate which domain of KdpD<sup>Sa</sup> interacts with c-di-AMP, full-length KdpD as well as truncated variants comprising only the N-terminal domain, the C-terminal domain or the KdpD and USP domains were produced in *E. coli*. While no clear overexpression was observed for the full-length membrane embedded KdpD<sup>Sa</sup> protein, all other variants were overproduced in *E. coli* and

## Results

protein bands of the expected size were clearly visible in whole cell lysates (Figure 2.4-1B). The ability of the truncated variants to bind to c-di-AMP was assessed by the differential radial capillary action of ligand assay (DRaCALA) (Corrigan *et al.*, 2013, Roelofs *et al.*, 2011) using whole cell lysates and radiolabelled c-di-AMP. As expected, full-length KdpD<sup>Sa</sup> interacted with c-di-AMP (Figure 2.4-1C). No interaction was observed between c-di-AMP and the C-terminal domain, but the N-terminal part of the protein and more specifically the USP domain retained the ability to bind c-di-AMP (Figure 2.4-1C).

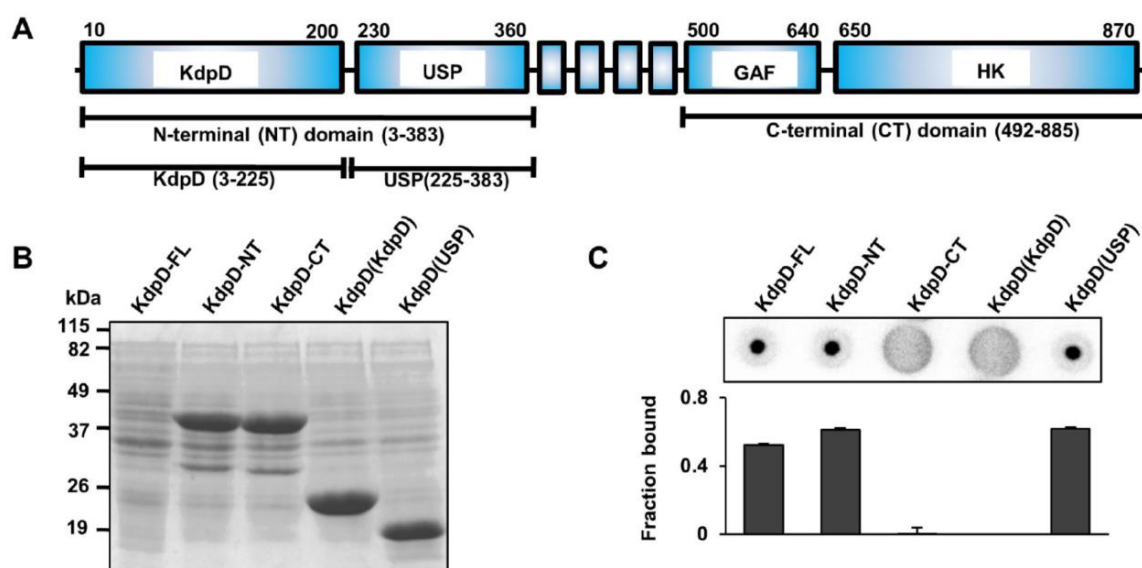


**Figure 2.4-1: c-di-AMP binds the USP domain of KdpD<sup>Sa</sup>.** (A) Schematic representation of the *S. aureus* KdpD protein and the truncated KdpD<sup>Sa</sup> variants generated in this study. The sensor histidine kinase contains an N-terminal cytoplasmic region with KdpD and universal stress protein (USP) domains, a central four transmembrane helix region, and a C-terminal cytoplasmic region with a GAF and histidine kinase (HK) domain. The different regions are drawn to scale with the amino acid numbers for the *S. aureus* KdpD protein indicated. (B) Coomassie stained gel of *E. coli* lysates overproducing the different KdpD variants. Whole cell lysates were prepared from *E. coli* strains expressing the full length (FL), the N-terminal cytoplasmic domain (NT), the C-terminal cytoplasmic domain (CT), the KdpD domain, or the USP domain of KdpD. Proteins were separated on a 12 % SDS gel and visualized by coomassie staining. Of note, no clear overproduction was observed for the full-length KdpD protein. The sizes of protein bands are indicated on the left and are given in kDa. (C) c-di-AMP binds to the USP domain of KdpD. DRaCALAs were performed using radiolabelled c-di-AMP and the *E. coli* extracts described in panel B. At least three independent experiments were performed. Representative DRaCALA spots are shown and the average fraction bound values and standard deviations from triplicates were determined and plotted as previously described (Corrigan *et al.*, 2013, Roelofs *et al.*, 2011). Experiments were performed by members of the Gründling lab (Imperial College London). The figure was taken from (Moscoso *et al.*, 2015) and was created by Joana Moscoso (Gründling lab, Imperial College London).

To confirm the interaction between c-di-AMP and the USP domain of KdpD<sup>Sa</sup>, the *kdpD<sup>Sa</sup>* DNA fragment coding for the KdpD(USP) domain (amino acids E225 to F383) was cloned into vector pMALX(E) and the recombinant maltose binding protein MBP-KdpD(USP) hybrid protein was purified over an amylose resin followed by size exclusion chromatography. c-di-AMP

interacted with the purified MBP-KdpD(USP) protein with a dissociation constant ( $K_d$ ) of  $2 \pm 0.18 \mu\text{M}$  (Figure 2.4-2A) and the binding was specific as only an excess of unlabelled c-di-AMP but none of the other nucleotides tested was able to compete for binding with radiolabelled c-di-AMP (Figure 2.4-2B). Taken together, these results show that c-di-AMP binds specifically to the USP domain of KdpD<sup>Sa</sup>.

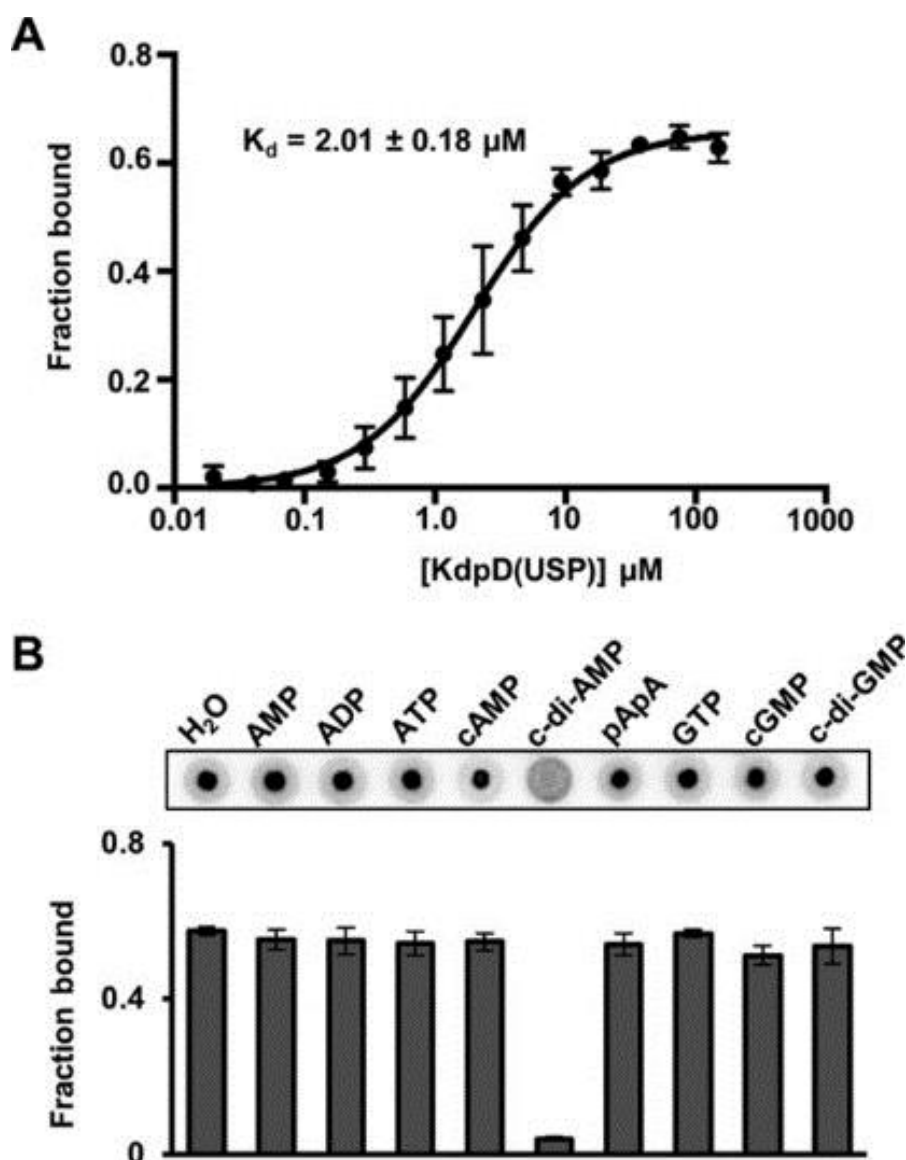


**Figure 2.4-2: c-di-AMP binds specifically and with a  $K_d$  of  $2 \pm 0.18 \mu\text{M}$  to the recombinant *S. aureus* MBP-KdpD(USP) protein.** (A) c-di-AMP binding curve and  $K_d$  determination using the purified MBP-KdpD(USP) hybrid protein. DRaCALAs were performed with radiolabelled c-di-AMP and protein concentrations ranging from 0.02 to 150  $\mu\text{M}$ . The average fraction bound values and standard deviations from three independent experiments were plotted against the protein concentration, the binding curve fitted using a one site – specific binding nonlinear regression and the  $K_d$  value determined as previously described (Corrigan *et al.*, 2013, Roelofs *et al.*, 2011). (B) DRaCALAs were performed with the purified MBP-KdpD(USP) protein, radiolabeled c-di-AMP and an excess (100  $\mu\text{M}$ ) of the indicated cold competitor nucleotide. Two independent experiments were performed. Representative DRaCALA spots are shown and the average fraction bound values and standard deviations from triplicate values are plotted. Experiments were performed by members of the AG Gründling (Imperial College London). The figure was taken from (Moscoso *et al.*, 2015) and was created by Joana Moscoso (Gründling lab, Imperial College London).

### 2.4.2 A conserved SxS-X<sub>20</sub>-FTAxY motif in KdpD<sup>Sa</sup>(USP) is involved in c-di-AMP binding.

To elucidate a potential c-di-AMP binding site in the USP domain of KdpD<sup>Sa</sup>, the USP domain sequences of 470 KdpD<sup>Sa</sup>(USP) homologues and the top 2000 KdpD<sup>Ec</sup>(USP) homologues were aligned separately and subsequently produced a Logo motif. Three regions with conserved motifs were identified in both alignments (Figure 2.4-3). The consensus sequences in regions II and III were similar in the *E. coli* and *S. aureus* KdpD(USP) domain alignments. However, the consensus in region I revealed the presence of a conserved SxS-X<sub>20</sub>-FTAxY motif in KdpD<sup>Sa</sup>(USP) homologues whereas KdpD<sup>Ec</sup>(USP) displayed a conserved RxxxR-X<sub>8</sub>-WxAVY motif. These analysis suggested that the SxS-X<sub>20</sub>-FTAxY motif, spanning amino acids 244 to 271 in KdpD<sup>Sa</sup>, might be required for the binding of c-di-AMP.

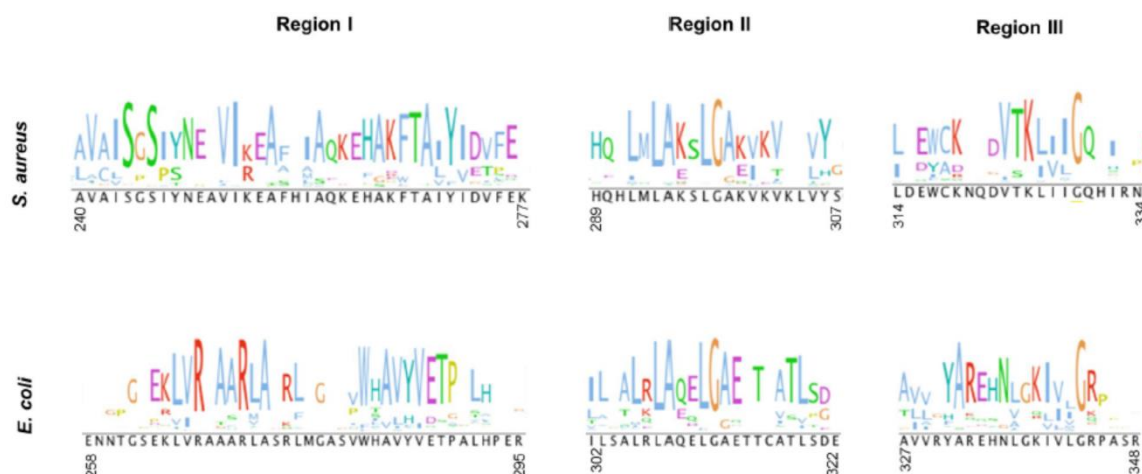


**Figure 2.4-3: Identification of a conserved amino acid motif in the *S. aureus* KdpD(USP) domain.** *S. aureus* and *E. coli* KdpD(USP) homologues were identified separately through BLAST searches. For each subset of USP domain sequences a multi-sequence alignment and a conserved sequence logo motif was generated with Clustal Omega (Sievers *et al.*, 2011). Three regions (labelled I, II and III) with highly conserved amino acid motifs were identified and are shown in this figure. While motifs II and III were similar in the *S. aureus* and *E. coli* KdpD(USP) domains, distinct conserved amino acids were observed in motif I. Specifically, a conserved SxS-X<sub>20</sub>-FTAxY motif ranging from amino acid 244 to 271 was found in the USP domain of the *S. aureus* KdpD protein and its homologues. The figure was taken from (Moscoso *et al.*, 2015) and was created by Joana Moscoso and Zong Zhang (Gründling lab, Imperial College London).

To investigate this further, plasmids for production of two MBP-KdpD<sup>Sa</sup>(USP) protein variants were generated in which amino acids S244 or Y271 were replaced with alanines. The MBP-KdpD(USP)<sub>S244A</sub> and MBP-KdpD(USP)<sub>Y271A</sub> hybrid proteins were produced in *E. coli* and purified, along with the MBP and MBP-KdpD<sup>Sa</sup>(USP) control proteins (Figure 2.4-4A). As assessed by DRaCALAs and shown in Figure 2.4-4B and C, the MBP-KdpD(USP)<sub>S244A</sub> and MBP-KdpD(USP)<sub>Y271A</sub> variants have impaired ability to bind c-di-AMP when compared to the

## Results

wild-type MBP-KdpD(USP). This suggests that these amino acids in the conserved SxS-X<sub>20</sub>-FTAxY motif in the USP domain of KdpD<sup>Sa</sup> are important for c-di-AMP binding.

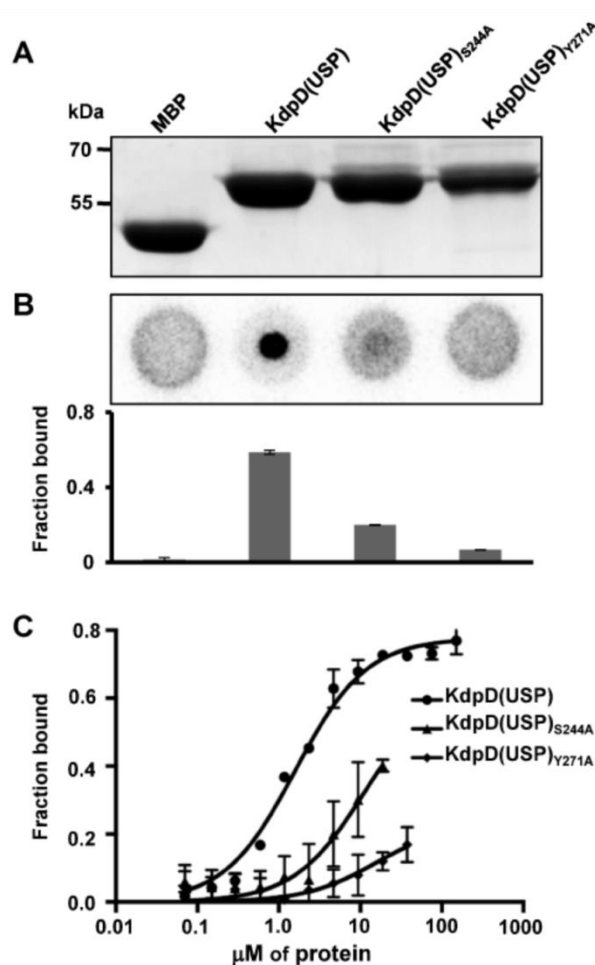


**Figure 2.4-4: *S. aureus* KdpD(USP) variants with alanine substitutions within the conserved SxS-X<sub>20</sub>-FTAxY motif show reduced binding to c-di-AMP.** (A) Coomassie stained gel with 10 μg of purified KdpD(USP) variants S244A and Y271A as well as the MBP protein and MBP-KdpD(USP) as negative and positive controls, respectively. The KdpD(USP) variants were created by replacing the first conserved serine residue or final conserved tyrosine residues with alanines and recombinant proteins were purified from *E. coli* as MBP hybrid proteins. (B) DRaCALAs with radiolabelled c-di-AMP and 10 μM of these four purified proteins. Two independent experiments were performed. Representative spots are shown and the average fraction bound values and standard deviation from three technical replicates are plotted. (C) c-di-AMP binding curve using the purified MBP-KdpD(USP) hybrid protein and the S244A and Y271A variants. DRaCALAs were performed with radiolabelled c-di-AMP and protein concentrations ranging from 0.02 to 150 μM for the wild-type MBP-KdpD(USP), 0.02 to 17.50 μM for the S244A variant and 0.02 to 35 μM for the variant Y271A. The average fraction bound values and standard deviations from three independent experiments were plotted against the protein concentration.  $K_d$  values could not be determined for the two variants, as the saturation point could not be reached. Experiments were performed by members of the AG Gründling (Imperial College London). The figure was taken from (Moscoso *et al.*, 2015) and was created by Joana Moscoso (Gründling lab, Imperial College London).

### 2.4.3 High levels of c-di-AMP inhibit the up-regulation of *kdpA* under salt stress.

Previous work by Price-Whelan *et al.* showed that the KdpDE two-component system is required for the up-regulation of the *kdpFABC* transporter genes under salt stress (Price-Whelan *et al.*, 2013). To investigate the impact of c-di-AMP on the function of KdpD, qRT-PCR experiments were carried out to monitor the transcript levels of the *kdpA* gene in the wild-type *S. aureus* strain LAC\* (WT) and an isogenic *gdpP* deletion strain, which has constitutively high levels of c-di-AMP (Corrigan *et al.*, 2011, Corrigan *et al.*, 2015). These two strains were grown to mid-log phase in LB 0 M NaCl or LB 1 M NaCl medium to induce expression of the *kdp* system. RNA was extracted and transcript levels of the *kdpA* gene, normalized to the levels of the *gyrB* housekeeping gene, were compared.

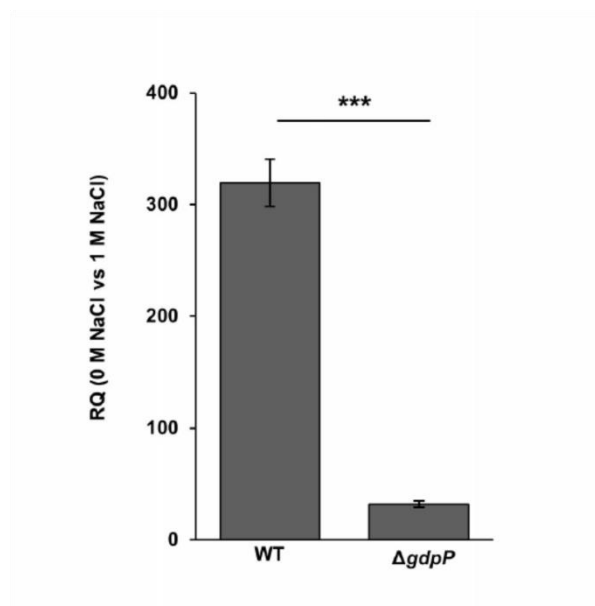


**Figure 2.4-5: High levels of c-di-AMP inhibits the expression of *kdpA*.** Relative quantification of transcript levels of *kdpA* measured by qRT-PCR in the wild-type *S. aureus* strain LAC\* (WT) and an isogenic *gdpP* ( $\Delta gdpP$ ) mutant strain (with constitutively high levels of c-di-AMP), normalized to *gyrB* transcript levels. The WT and mutant *S. aureus* strains were grown to an OD<sub>600</sub> of 0.7 in LB medium without salt (0 M NaCl) or containing 1 M NaCl, RNA extracted and used in qRT-PCR experiments performed as described in the materials and method section. Three independent experiments with triplicates were performed and a representative result is shown. The data from one independent experiment are plotted and were analysed using a two tailed Student's *t*-test. A statistically significant difference with a p-value < 0.01 was observed between the values and is indicated by asterisks. Experiments were performed by members of the AG Gründling (Imperial College London). The figure was taken from (Moscoso *et al.*, 2015) and was created by Joana Moscoso (Gründling lab, Imperial College London).

As expected, the levels of *kdpA* transcripts increased dramatically (320-fold) under salt stress in the WT strain (Figure 2.4-5). In the *gdpP* mutant, the levels of *kdpA* transcripts under salt stress were only slightly increased (30-fold) when compared to the WT strain (Figure 2.4-5). This indicates that c-di-AMP binding to KdpD negatively affects the expression of the *kdpA* transporter genes. Combined with previous work, which suggested a function of c-di-AMP as

negative regulator of the *S. aureus* Ktr potassium transport system (Corrigan *et al.*, 2013), this implicates this signalling nucleotide as a general negative regulator of potassium transport systems in *S. aureus*.

#### 2.4.4 Influence of c-di-AMP on KdpD<sup>Sa</sup> activity *in vitro*

As it was found that c-di-AMP binds to KdpD<sup>Sa</sup> and downregulates expression of *kdpA* we next wanted to analyse the influence of c-di-AMP on kinase and phosphatase activities of KdpD<sup>Sa</sup> *in vitro*. The heterologous overproduction of KdpD<sup>Sa</sup> turned out to be challenging and could only be accomplished in strain *E. coli* arctic express (DE3) RIL $\Delta$ *atpIBEFHA* carrying plasmid pET28b-*kdpD-His* after overnight cultivation at 16°C (Figure 2.4-6A).

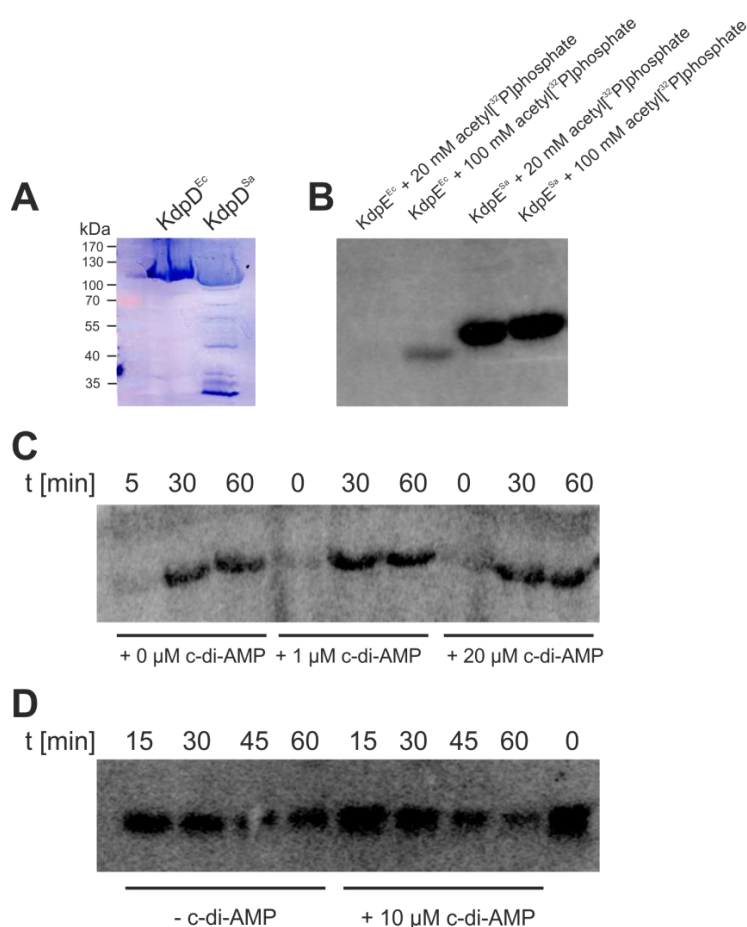


**Figure 2.4-6: Influence of c-di-AMP on KdpD<sup>Sa</sup> activity.** (A) Western Blot of membrane vesicles containing KdpD<sup>Ec</sup> (*E. coli*) and KdpD<sup>Sa</sup> (*S. aureus*). Membrane vesicles containing 100  $\mu$ g (total protein) were mixed with SDS loading dye and analysed by SDS-PAGE and Western Blot as described in Material and Methods. (B) Phosphorylation of KdpE<sup>Ec</sup> and KdpE<sup>Sa</sup> *in vitro* with radiolabelled acetyl[<sup>32</sup>P]phosphate. Synthesis of radiolabelled acetyl[<sup>32</sup>P]phosphate and phosphorylation was performed as described in Materials and Methods. Samples were loaded on a SDS-gel exposed to a phosphoscreen. (C) Time-dependent autokinase activity of KdpD<sup>Sa</sup> in membrane vesicles was monitored by incubation with [ $\gamma$ -<sup>32</sup>P]ATP in the presence and absence of c-di-AMP. Samples were loaded on a SDS-gel exposed to a phosphoscreen. (D) Time dependent phosphatase activity of KdpD<sup>Sa</sup> in the absence and presence of c-di-AMP. KdpE<sup>Sa</sup> was phosphorylated with radiolabelled acetyl[<sup>32</sup>P]phosphate *in vitro*. Subsequently KdpD<sup>Sa</sup> was added and samples were taken at indicated time points and loaded on a SDS-gel. Phosphorylated KdpE<sup>Sa</sup> was visualized by exposure of the gels to a phosphoscreen.

## Results

Autophosphorylation of KdpD<sup>Sa</sup> in membrane vesicles was detectable after 30 minutes incubation with [ $\gamma$ -<sup>32</sup>P]ATP (Figure 2.4-6C), whereas autokinase activity of KdpD<sup>Ec</sup> is clearly visible after 30 seconds (see for example Figure 2.1-2B). Furthermore we did not observe any influence of c-di-AMP on autophosphorylation activity (Figure 2.4-6C) or phosphotransfer to the response regulator KdpE<sup>Sa</sup> (data not shown). To further analyse if c-di-AMP could influence KdpD<sup>Sa</sup> phosphatase activity, we therefore had to phosphorylate KdpE<sup>Sa</sup> *in vitro* using radiolabelled acetyl[<sup>32</sup>P]phosphate (Figure 2.4-6B). Purified KdpE<sup>Sa</sup> was provided by Joana Moscoso and phosphorylated *in vitro* as described in Materials and Methods. Subsequently membrane vesicles containing KdpD<sup>Sa</sup> were added and dephosphorylation of phospho-KdpE<sup>Sa</sup> in the presence and absence of 10  $\mu$ M c-di-AMP was monitored over time (Figure 2.4-6D). The amount of phospho-KdpE<sup>Sa</sup> decreased within 60 minutes, however there was no significant difference between the absence and presence of c-di-AMP, respectively (Figure 2.4-6D). Taken together we could not prove a direct influence of c-di-AMP on KdpD<sup>Sa</sup> *in vitro*, however autophosphorylation activity was low and homologous overproduction of KdpD<sup>Sa</sup> in *S. aureus* and heterologous overproduction in different *E. coli* strains failed in almost all cases (data not shown). Therefore it is likely that KdpD<sup>Sa</sup> is not folded correctly under the tested cultivation conditions. Moreover the phospholipid composition of the cytoplasmic membrane might influence protein activity.

### 3 Discussion

#### 3.1 K<sup>+</sup> sensing and signal transduction in the histidine kinase KdpD

Conservation of crucial resources in fluctuating environments is particularly challenging for unicellular organisms. Under K<sup>+</sup>-limiting conditions, induction of *kdpFABC* expression is controlled by the bifunctional sensor kinase KdpD via KdpE, which ultimately leads to production of the high-affinity KdpFABC transport system (Figure 2.1-1A and B). In this study we have shown that KdpD is able to monitor concentrations of both extra- and intracellular K<sup>+</sup> and to regulate its dual function as an autokinase and a KdpE-specific phosphatase according to the K<sup>+</sup> concentrations of the two K<sup>+</sup> pools (Figure 2.1-1C and D). The observed  $K_{0.5}$  value for autokinase activity is in the range of environmental K<sup>+</sup> concentrations at which induction is observed *in vivo*, and amino acid replacements in the periplasmic loop of KdpD lead to loss of its sensitivity to external K<sup>+</sup>. Furthermore, we demonstrated that the phosphatase activity is stimulated by intracellular K<sup>+</sup> via a sensor module located in the C-terminal cytoplasmic domain of KdpD (Figure 2.1-1, Figure 2.1-2, Figure 2.1-5).

These results led us to formulate a novel dual-sensing, dual-regulation model for K<sup>+</sup>-dependent KdpD signalling (Figure 2.1-8A), which reproduces the basic features of the system (Figure 2.1-8B and C). When the extracellular K<sup>+</sup> concentration is high (>5 mM), K<sup>+</sup> is recognized by the periplasmic loop and inhibits the autokinase activity. At the same time intracellular K<sup>+</sup> is sensed by the C-terminal cytoplasmic domain and stimulates the phosphatase activity. Consequently KdpD acts as a phosphatase on KdpE-P, and production of the high-affinity K<sup>+</sup> transporter is prevented. When environmental levels of K<sup>+</sup> fall below the threshold for autokinase activation, *kdpFABC* expression is initiated; however, as long as the intracellular K<sup>+</sup> concentration remains high, the KdpD phosphatase activity remains stimulated. Under these conditions, the intracellular response is attenuated for as long as the high intracellular K<sup>+</sup> concentration is sufficient for all cellular processes. The longer the cells are exposed to K<sup>+</sup> limitation or extreme K<sup>+</sup> limitation, the larger the drop in intracellular K<sup>+</sup> levels. Eventually, the phosphatase activity is no longer stimulated and higher amounts of KdpE become phosphorylated, resulting in maximal production of KdpFABC.

Importantly, this dual-sensing, dual-regulation mechanism allows *E. coli* not only to respond to impending limitation by sensing the extracellular K<sup>+</sup> concentration, but also to regulate the activation level in response to changing intracellular K<sup>+</sup> requirements. In particular, the demand for K<sup>+</sup> is determined by the cellular growth rate. In media that permit rapid growth, intracellular K<sup>+</sup> could become depleted even though it is abundant in the environment. Under these

conditions, sensing of the intracellular  $K^+$  level allows the cell to fine-tune its uptake rate to match the demand. Moreover, it has been shown previously that both extracellular  $Cs^+$  and low pH significantly reduce the availability of free intracellular  $K^+$  and lead to induction of *kdpFABC* expression (Jung *et al.*, 2001, Roe *et al.*, 2000). Furthermore,  $K^+$  uptake is linked to carbohydrate metabolism (Lüttmann *et al.*, 2009). We included this cellular scenario in our mathematical model, and used simulations to compare the dual-sensing strategy to strategies with sensing of only one  $K^+$  pool under variation of both environmental  $K^+$  and growth rate. We found that the dual-sensing strategy was better able to maintain intracellular  $K^+$  within the tolerable range, and therefore was able to outcompete single-sensing strategies (Figure 2.1-10). Dual sensing by a bifunctional histidine kinase thus emerges as a highly optimized regulation strategy. While bifunctionality of sensor kinases ensures robustness to changes in the protein concentrations (Batchelor & Goulian, 2003, Shinar *et al.*, 2007), regulation of both activities is needed to achieve stable homeostasis in changing environments. The key advantage of this strategy is the ability to directly sense changes in both supply of and demand for the limiting resource. It is in fact analogous to strategies that are widely used in control engineering (Kilian, 2005). For example, temperature controllers often monitor both internal and external temperature to control heating and cooling elements (Figure 3.1-1). In this case, dual sensing keeps room temperature constant in the face of unpredictable changes in the weather or when variables such as incident sunlight, room occupancy or the opening of doors affect heat influx and leakage. However, whereas engineered control systems usually have separate sensors, controllers and actuators, bacteria have found a remarkably compact and integrated solution in the case of the Kdp system, with KdpD providing the functions of the sensors, the controller, and, aided by KdpE, also the actuator (Figure 3.1-1).

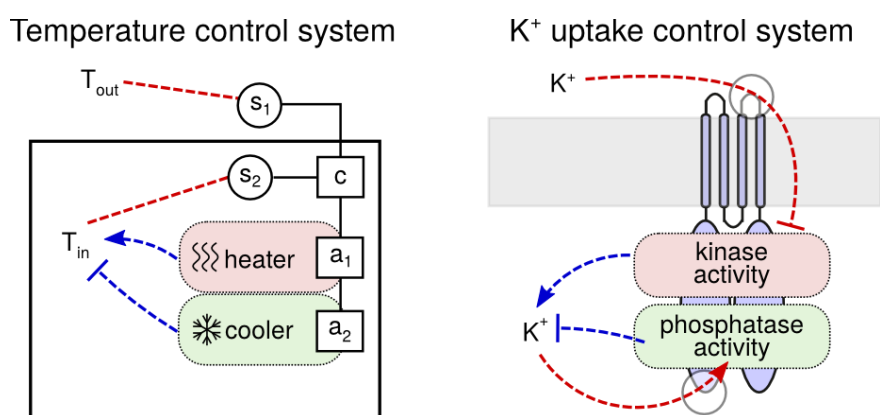


**Figure 3.1-1: Schematic comparison of a temperature control system with KdpD.** A temperature controller (c) integrates measurements of the internal and external temperatures from individual sensors (s) into signals that regulate the actuators (a) of a heater and a cooler. KdpD is an all-in-one control system for  $K^+$  uptake: it combines extracellular and intracellular sensing functions which control its autokinase and phosphatase activities, respectively, as well as the actuators of the downstream pathway. The figure was created by Filipe Tostevin.

The combination of extra- and intracellular sensing has been shown previously for  $Mg^{2+}$  homeostasis in the pathogen *Salmonella enterica* serovar *typhimurium*, albeit via a very different mechanism. The PhoP/PhoQ two-component system in *Salmonella* senses external  $Mg^{2+}$  limitation to activate target gene expression (Garcia Vescovi *et al.*, 1996). In addition, transcription of the gene encoding the  $Mg^{2+}$  transporter MgtA is influenced by intracellular  $Mg^{2+}$ . More precisely intracellular  $Mg^{2+}$  binds to the *mgtA* 5'UTR and terminates transcription via stem-loop formation (Cromie *et al.*, 2006). The expression of *mgtA* is thus regulated by both the intra- and extracellular  $Mg^{2+}$  concentrations. However, unlike the Kdp system, the two signals are not integrated at the level of the sensor kinase, but instead act at different levels of the response pathway. For most signal transduction pathways the precise signalling mechanism has remained elusive up to now and it is conceivable that dual sensing by bifunctional histidine kinases and other similarly elaborate mechanisms that integrate multiple signals are the rule rather than the exception.

Our data do not identify the specific molecular transitions that determine the catalytic activities of KdpD, although we suggest that KdpD integrates distinct  $K^+$  signals from at least two sensory domains. Structural data for conserved sensor kinase domains support the existence of distinct conformational states of bifunctional sensor kinases with autokinase or phosphatase activity (Marina *et al.*, 2005, Ferris *et al.*, 2012, Huynh & Stewart, 2011). Here we have used the simplest generalization of this conformational model to incorporate a third, enzymatically inactive, state. However, the multidomain structure of KdpD potentially allows for a far larger number of conformations, as each domain may respond differently in the presence of distinct stimuli (Bhate *et al.*, 2015). It therefore remains to be determined precisely how the dual  $K^+$  stimuli are encoded in KdpD dynamics at a molecular scale.

Furthermore the mechanism of intracellular  $K^+$  sensing in the C-terminal cytoplasmic domain remains obscure. In this study we attempted to localise a  $K^+$  recognition site within the GAF domain. However, the analysed KdpD variants showed either a wild-type-like response or were characterised by altered signalling properties. The hybrid protein KdpD-GAF 3E0Y showed deregulated enzymatic activities, indicating the importance of the GAF domain for signal transduction to the output domain. However, the hybrid proteins containing the GAF domains of *S. aureus* and *V. cholera* KdpD displayed wild-type-like behaviour *in vivo*. Thus – despite low amino acid identity – the overall structure of the domain seems to be similar in these organisms. Consequently, from these data we cannot draw conclusions about the mechanism of  $K^+$  binding in the GAF domain. Even though a defined  $Na^+$ -binding site was identified in the GAF domain of the adenylyl cyclases CyaB1 and CyaB2 from *Anabaena* PCC7120

(Camn, 2007a), it is conceivable that more than one  $K^+$  binds to or covers the surface of the GAF domain.

Interestingly a truncated KdpD variant, in which the GAF domain was missing, showed an inverted response *in vitro* (chapter 2.2.3). In subsequent experiments we identified several hydrophobic amino acid located on the third helix of the GAF domain that could be important for dimerization. KdpD variants, in which these amino acids were replaced with alanines, resulted in a decreased output response. KdpD autophosphorylation occurs *in trans*, that means one monomer binds ATP and the phosphoryl group is transferred to the conserved histidine of the other monomer (Heermann *et al.*, 1998). Thus the decreased output response could be explained by lower autophosphorylation as a consequence of dimerization defects. Furthermore the KdpD variant in which L630 and L631 were replaced with alanine did not show any activity *in vivo* and we could not detect this variant by Western blot analysis (Figure 2.2-9B & C). It is possible that dimerization of KdpD contributes to protein stability and that monomeric KdpD proteins are degraded *in vivo*.

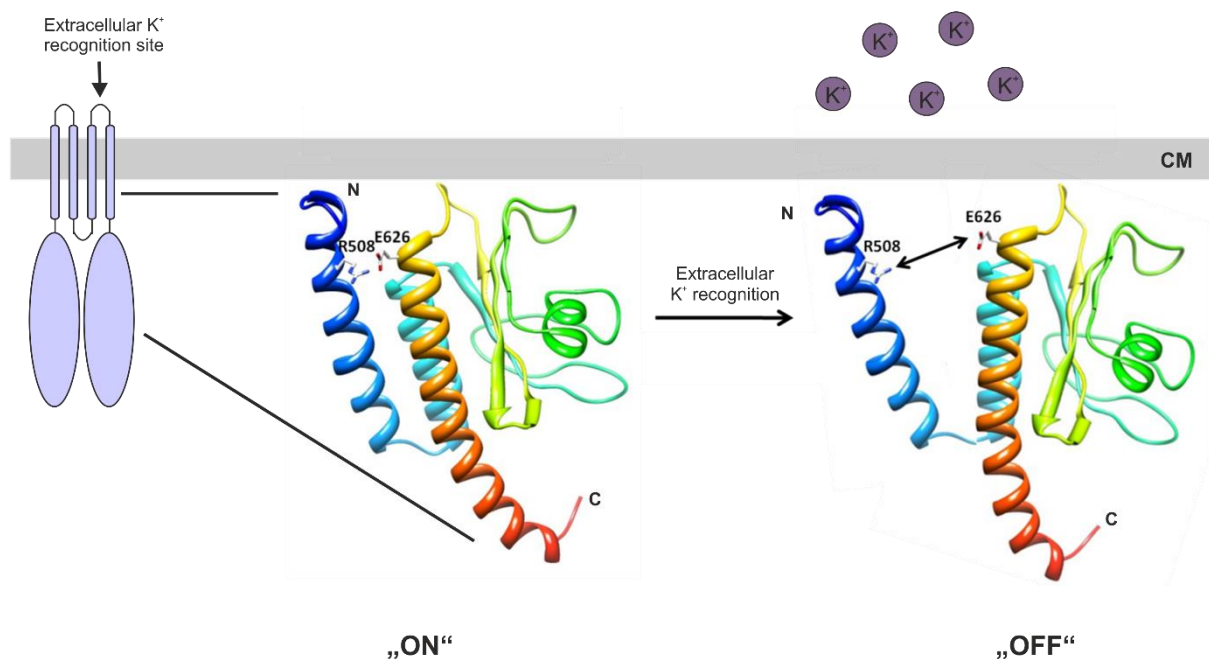


**Figure 3.1-2: Schematic model of  $K^+$  dependent signaling across the membrane.** Electrostatic interactions between R508 and E626 keep KdpD in the kinase “ON” state. Extracellular  $K^+$  recognition causes movements of the extended TM4 (dark blue) and therefore an “OPEN” conformation. The “OPEN” conformation shifts KdpD in the kinase inactive (“OFF”) state and thus KdpFABC is not produced in the presence of  $K^+$ . The figure was modified from (Schramke, 2011). CM: cytoplasmic membrane.

By modelling the structure of the GAF domain we identified interaction sites between the extended TM4 and the last  $\alpha$ -helix of the GAF domain. Electrostatic interactions between the side chains of amino acid R508 and E626 are important for modulating KdpD activity (Figure 2.2-10, Figure 2.2-11). More specifically, the insertion of repellent charges resulted in an inactive

protein. Therefore we propose that this kind of interactions are responsible for an “open” or “closed” conformation within the protein, which is in turn responsible for activating the kinase or phosphatase activities. According to our data the “open” conformation results in a kinase inactive state, whereas the “closed” conformation would activate kinase activity (Figure 3.1-2). In the future it would be interesting to unravel the course of movement of TM4 upon ligand binding. There are several mechanisms known how signalling across the membrane can occur. For the chemoreceptor Tar and the histidine kinase DcuS of *E. coli* it has been shown that the signal is transferred via a piston-like movement (Ottemann *et al.*, 1999, Monzel & Uden, 2015), the histidine kinases LuxPQ involved in quorum sensing in *Vibrio harveyi* transmits the signal by a rotation mechanism of the TM helices (Neiditch *et al.*, 2006) whereas for a hybrid two-component system of *Bacteroides* it was shown that transmembrane signalling is accomplished by a scissor blade-like closing mechanism (Lowe *et al.*, 2012). The model presented in Figure 3.1-2 favours a scissor blade-like movement. However, it should be considered that a piston-like movement or rotation of TM4 would affect electrostatic interactions between R508 and E626 as well. Accessibility studies could provide further insights in the movement of TM4 upon stimulus perception.

To date KdpD is a unique example for a histidine kinase that senses the same stimulus extra- and intracellularly (see chapter 2.1 and 3.1). In this respect another interesting point would be, whether K<sup>+</sup> binding occurs cooperatively. In chapter 2.1 we found that extracellular K<sup>+</sup> influences the kinase and phosphatase activities, however there was no influence of intracellular K<sup>+</sup> on the kinase activity. Potentially the intracellular K<sup>+</sup> binding site is only accessible in a specific conformation of the protein.

### 3.2 Interconnection of Kdp mediated K<sup>+</sup> homeostasis and other cellular processes

Besides direct K<sup>+</sup> sensing KdpD is known to interact with other proteins like UspC and EIIA<sup>Ntr</sup> to couple K<sup>+</sup> homeostasis to stress responses and metabolism. In this study we investigated the influence of other cellular processes on the Kdp system *in vivo* and *in vitro*. In chapter 2.3 we found that cells lacking the two constitutively produced K<sup>+</sup> transporters Trk and Kup and the sensor kinase KdpD are not able to grow under K<sup>+</sup> limitation, as synthesis of KdpFABC cannot be induced. However these cells grow again after an initial lag phase of 22 hours. Recovery of growth arrest was dependent on an intact phosphorylation site within KdpE and resulted in *kdpFABC* expression. Whole genome sequencing revealed a suppressor mutation in the *pstC* gene and further experiments confirmed that a deletion in *pstC* or *phoU* – known to switch the histidine kinase PhoR in the constitutive kinase “ON” state – induced *kdpFABC* expression in the absence of the partner histidine kinase KdpD. Therefore we reasoned cross-talk regulation between these two systems. Up to now it is not completely understood how specificity between two-component signal transduction systems is maintained. Podgornaia & Laub suggest three key mechanisms to enable specificity between signal transduction systems: molecular recognition, phosphatase activity and substrate competition (Podgornaia & Laub, 2013). According to the authors the prevalent specificity mechanism is molecular recognition, that is the strong kinetic preference of a histidine kinase to its partner response regulator *in vitro* (Skerker *et al.*, 2005). Commonly histidine kinases are bifunctional enzymes having both kinase and phosphatase activities (Willett & Kirby, 2012) and phosphatase activity is supposed to counteract unspecific phosphorylation by non-partner histidine kinases *in vivo* (Alves & Savageau, 2003). Even though cross talk between two-component systems has been described several times, it mostly occurs in the absence of either the partner histidine kinase or partner response regulator respectively (Siryaporn & Goulian, 2008, Silva *et al.*, 1998, Fisher *et al.*, 1995, Haldimann *et al.*, 1997). Therefore it is not clear whether cross-talk between two-component systems is a widespread but more undirected phenomenon, or if it could be of physiological importance *in vivo*. Here we show that PhoR/KdpE and KdpD/PhoB cross-regulation affects target gene expression in both directions even in the presence of the partner histidine kinase. We found that both histidine kinases are able to phosphorylate their non-partner response regulators *in vitro* and we observed cross-regulation between these two-component systems *in vivo*. Thus in our current model we assume that PhoR directly activates KdpE and KdpD directly activates PhoB under K<sup>+</sup> and PO<sub>4</sub><sup>3-</sup> limitation (Figure 3.2-1).

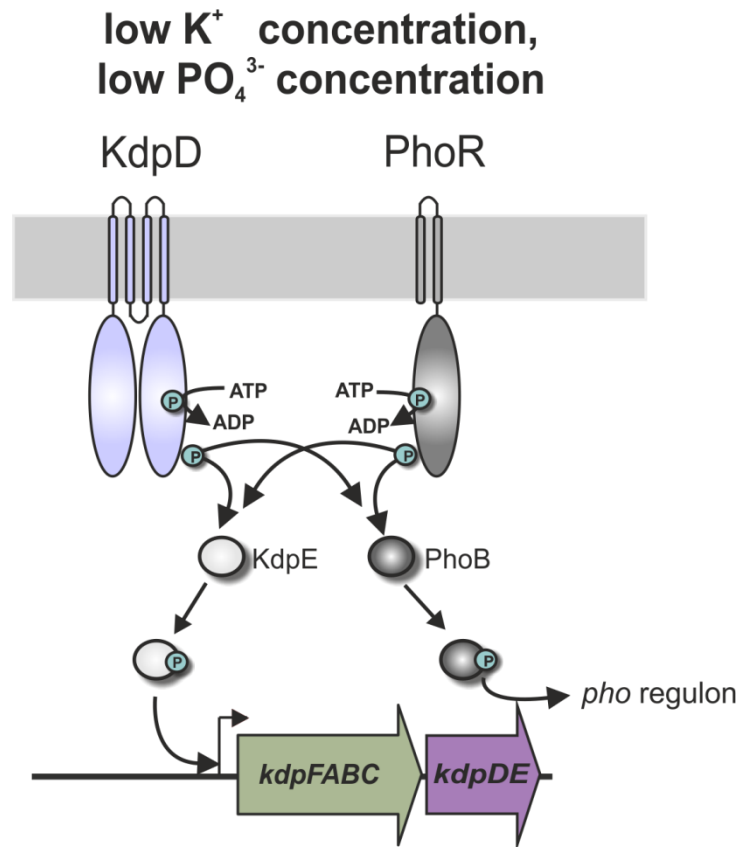


**Figure 3.2-1: Cross-talk between the KdpD/KdpE and PhoR/PhoB two-component system couples  $K^+$  and  $PO_4^{3-}$  homeostasis in *E. coli*.** KdpD and PhoR phosphorylate their partner response regulators KdpE and PhoB, respectively. If both stimuli are limited an additional increase of target gene expression can be achieved by direct cross-regulation of these two two-component systems and therefore might contribute to maintain the balance of positively and negatively charged ions within the cell.

If  $PO_4^{3-}$  is limited PhoR autophosphorylates and transfers the phosphoryl group to the partner response regulator PhoB, which in turn activates transcription of the *pho* regulon. Furthermore PhoR phosphorylates the non-partner response regulator KdpE. However, if intra- and extracellular  $K^+$  levels are sufficient, the counteracting phosphatase activity of KdpD results in KdpE dephosphorylation and prevents *kdpFABC* expression. If additionally the  $K^+$  concentration is low, KdpD is in the kinase active state and phosphorylates KdpE as well as the non-partner response regulator PhoB, finally leading to higher  $K^+$  uptake and transcription of the *pho* regulon (Figure 3.2-1). Our hypothesis that interconnection of these two pathways is beneficial for the cell is further supported by early studies, which revealed that  $K^+$  is important for  $PO_4^{3-}$  uptake (Weiden et al., 1967). Moreover it has been shown previously that in the absence of PhoR the response regulator PhoB can be activated by non-partner histidine kinases, amongst others KdpD (Zhou, 2005). Furthermore a potential link between these two-component systems has been described recently. The phosphotransferase protein EIIA<sup>Ntr</sup> of *E. coli* has been shown to interact with KdpD, stimulate its activity and thereby couples carbon metabolism with  $K^+$  homeostasis (Lüttmann et al., 2009). More recent studies revealed that enzyme IIA binds to

and regulates activity of PhoR in a similar way (Lüttmann *et al.*, 2012). We therefore propose that cross-regulation between these two-component systems is of physiological relevance and ensures the maintenance of the ratio between positively and negatively charged ions in the cell. It should be noted that very recently Moreau & Loiseau published studies about suppressor mutants generated under phosphate starvation. Interestingly one of the mutations the authors identified was located in the *kdpD* gene and resulted in a constitutively active KdpD protein (Moreau & Loiseau, 2016). According to our results a constitutively active KdpD protein could rescue growth under phosphate starvation by directly activating the non-partner response regulator PhoB.

In Chapter 2.4 we investigated an accessory influence on the Kdp system in *S. aureus*. It was shown previously that the second messenger c-di-AMP, which is common among Gram-positive bacteria, binds to *S. aureus* KdpD (Corrigan *et al.*, 2013). The influence of c-di-AMP on KdpD<sup>Sa</sup> activity was analysed in more detail and the data suggest that c-di-AMP dampens the production of the Kdp K<sup>+</sup> transport system under osmotic stress. Using truncated and modified KdpD variants, it was shown that c-di-AMP interacts specifically with the USP domain of the *S. aureus* KdpD protein (Figure 2.4-1, Figure 2.4-2, Figure 2.4-4). USP domains (Pfam accession number PF00582) are widespread among many organisms including archaea, bacteria, fungi, plants and even a few animals (Finn *et al.*, 2014). They are generally associated with responses to different stresses and bacterial species can have one or several USP domain containing proteins. Among the USP proteins that are able to bind ATP, a conserved G-X<sub>2</sub>-G-X<sub>9</sub>-G(S/T) amino acid motif is found (Tkaczuk *et al.*, 2013). However, the actual functional consequence of nucleotide binding to these USP domains is not known. The USP-domain of KdpD<sup>Sa</sup> does not contain a recognizable ATP-binding motif, but multiple protein sequence alignments revealed a region that is conserved in species that have a KdpD<sup>Sa</sup>-like USP domain and diverges from the same region of *E. coli* KdpD homologues (Figure 2.4-3). Within this region a conserved SxS-X<sub>20</sub>-FTAxY motif was identified and shown to be required for c-di-AMP binding (Figure 2.4-4). The data presented here indicate that high levels of c-di-AMP prevent the up-regulation of the *kdp* transporter genes under salt stress (Figure 2.4-5). Therefore, c-di-AMP binding to KdpD seems to impact, by a yet unknown mechanism, KdpDE signalling, thus preventing production of the Kdp K<sup>+</sup> transporter. In light of this, it is conceivable that in the absence of stress, production of the Kdp K<sup>+</sup> transporter is inhibited until absolutely required by c-di-AMP binding to KdpD; and that, under salt stress, this inhibition is relieved or bypassed. Similar to the observed inhibitory effect of c-di-AMP on the Kdp system, previous work by Bai *et al.* suggested that c-di-AMP impairs K<sup>+</sup> uptake via

## Discussion

the Ktr system in *Streptococcus pneumoniae* by binding to the cytoplasmic gating component (Bai *et al.*, 2014). This implicates c-di-AMP as a more general negative regulator of K<sup>+</sup> uptake systems in Gram-positive bacteria. Even though we were able to overproduce KdpD<sup>Sa</sup> heterologously in *E. coli*, the *in vitro* activity of the protein was rather low. For this reason future work about the direct influence of c-di.AMP binding on KdpD<sup>Sa</sup> kinase or phosphatase activity would be interesting.

Taken together, in this study we identified a connection between PO<sub>4</sub><sup>3-</sup> and K<sup>+</sup> homeostasis in *E. coli* and an influence of c-di-AMP on KdpD regulated target gene expression in *S. aureus*. As KdpD harbours an extraordinary large input domain, it is conceivable that a multitude of other cellular components influences KdpD activity and thereby couples K<sup>+</sup> uptake to other stress responses or different metabolic states.

## 4 Materials and Methods

Experiments presented in chapter 2.4.1-2.4.4 were performed by Joana Moscoso, Yong Zhang, Tommaso Tosi and Amina Debhi in the lab of Angelika Gründling. All strains, plasmids and experimental procedures are already published (Moscoso *et al.*, 2015) and are therefore not listed here.

### 4.1 Materials

Ni<sup>2+</sup>-NTA resin and the Penta-His antibody were obtained from Qiagen (Hilden, Germany). NAP-5 columns and [ $\gamma$ -<sup>32</sup>P]ATP were purchased from GE Healthcare (Freiburg, Germany) and Perkin Elmer (Groningen, Netherlands), respectively. Goat anti-(rabbit IgG)-alkaline phosphatase was obtained from Biomol (Hamburg, Germany), and silicone oil (DC550) was from Serva (Heidelberg, Germany). All other reagents were reagent grade and obtained from commercial sources.

### 4.2 Strains, plasmids, oligonucleotides used in this study

Strains, plasmids and oligonucleotides used in this study are listed in Table S1, Table S2 and Table S3, respectively. *E. coli* strain MG1655 (wild type K-12 strain) was used for measurements of intracellular K<sup>+</sup> concentrations. *E. coli* strain HAK006 was used for reporter assays with plasmid encoded *kdpD* (Nakashima *et al.*, 1993). For protein overproduction of soluble proteins *E. coli* BL21 (DE3/pLysS) and for preparation of membrane vesicles *E. coli* TKR2000 was used. For overproduction of *S. aureus* KdpD we used strain ArcticExpress(DE3)RIL $\Delta$ *atpIBEFHA*.

Strains carrying chromosomal point mutations within *kdpD* (HS2, HS3 and HS4) are based on the reporter strain LF3 and were generated by using Red<sup>®</sup>/ET<sup>®</sup> recombination technology in combination with *rpsL* counter-selection (Heermann *et al.*, 2008). The kanamycin cassette was inserted in *kdpD* by amplification of the kanamycin cassette using primers KdpD\_up + KdpD\_low and subsequent homologous recombination in LF3 resulting in strain HS1. The linear DNA fragments for the second homologous recombination carrying corresponding point mutations were amplified from plasmids pBD/#3, pBD/T677A and pBD/#4 (see Table S3), respectively, by using primers NotI\_s and Kdp730\_as (see Table S2).

Strain LB2240 $\Delta$ *kdpD* and LB2240 $\Delta$ *kdpD,kdpE*<sup>D52N</sup> were constructed in two steps by using Red<sup>®</sup>/ET<sup>®</sup> recombination technology in combination with *rpsL* counter-selection (Heermann *et al.*, 2008). Briefly, in the first step we inserted a linear DNA fragment encoding a kanamycin cassette as selection marker in the *kdpD* (for LB2240 $\Delta$ *kdpD*) and *kdpE* gene (for

LB2240 $\Delta kdpD, kdpE^{D52N}$ ), respectively (primer pairs for amplification of kanamycin cassette: 50bp*kdpD\_rpsL*- kan\_sense + 50bp*kdpD\_rpsL*- kan\_antisense; 50bp*kdpE\_rpsL*- kan sense + 50bp*kdpE\_rpsL*/ kan\_antisense). In the second step the kanamycin cassette was replaced with a linear DNA fragment encoding the *kdpD* deletion and the *kdpE*<sup>D52N</sup> substitution, respectively. The linear DNA fragments for *kdpD* deletion was derived by a two-step PCR using genomic DNA of LB2240 as template and primer pairs *kdpCDforI\_sense* +  $\Delta kdpD$ \_antisense and  $\Delta kdpD$ \_sense + *kdpE*\_antisense, respectively. The linear DNA fragment for *kdpE*<sup>D52N</sup> substitution was derived from DNA amplification of pPV-2/D52N as a template and primer pairs *kdpE\_sense* + *kdpE*\_antisense. Strains LB2240 $\Delta kdpD\Delta pta\Delta ackA$  and LF3 $\Delta kdpD$  were constructed using the “Quick and Easy *E. coli* Gene Deletion and Bac Modification Kits” (Gene Bridges) as previously described (Heermann *et al.*, 2008). Briefly, we inserted a linear DNA fragment encoding a kanamycin cassette as selection marker in the genes *pta, ackA* (parental strain LB2240 $\Delta kdpD$ ) and *kdpD* (parental strain LF3), respectively (primer pairs for amplification of the kanamycin cassette: 50bp*ackApta\_rpsL*-kan\_sense + 50bp*ackApta\_rpsL*- kan\_sense and delta *KdpD\_up* + delta *KdpD\_down*). To avoid effects of the kanamycin resistance cassette on *kdpE* expression levels, we removed the selection marker in LF3 $\Delta kdpD$  using the pCP20 helper plasmid as described previously (Baba *et al.*, 2006). Strains LB2240 $\Delta pstC$ , LB2240 $\Delta kdpD\Delta pstC$  and all other LF3 deletion mutants (Table S1) were constructed by P1 transduction (Miller, 1972). Strains JW3705 (*pstC::npt*), JW0390 (*phoR::npt*) and JW3702 (*phoU::npt*) were used as donor strains. Preparation of phage lysate of donor strains and transduction to recipient strains was performed as described previously (Leder *et al.*, 1977). For double or triple deletions the kanamycin cassette was removed in between using the helper plasmid pCP20 plasmid as previously described (Datsenko & Wanner, 2000). Successful deletion was confirmed by PCR using appropriate primers listed in Table 3.

Strain ArcticExpress(DE3)RIL $\Delta atpIBEFHA$  was constructed using the “Quick and Easy *E. coli* Gene Deletion and Bac Modification Kits” (Gene Bridges) as previously described (Heermann *et al.*, 2008). Briefly, we inserted a linear DNA fragment encoding a kanamycin cassette as selection marker in the genes *atpIBEFHA* (parental strain ArcticExpress(DE3)RIL) (primer pairs for amplification of the kanamycin cassette: delta *ATP (IBEFHA)\_up* + delta *ATP (IBEFHA)\_down*). To avoid effects of the kanamycin resistance cassette on expression levels, we removed the selection marker in using the pCP20 helper plasmid as described previously (Baba *et al.*, 2006).

All plasmid based point mutations were introduced in pBD via overlap PCR using the primers XmaI\_s, NotI\_s, HindIII\_as and the corresponding primers containing point mutations (Table S2). The products were ligated into pBD using XmaI or NotI and HindIII restriction enzymes.

The truncated variant *kdpD*/Δ2-498 was generated with the listed primers and cloned into pET16b using NdeI and BamHI restriction sites (resulting in plasmid pET16b/C3). Plasmid pBD/ΔTM1-4/loop3 was created in two steps. In the first step nucleotides encoding amino acids of TM4 were removed by a two-step overlap PCR using primer pairs XmaI\_s + delta TM4\_as and delta TM4\_s + HindII\_as and subsequent cloning in pBD using SpeI and HindII restriction sites. The resulting plasmid was used as template for the second step, in which nucleotides encoding amino acids of TM1-3 were removed by another two-step overlap PCR using primer pairs XmaI\_s + delta TM1-3\_as and delta TM1-3\_s + HindIII\_as. Subsequent cloning in pBD using SpeI and HindIII restriction sites resulted in plasmid pBD/ΔTM1-4/loop3.

For construction of pBD/NarX S-helix, pBD/Tsr S-helix, pBD/KdpD S-helix and pBD/all088 S-helix synthetic genes were ordered from Genewiz® and subsequently cloned in pPV/5-3 using MluI and NheI restriction enzymes. Afterwards *kdpD* variants were cloned in pBD using XbaI and HindIII.

Truncated *kdpD* variants *kdpD*/Δ625-632, *kdpD*/Δ633-640 and *kdpD*/Δ641-648 were constructed by two-step PCR using primer pairs NotI + corresponding antisense primer and corresponding sense primer + HindII\_as and subsequent cloning in pBD.

Plasmids for the bacterial adenylate cyclase assays (BACTH) were constructed by DNA amplification using genomic DNA of *E. coli* MG1655 as template with primer pairs listed in Table 3 and subsequent cloning in indicated vectors. Successful insertion was confirmed by restriction with appropriate enzymes.

Plasmid pBR-Cherry pPstS was constructed by amplification of the upstream region of the *pstS* gene (~500bp) using primers pPstS\_BamHI\_s and pPstS\_XmaI\_as using genomic DNA of *E. coli* MG1655 as template. After restriction with enzymes XmaI and BamHI the DNA fragment was ligated in vector pBR-Cherry. Successful cloning was confirmed by restriction and sequencing analysis.

### 4.3 Molecular biological techniques

Plasmid DNA was isolated using a “HiYield plasmid minikit” (Suedlaborbedarf) or “QIAprep spin miniprep kit” (Qiagen), respectively. Genomic DNA was isolated using the “DNeasy tissue kit” (Qiagen). DNA fragments were purified from agarose gels using a “HiYield PCR cleanup

and gel extraction kit” (Suedlaborbedarf) or “QIAquick gel extraction kit” (Qiagen), respectively. Q5 DNA polymerase (New England BioLabs) and OneTaq DNA polymerase (New England BioLabs) were used according to the supplier’s instructions. Restriction enzymes and other DNA-modifying enzymes were also purchased from New England BioLabs and used according to the manufacturer’s directions.

### 4.4 Random mutagenesis

Random mutagenesis was performed with a PCR based method as described previously (Wilson & Keefe, 2001). DNA fragments were amplified using pBD/E643A (Schramke, 2011) as template with primer pairs NotI<sub>s</sub> and HindII<sub>as</sub>. Subsequently fragments were ligated in pBD/-MluI (Schramke, 2011) using MluI and NheI restriction sites. To screen for less K<sup>+</sup> sensitive KdpD variants, strain HAK006 was transformed with mutagenized plasmids and plated on KML plates containing ampicillin and X-Gal. Plasmids from blue colonies were isolated and point mutations were identified by sequencing.

### 4.5 Growth conditions

KML (1% KCl, 1% tryptone, 0.5% yeast extract) was used as standard medium for strain LB2240 and derivatives and LB (1% NaCl, 1% tryptone, 0.5% yeast extract) for LF3 and derivatives, respectively. To analyse K<sup>+</sup> dependent growth and reporter gene expression we used a phosphate buffered minimal medium containing indicated K<sup>+</sup> concentrations (K115 contains 46 mM K<sub>2</sub>HPO<sub>4</sub>, 23 mM KH<sub>2</sub>PO<sub>4</sub>, 8 mM (NH<sub>4</sub>)<sub>2</sub>SO<sub>4</sub>,; 0.4 mM MgSO<sub>4</sub>, 6 µM FeSO<sub>4</sub>, 1 mM sodium citrate) (Epstein & Kim, 1971). For cultivation of cells at different phosphate concentrations we used a Tris-maleic acid minimal medium (TMA, 100 mM Tris, 100 mM maleic acid, NaOH to a final pH of 7.4, 10 mM NH<sub>4</sub>Cl, 1 mM Na<sub>2</sub>SO<sub>4</sub>, 0.4 mM MgSO<sub>4</sub>) (Weiden *et al.*, 1967) and KCl and Na<sub>2</sub>HPO<sub>4</sub> were added as indicated. Glucose was added as C-source in a final concentration of 0.4%. Whenever necessary, thiamine was added in a final concentration of 1 µg/ml. Appropriate antibiotics were added in a final concentration of 100 µg/ml (ampicillin), 50 µg/ml (kanamycin) and 25 µg/ml (chloramphenicol). For cultivation on plates 1.5% (w/v) agar was added to the corresponding medium. Unless otherwise stated, cells were grown under aeration at 37°C.

### 4.6 β-galactosidase activity assays (determination of *kdpFABC* expression *in vivo*)

*In vivo kdpFABC* expression was analysed using strains HAK006 carrying plasmids pBD and derivatives, as well as LF3 and its derivatives (*P<sub>kdpFABC</sub>::lacZ*) (Table S1). Unless otherwise

stated cells were aerobically grown at 37°C in minimal media containing indicated K<sup>+</sup> concentrations (Epstein & Kim, 1971, Weiden *et al.*, 1967) and harvested in the late exponential growth phase by centrifugation.  $\beta$ -galactosidase activity was determined as described (Miller, 1992) and is given in Miller Units.

#### 4.7 **P<sub>pstS</sub> promoter activity assays**

*E. coli* MG1655 carrying plasmid pBR-Cherry-pPstS was cultivated in TMA medium supplemented with the indicated KCl and Na<sub>2</sub>HPO<sub>4</sub> concentration. Cells were grown aerobically in a microtiter plate in a final volume of 150  $\mu$ l at 37°C. Optical density (wavelength 600 nm) and fluorescence (excitation wavelength 560 nm, emission wavelength 612 nm) were determined with a Tecan Infinite F500 system. Promoter activity was calculated as described previously (Bren *et al.*, 2013).

#### 4.8 **RNA isolation, cDNA synthesis and qRT-PCR**

At indicated time points, cells were harvested and RNA was isolated using the “RNeasy mini kit” (Qiagen) according to the manufacturer’s directions. RNA concentration was adjusted to 20  $\mu$ g/ml and treated with “RNase free DNase” (New England Biolabs) for 60 min at 37°C to remove residual chromosomal DNA. Subsequently DNase was heat inactivated for 5 min at 70°C and RNA was stored at -20°C. cDNA was synthesised using the “RevertAid first strand cDNA synthesis kit” (Fermentas) according to the manufacturer’s directions. Samples were cooled down to 4°C and immediately frozen at -20°C. Quantitative real-time PCR (qRT-PCR; iQ5 real-time PCR detection system; Bio-Rad) was performed using specific primers for *kdpA*, *kdpD* and *gap* (see Table S3). The cycle threshold (CT) value was determined after 40 cycles using iQ software (Bio-Rad) and values were normalized with reference to the value of *gap*. The average of three technical replicates was calculated and is representative for three biological experiments.

#### 4.9 **Cell fractionation and preparation of membrane vesicles**

*E. coli* strain TKR2000 transformed with plasmids pBD or its derivatives was grown aerobically at 37°C in KML complex medium supplemented with ampicillin (100  $\mu$ g/ml). Cells were induced at OD<sub>600</sub>=0.5 with 0.2% (w/v) arabinose and grown for another three hours. After harvesting, the cells were washed with buffer (50 mM Tris/HCl pH 7.5, 10 mM MgCl<sub>2</sub>) and disrupted by passage through a Cell disruptor (Constant Cell Disruption Systems, Northants, UK) at 1.35 kbar and 4°C in disruption buffer [50 mM Tris/HCl pH 7.5, 10% (v/v) glycerol,

10 mM MgCl<sub>2</sub>, 1 mM dithiothreitol, 0.5 mM phenylmethylsulfonylfluoride, and 0.03 mg/ml DNase]. After removal of intact cells and cell debris by centrifugation (9.000 × g, 10 min), membrane vesicles were collected by centrifugation at 160.000 × g for 60 min. Membrane vesicles were washed with low ionic strength buffer (10 mM Tris/HCl, pH 7.5, 3 mM EDTA), centrifuged again and resuspended in 50 mM Tris/HCl, pH 7.5 containing 10% (v/v) glycerol. Vesicles were frozen in liquid nitrogen and stored at -80°C until use.

For preparation of membrane vesicles containing *S. aureus* KdpD we used strain ArcticExpress (DE3) RIL $\Delta$ atpIBEFHA carrying plasmid pET28b-KdpD (Table S1, Table S2). Cells were cultivated in LB under aeration at 37°C until OD<sub>600</sub>=0.5, IPTG was added in a final concentration of 0.5 mM and cultivation continued overnight at 16°C. Afterwards cells were harvested and membrane vesicles were prepared as described above.

#### 4.10 Overproduction and purification of soluble proteins

*E. coli* strain BL21(DE3/pLysS) transformed with plasmids pET16b/C3 (coding for *kdpD*/ $\Delta$ 2-498-6His), pDL39 (coding for *phoB*-10His), pDL40 (coding for *phoR*(codon 52-431)-10His) and pEE(coding for *kdpE*-10His), respectively, was grown aerobically at 37°C in LB complex medium supplemented with ampicillin (100 µg/ml). Gene expression was induced at OD<sub>600</sub>=0.5 with 0.5 mM IPTG and cells were grown for another three hours. In case of pDL39 and pDL40 cells were cultivated at 16°C overnight after induction. After harvesting the cells were washed with buffer (50 mM Tris/HCl pH 7.5, 10 mM MgCl<sub>2</sub>) and disrupted by passage through a Cell disruptor (Constant Cell Disruption Systems, Northants, UK) at 1.35 kbar and 4°C in disruption buffer [50 mM Tris/HCl pH 7.5, 10% (v/v) glycerol, 10 mM MgCl<sub>2</sub>, 1 mM dithiothreitol, 0.5 mM phenylmethylsulfonylfluoride, and 0.03 mg/ml (w/v) DNase]. After removal of intact cells and cell debris by centrifugation (9.000 × g, 10 min), the cytosol was frozen at -80°C. Despite the fact that the truncated version of PhoR lacks the transmembrane domains, we found a large proportion of the protein located in the membrane fraction. Therefore we solubilized the membrane fraction as described previously (Jung *et al.*, 1997) prior purification. Purification was performed as described before (Heermann *et al.*, 2003a). Deviating from this purification protocol, KdpD/ $\Delta$ 2-498 (pET16b/C3) was eluted with 250 mM imidazole.

#### 4.11 Phosphorylation and dephosphorylation assays

Purified PhoR (0.2 mg/ml, final concentration) or membrane vesicles containing approximately 0.2 mg/ml KdpD were incubated in phosphorylation buffer [50 mM Tris/HCl, pH 7.5, 10% glycerol (v/v), 0.5 M NaCl, 10 mM MgCl<sub>2</sub> and 2 mM dithiothreitol] at room temperature.

Phosphorylation was initiated by addition of 20  $\mu\text{M}$  [ $\gamma$ - $^{32}\text{P}$ ]ATP (2.38 Ci/mmol). At different times, aliquots were removed and the reaction was stopped by mixing with SDS sample buffer (Jung *et al.*, 1997). After incubation for 3.5 min, purified response regulator was added at a final concentration of 0.1 mg/ml to the histidine kinase-containing samples (resulting in a 1:2 dilution of histidine kinase, ATP and  $\text{K}^+$  concentration) and the incubation was continued. Additional aliquots were removed at different times and mixed with SDS sample buffer. For dephosphorylation assays, 10His-KdpE- $^{32}\text{P}$  was obtained as described (Jung & Altendorf, 1998a). Dephosphorylation was initiated by the addition of membrane vesicles containing approximately 0.1 mg/ml of either KdpD or the purified C-terminal cytoplasmic domain KdpD/ $\Delta$ 2-498 (0.1 mg/ml), 20 mM  $\text{MgCl}_2$  in presence of 20  $\mu\text{M}$  ATP- $\gamma$ -S. To test for  $\text{K}^+$ -dependent dephosphorylation of KdpE, we added KCl at the indicated concentrations. The ionic strength was always kept constant at 0.5 M by supplementing with NaCl. At different times, aliquots were removed, and the reaction was stopped by the addition of SDS sample buffer. All samples were immediately subjected to SDS-polyacrylamide gel electrophoresis. Shortly before the end of electrophoresis an [ $\gamma$ - $^{32}\text{P}$ ]ATP standard was loaded onto the gels. Gels were then dried and protein phosphorylation was detected by exposure of the gels to a Storage Phosphor Screen. Phosphorylated proteins were quantified by image analysis using Image Quant® software (GE Healthcare, Freiburg, Germany).

#### 4.12 Determination of extracellular and intracellular $\text{K}^+$ concentrations

$\text{K}^+$  concentrations were determined by atomic absorption spectroscopy (Bossemeyer *et al.*, 1989). Briefly, *E. coli* MG1655 (Table S1) was cultivated in minimal medium containing 10 mM  $\text{K}^+$  (Epstein & Kim, 1971). Cells were collected by centrifugation and transferred into pre-warmed minimal medium containing 0.1, 1 and 10 mM  $\text{K}^+$ , respectively, and then incubated aerobically at 37°C for 2 h. Aliquots (1 ml) were taken and centrifuged through 200  $\mu\text{l}$  of silicone oil (DC550, Serva) at 13,000 rpm for 2 min. The  $\text{K}^+$  content of the cell pellets and the supernatants was then determined in an atomic absorption spectrometer (Varian AA240 Spectroscopy Instrument, Agilent Technologies, Böblingen). To determine the fraction of bound and freely diffusible  $\text{K}^+$ , 0.5-ml samples were collected and diluted in either 0.5 ml of medium (total  $\text{K}^+$ ) or 0.5 ml  $\text{d}_2\text{H}_2\text{O}$  (bound  $\text{K}^+$ ) (Bossemeyer *et al.*, 1989). After centrifugation through silicone oil, the  $\text{K}^+$  content of the cell pellets was determined by atomic absorption spectroscopy. The fraction of free  $\text{K}^+$  is defined as the difference between the total  $\text{K}^+$  content and the bound  $\text{K}^+$  content. The intracellular concentrations were calculated by taking the number of cells per sample and the cytoplasmic

volumes into account. Since it has been shown that cell volumes remain more or less constant during the experiments, an average value of  $8.12 \times 10^{-16}$  l per cell was used in all calculations (Heermann *et al.*, 2014).

#### **4.13 Determination of KdpFABC production by quantitative Western blot analysis.**

Levels of KdpFABC in *E. coli* strains were determined by quantitative Western blot analysis. *E. coli* strains LF3, HS2, HS3, and HS4 (Table S1) were grown aerobically at 37°C to  $OD_{600}=0.5$  in minimal media containing 10 mM  $K^+$  (Epstein & Kim, 1971). Then the cells were shifted to minimal medium containing the indicated  $K^+$  concentrations. After 2 h the  $OD_{600}$  was adjusted to 1 and aliquots of the cultures were collected by centrifugation. Cells were resuspended in SDS sample buffer and subjected to SDS- polyacrylamide gel electrophoresis. Proteins were electroblotted onto a nitrocellulose membrane, and the blots were blocked with 5% (w/v) skim milk in buffer A (10 mM Tris/HCl pH 7.4, 0.15 M NaCl) for 1 h. Anti-KdpB antibody (Heermann *et al.*, 2009b) was added at a final dilution of 1:10,000 and incubation was continued for 1 h. After washing with buffer A, goat anti-(rabbit IgG) conjugated with alkaline phosphatase was added in a final dilution of 1:2,500, and incubation was continued for 1 h. After washing thoroughly, blots were developed with substrate solution [50 mM  $Na_2CO_3$ , pH 9.5, 0.01% (w/v) nitro-blue-tetrazolium, 5 mg/ml 5-bromo-4-chloro-3-indoly]phosphate]. Blots were scanned at high resolution in 256 grey scales, imported as TIF files into ImageJ, and the amount of KdpB was quantified. For each biological replicate we calibrated the mean of two technical replicates using previously measured molecule numbers (Heermann *et al.*, 2014), by finding a linear scaling coefficient that minimized the total squared deviation for the wild-type strain at the  $K^+$  concentrations for which measurements were available in both data sets. The scaling coefficient was applied to all samples on a given blot. Data represent the average values and standard deviation of three independent biological replicates.

#### **4.14 Synthesis of radiolabelled acetyl phosphate**

Acetyl[ $^{32}P$ ]phosphate was synthesised using a modified protocol as described previously (Stadtman, 1957) and was dissolved in a buffer (50 mM Tris-HCl [pH 7.5], 5% [v/v] glycerol, 0.1 mM EDTA, 1 mM DTT). The concentration was determined as described previously (Lipmann & Tuttle, 1945). Phosphorylation of 0.2 mg/ml 6His-KdpE<sup>Ec</sup> and 0.5 mg/ml 6His-KdpE<sup>Sa</sup> was performed at 30°C with 20 mM  $MgCl_2$  and 20 mM acetyl[ $^{32}P$ ]phosphate for 60 min. The reaction was stopped by adding SDS sample buffer. Samples were loaded onto an

SDS-polyacrylamide gel. Phosphorylated KdpE was detected by after exposure to a phosphor screen.

#### **4.15 Analytical Procedures**

The concentration of soluble proteins was determined as described by Lowry (Lowry *et al.*, 1951) and for membrane proteins using a modified Lowry method (Peterson, 1977), using bovine albumin as a standard. Immunodetection of KdpD was performed with polyclonal antibodies against KdpD as previously described (Voelkner *et al.*, 1993).

#### **4.16 Bacterial adenylate cyclase two-hybrid assay (BACTH)**

Protein-protein interactions were assayed with the bacterial adenylate cyclase based two-hybrid system (BACTH) essentially as described previously (Karimova & Ladant, 2005). *E. coli* BTH101 was transformed with different pUT18, pUT18C and pKT25 derivatives (Table S2) to test for interactions. We used pUT18C and pKT25 as negative control and the leucine zipper fusion constructs as positive control, respectively (Table S2). Cells were grown under aeration for 48 hours in LB medium supplemented with appropriate antibiotics and 0.5 mM isopropyl- $\beta$ -D-thiogalactopyranoside (IPTG) at 25°C. Subsequently cells were harvested for determination of  $\beta$ -galactosidase activities, which are given in Miller units (Miller, 1992). For bacterial adenylate cyclase two-hybrid assays on plates 1.5% (w/v) agar was added to the indicated medium, which additionally contained 0.4% (w/v) glucose, 0.5 mM isopropyl- $\beta$ -D-thiogalactopyranoside (IPTG), 100  $\mu$ g/ml ampicillin, 50  $\mu$ g/ml kanamycin and 40  $\mu$ g/ml 5-bromo-4-chloro-3-indolyl- $\beta$ -D-galactopyranoside (final concentrations). After washing cells from overnight cultures with TMA medium without KCl and Na<sub>2</sub>HPO<sub>4</sub>, equal cell counts were dropped on the plates and incubated at 25°C for 72 hours.

#### **4.17 Structural modelling**

The structure of the GAF domain was modelled using HHPred (Söding *et al.*, 2005). Homology detection was performed using amino acids sequence H514-E651 and subsequently the tertiary structure was modelled using 3E0Y as a template. Additionally, we developed a structural model of the GAF domain using Phyre2 (Kelley & Sternberg, 2009) to identify potential interaction sites between between the GAF domain and the cluster of arginines located on the extended transmembrane helix four (R506, R508, R511). All structural models were visualized with the UCSF Chimera program (Pettersen *et al.*, 2004).

#### 4.18 Fitting of autokinase and phosphatase $K^+$ dependency

Fitting of autokinase and phosphatase  $K^+$  dependency was done by Filipe Tostevin. In order to determine the initial reaction rate, samples were taken after 10 and 20 sec for the autokinase activity and after 1 and 2 min to determine  $K^+$ -dependent dephosphorylation of KdpE. This slope was used as a measure of the enzymatic activity. To minimize day-to-day variability, the activities in each replicate data set were scaled by a constant factor, chosen to minimize the mean-squared deviation between all data sets (3 independent experiments for autokinase activity of wild-type KdpD; 2 independent experiments each for phosphatase activity of wild-type KdpD, KdpD/ $\Delta$ 2-498, and KdpD<sup>1</sup>). The different data sets were then pooled, and non-linear least-squares fitting was performed on the pooled data via the Levenberg-Marquardt method. For autokinase activity of wild-type KdpD model of the form  $c_1 + c_2 \frac{K_{0.5}}{[K^+] + K_{0.5}}$  was assumed. The resulting best-fit parameter values were  $c_1=0.18$  a.u.,  $c_2=0.82$  a.u.,  $K_{0.5}=2.7$  mM. A model of the form  $c_1 + c_2 \frac{[K^+]}{[K^+] + K_{0.5}}$  was used for fitting of the phosphatase activity. Best-fit parameter values were, for wild-type KdpD:  $c_1=0.25$  a.u.,  $c_2=0.75$  a.u.,  $K_{0.5}=4.2$  mM; for KdpD/ $\Delta$ 2-498:  $c_1=0.11$  a.u.,  $c_2=0.89$  a.u.,  $K_{0.5}=34$  mM; for KdpD<sup>1</sup>:  $c_1=0.33$  a.u.,  $c_2=0.67$  a.u.,  $K_{0.5}=32$  mM. Confidence regions were estimated by randomly sampling parameter space and including or excluding parameter sets according to F-test relative to the best-fit parameters.

#### 4.19 Mathematical model – KdpD switching dynamics

The mathematical model was developed by Filipe Tostevin and Ulrich Gerland. The enzymatic activities of KdpD were modeled by assuming that the protein has three conformational states, which were labelled as  $K$ ,  $P$  and  $O$ . The occupancy of these states across the population of KdpD molecules is assumed to be in a dynamic equilibrium (see Figure S1A). The autokinase activity is taken to be proportional to the probability of the system to be in the  $K$  state, while the phosphatase activity is proportional to the probability of being in the  $P$  state. The occupancies are given, in terms of the equilibrium constants of the transitions to and from the catalytically inactive  $O$  state, by  $\varphi_K = \frac{K_2}{K_1 + K_2 + K_1 K_2}$ ,  $\varphi_P = \frac{K_1}{K_1 + K_2 + K_1 K_2}$ . Considering the requirement for external  $K^+$  sensing for autokinase activity regulation, and that phosphatase regulation does not require external  $K^+$  sensing, the equilibrium constants were taken to depend on different  $K^+$  pools according to  $K_1([K_{ex}^+]) = \frac{a_k + b_k [K_{ex}^+]}{c_k + [K_{ex}^+]}$ ,  $K_2([K_{in}^+]) = \frac{a_p + b_p [K_{in}^+]}{c_p + [K_{in}^+]}$ .

To estimate the parameters appearing in these equilibrium constants the *in vitro* measured activity data were used. Substituting the above expressions for  $K_1$  and  $K_2$  into  $\varphi_K$  and  $\varphi_P$ , the result is a two-dimensional regulation function for each enzymatic activity. However, out *in vitro* activity measurements do not span this input space, as it is not possible to selectively apply different  $K^+$  concentrations to the extracellular and intracellular portions of the protein. The *in vitro* activity measurements for wild-type KdpD provide us with the values of the enzymatic activities only along one lines in input space, namely  $[K_{\text{ex}}^+] = [K_{\text{in}}^+]$ . However, it was reasoned that the activity of the KdpD<sup>1</sup> variant that is insensitive to extracellular  $K^+$ , is equivalent to the enzymatic activities along the line  $[K_{\text{ex}}^+] = 0$  (see Figure S1).

The values of the parameters were estimated that best reproduced the activity regulation *in vitro* by simultaneous least-squares fitting to the autokinase and phosphatase data from wild-type KdpD and KdpD<sup>1</sup> (Figure 2.1-1C&D, Figure 2.1-2B and Figure 2.1-6). Since the enzymatic activity measurements cannot identify the actual occupancy of each state, but only relative changes in occupancy, additional weighting factors  $\alpha_k$  and  $\alpha_p$  were introduced to account for the scaling of occupancy to activity. Ultimately, therefore, the Levenberg-Marquardt method was used to estimate the parameters that minimize the function

$$\sum_{i \in \text{data points}} \left[ \frac{\varphi_K([K_i^+], [K_i^+])}{\alpha_k} - k_i^{\text{WT}} \right]^2 + \sum_{i \in \text{data points}} \left[ \frac{\varphi_P([K_i^+], [K_i^+])}{\alpha_p} - p_i^{\text{WT}} \right]^2 + \sum_{i \in \text{data points}} \left[ \frac{\varphi_K(0, [K_i^+])}{\alpha_k} - k_i^1 \right]^2 + \sum_{i \in \text{data points}} \left[ \frac{\varphi_P(0, [K_i^+])}{\alpha_p} - p_i^1 \right]^2,$$

where  $k_i$  and  $p_i$  are the individual autokinase and phosphatase activity measurements, and the superscript denotes either wild-type or the KdpD<sup>1</sup> variant. The resulting best-fit parameter values (Figure S1) were  $a_k=18.4$  mM,  $b_k=11.7$ ,  $c_k=9.09$  mM,  $\alpha_k=0.31$ ,  $a_p=59.3$  mM,  $b_p=4.35$ ,  $c_p=4.76$  mM,  $\alpha_p=0.16$ .

**Mathematical model - *in vitro*.** A model of KdpD/KdpE phosphorylation was developed that was consistent with the dynamics measured *in vitro* for all KdpD variants. The proposed phosphorylation and phosphotransfer reactions were incorporated into a pair of differential equations describing how the concentration of phosphorylated KdpD (Dp) and phosphorylated KdpE (Ep) changes over time:

$$\frac{dDp}{dt} = \frac{\kappa_{\text{auto}}}{v} \left[ \varphi_K((1 - \delta_1)[K^+], [K^+]) (Dt_{\text{tot}} - Dp) - K_{\text{auto}} Dp \right] - \frac{\kappa_{\text{trans}}}{1 + \delta_2 \gamma} [Dp (Et_{\text{tot}} - Ep) - K_{\text{trans}} (Dt_{\text{tot}} - Dp) Ep], \quad (1)$$

$$\frac{dEp}{dt} = \frac{\kappa_{\text{trans}}}{1+\delta_2\gamma} [Dp(E_{\text{tot}} - Ep) - K_{\text{trans}}(D_{\text{tot}} - Dp)Ep] - \kappa_p \varphi_p((1 - \delta_1)[K^+], [K^+])(D_{\text{tot}} - Dp)Ep. \quad (2)$$

Here  $D_{\text{tot}}$  and  $E_{\text{tot}}$  denote the total concentrations of KdpD and KdpE in the system and  $v$  is the relative system volume. The first two reactions in Eq. 1 describe the reversible phosphorylation of KdpD. It was assumed that KdpD molecules in the  $K$  state undergo autophosphorylation (Figure 2.1-8A) with a rate that depends on the ATP concentration (see below). Phosphorylated KdpD cannot catalyze any reaction but phosphotransfer to KdpE. The last two terms in Eq. 1 and the corresponding complementary terms in Eq. 2 describe the reversible phosphotransfer between KdpD and KdpE. Phosphotransfer is assumed to occur at a constant rate, insensitive to  $K^+$ . Following phosphotransfer, unphosphorylated KdpD rapidly equilibrates between the three conformational states (Figure 2.1-8A). Finally, the last term of Eq. 2 models dephosphorylation of phospho-KdpE by KdpD; it was assumed that only unphosphorylated KdpD acts as a phosphatase in this reaction. The influence of  $K^+$  on the enzymatic activity is introduced via the occupancy functions  $\varphi_K$  and  $\varphi_P$ , described above. Since in our *in vitro* assay both the periplasmic and cytoplasmic sides of the KdpD protein are exposed to the same medium, the same  $[K^+]$  for both external and internal sensing was used. The KdpD<sup>2</sup> mutation in the state-switching model was simulated by assuming that the  $P$  conformation was inaccessible, and recalculating the occupancy of the  $K$  state according to  $K_1([K^+_{\text{ex}}])$  only.

The indicator functions  $\delta_i$  are used to denote variants of the KdpD protein, with  $\delta_1=1$  if KdpD carries the amino-acid substitutions of variant 1 (KdpD<sub>1</sub> or KdpD<sub>1+2</sub>) and  $\delta_1=0$  otherwise (wild-type or KdpD<sub>2</sub>), and similarly for variant 2. It was found that removal of KdpD autokinase activity in the model was not sufficient to reproduce the experimental results for the KdpD<sup>2</sup> and KdpD<sup>1+2</sup> variants, resulting in a faster decrease in the level of phospho-KdpD upon addition of KdpE than observed experimentally. Agreement with experiment was improved only if variation 2 was allowed, in addition to eliminating KdpD phosphatase activity, to alter the rates of phosphotransfer between KdpD and KdpE compared to wild-type. This is incorporated via the parameter  $\gamma$ . Such an effect may arise, for example, because the variation also indirectly changes the KdpD-KdpE binding affinity. Initially  $Dp=E_{\text{tot}}=Ep=0$   $\mu\text{M}$ ,  $D_{\text{tot}}=2$   $\mu\text{M}$  were set and  $v=1$  at time  $t=0$ . To model the later addition of KdpE  $E_{\text{tot}}=8$   $\mu\text{M}$  at  $t=3.5$  min was set. The addition of KdpE also doubles the volume of the system; therefore at this time also the concentrations  $[K^+]$ ,  $D_{\text{tot}}$  and  $Dp$  was halved and set  $v=2$ . The inclusion of the factor  $v^{-1}$  in the first term of Eq. 1 models the slowing down of KdpD (de-)phosphorylation due to the dilution of ATP and ADP in the medium.

The values of the kinetic rate parameters  $\kappa_{\text{auto}}$ ,  $\kappa_{\text{trans}}$  and  $\kappa_{\text{p}}$ , equilibrium constants  $K_{\text{auto}}$  and  $K_{\text{trans}}$ , and variant effect  $\gamma$ , were determined by Monte Carlo fitting to the experimental data. Initial trial parameter values were chosen from a log-normal distribution with median 1 and scale parameter  $\sigma=5$ . The trajectory of the system was evaluated for these parameters, and the total squared deviation from the experimental time-course data weighted by the data value,  $Z^2 = \sum_{i \in \text{data points}} \frac{(x^{(i)}_{\text{experiment}} - x^{(i)}_{\text{model}})^2}{x^{(i)}_{\text{experiment}}}$ , was determined. The value of one randomly chosen parameter was then multiplied by a factor  $e^{\xi}$  with  $\xi$  chosen from a Gaussian distribution with zero mean and standard deviation 0.1. The trajectories and deviation  $Z$  were then re-evaluated for the new parameter set. If the new parameters did not provide an improved fit (i.e. if they resulted in a larger  $Z$ ), then the parameters were reverted to their previous value and a new random modification was made; otherwise, the current parameters were retained and modified in the next round. This procedure was repeated for a total of  $10^6$  iterations. It revealed that a small fraction of optimization runs (~5%) became trapped in poorly-fitting regions of parameter space, while the majority of realizations converged to a single consensus parameter set ( $\kappa_{\text{auto}}=0.19 \text{ min}^{-1}$ ,  $K_{\text{auto}}=0.47$ ,  $\kappa_{\text{trans}}=4.3 \mu\text{M}^{-1} \text{ min}^{-1}$ ,  $K_{\text{trans}}=0.25$ ,  $\gamma=14$  and  $\kappa_{\text{p}}=8.9 \mu\text{M}^{-1} \text{ min}^{-1}$ ) when initialized with a range of initial parameter combinations.

**Mathematical model – *in vivo* model and parameter fitting.** In the *in vivo* model the same reactions scheme as above was used to describe the dynamics of KdpD/KdpE phosphorylation. However, now the different pools of extracellular and intracellular  $\text{K}^+$  were introduced. As most intracellular  $\text{K}^+$  is bound to macromolecules, it is important to distinguish between bound and free ions when considering the effects of intracellular  $\text{K}^+$ . To this end a linear relationship  $[\text{K}^+_{\text{free}}] = f_0 + f_{\text{free}}[\text{K}^+_{\text{in}}]$  was fitted to the experimentally-measured intracellular total and free  $\text{K}^+$  concentrations using the Deming method with the residuals at each point weighted by the corresponding variance in the experimental measurements. The resulting best fit parameters were  $f_0=-14 \text{ mM}$  and  $f_{\text{free}}=0.27$  (Figure S2). For any  $[\text{K}^+_{\text{in}}]$  that this relationship indicated a negative  $[\text{K}^+_{\text{free}}]$ ,  $[\text{K}^+_{\text{free}}]$  was set equal to zero. The KdpD/KdpE phosphotransfer reactions therefore became

$$\frac{dDp}{dt} = \kappa_{\text{auto}} \left[ \varphi_{\text{K}} \left( (1 - \delta_1) [\text{K}^+_{\text{ex}}], [\text{K}^+_{\text{free}}] \right) (D_{\text{tot}} - Dp) - K_{\text{auto}} Dp \right] - \frac{\kappa_{\text{trans}}}{1 + \delta_2 \gamma} [Dp(E_{\text{tot}} - E_p) - K_{\text{trans}}(D_{\text{tot}} - Dp)E_p], \quad (3)$$

$$\frac{dE_p}{dt} = \frac{\kappa_{\text{trans}}}{1 + \delta_2 \gamma} [Dp(E_{\text{tot}} - E_p) - K_{\text{trans}}(D_{\text{tot}} - Dp)E_p] - \kappa_{\text{p}} \varphi_{\text{P}} \left( (1 - \delta_1) [\text{K}^+_{\text{ex}}], [\text{K}^+_{\text{free}}] \right) (D_{\text{tot}} - Dp)E_p. \quad (4)$$

It was assumed that the total concentration of KdpD and KdpE are constant, and set these values to  $D_{tot}=0.04 \mu\text{M}$ ,  $E_{tot}=0.08 \mu\text{M}$  (Surmann *et al.*, 2014). These equations were then supplemented by a model of KdpFABC production,  $\text{K}^+$  import, and population growth.

As described in chapter 1.2,  $\text{K}^+$  ions are imported into the cell by the high-affinity (HA) KdpFABC transporter and by constitutively produced low-affinity (LA) transporters. The rates of each of these reactions were described as a Michaelis-Menten function of the external  $\text{K}^+$  concentration,  $[\text{K}_{ex}^+]$ , such that  $[\text{K}_{in}^+]$  evolves according to

$$\frac{d[\text{K}_{in}^+]}{dt} = v_{LA} \frac{[\text{K}_{ex}^+]}{[\text{K}_{ex}^+] + K_{m,LA}} + v_{HA} F \frac{[\text{K}_{ex}^+]}{[\text{K}_{ex}^+] + K_{m,HA}} - \mu[\text{K}_{in}^+], \quad (5)$$

where  $F$  is the concentration of KdpFABC transporters. The transporter affinities have been estimated previously and are set to  $K_{m,LA}=2 \text{mM}$  and  $K_{m,HA}=2 \mu\text{M}$  (Schlösser *et al.*, 1995, Rhoads *et al.*, 1976). It was assumed that export of  $\text{K}^+$  is negligible under our experimental conditions. The final term in Eq. 5 models dilution of  $\text{K}^+$  by population growth with growth rate  $\mu$ . The depletion of  $\text{K}^+$  from the environment was described by the complement of the transport terms in Eq. 5, but scaled by the ratio of total cell volume to system volume,  $V(\ll 1)$ ,

$$\frac{d[\text{K}_{ex}^+]}{dt} = -V \left[ v_{LA} \frac{[\text{K}_{ex}^+]}{[\text{K}_{ex}^+] + K_{m,LA}} + v_{HA} F \frac{[\text{K}_{ex}^+]}{[\text{K}_{ex}^+] + K_{m,HA}} \right]. \quad (6)$$

Next the regulation of KdpFABC levels was considered. Phospho-KdpE dimerizes and binds to the *kdpFABC* promoter, thereby activating the transcription of the *kdpFABC* operon encoding the high-affinity  $\text{K}^+$  transporter complex (Nakashima *et al.*, 1993). It was assumed that both the dimerization of phospho-KdpE and the binding to DNA are fast, and thus simply the probability that the *kdpFABC* activator site is bound at any time was taken to be given by

$$p(\text{Ep}) = \frac{\text{Ep}^2}{\text{Ep}^2 + K_{\text{DNA}}^2}. \quad (7)$$

$K_{\text{DNA}}=0.25 \mu\text{M}$  was taken, in the range of previous measurements (Narayanan *et al.*, 2012). It was then assumed that the concentration of KdpFABC transporters,  $F$ , evolves according to

$$\frac{dF}{dt} = k_{tr} p(\text{Ep}) - [\mu + k_{deg}(F)]F. \quad (8)$$

For simplicity transcription and translation in detail was not modelled, but rather assumed that KdpFABC is produced at an effective production rate  $k_{tr}$  when KdpE binds to the *kdpFABC* promoter. The second term in Eq. 8 accounts for both dilution due to growth, and potentially non-linear turnover of KdpFABC (Heermann *et al.*, 2014) with rate

$$k_{\text{deg}}(F) = k_{\text{deg},0} + k_{\text{deg},F}F. \quad (9)$$

Finally, the growth of the population over time was accounted. It was assumed that the cell mass, or equivalently the volume fraction, increases according to

$$\frac{dV}{dt} = \mu V. \quad (10)$$

Since the detailed effects of changing intracellular  $K^+$  concentration on population growth are not known, a phenomenological growth model was used wherein the growth rate depends on the intracellular  $K^+$  concentration according to  $\mu([K_{\text{in}}^+]) = \mu_{\text{max}} \frac{[K_{\text{in}}^+]^3}{[K_{\text{in}}^+]^3 + K_{\mu}^3}$ . This form together with the parameter values  $\mu_{\text{max}} = 0.011 \text{ min}^{-1}$  and  $K_{\mu} = 70 \text{ mM}$  were chosen such that the resulting population dynamics match the experimentally measured growth curves when the simulated intracellular  $K^+$  concentration also follows the corresponding experimentally observed values.

Once again parameter combinations were sought that give the best fit to the experimental data. For this purpose the four data sets describing the *in vivo* response were used that are shown in Figure 2.1-8: time-course measurements of (i) intracellular and (ii) extracellular  $K^+$  concentrations and (iii)  $\text{OD}_{600}$ , for initial environmental  $K^+$  concentrations of 10 mM, 1 mM and 0.1 mM; and (iv) KdpFABC protein copy numbers two hours after transfer to media with varying environmental  $K^+$  levels. Since it would not be expected that the parameters for the KdpD/KdpE phosphorylation reactions *in vivo* match with their *in vitro* values, these were initialized with their *in vitro* values but were subsequently allowed to vary. The additional parameters remaining to be determined that could not be estimated from previous measurements were: the transporter rates  $v_{\text{LA}}$  and  $v_{\text{HA}}$ ; the maximal KdpFABC production rate  $k_{\text{tr}}$ ; and the parameters of the KdpFABC degradation function,  $k_{\text{deg},0}$  and  $k_{\text{deg},F}$ . A similar optimization procedure was employed as described above for the *in vivo* model. However, rather than the score function  $Z$  described above, the residual of the model was scaled from the data by the experimental uncertainty:

$$Z^2 = \sum_{i \in \text{data points}} \frac{(x(i)_{\text{model}} - x(i)_{\text{experiment}})^2}{\sigma(i)_{\text{experiment}}^2},$$

where  $x(i)_{\text{experiment}}$  and  $\sigma(i)_{\text{experiment}}$  are respectively the mean and standard deviation of the experimental data and the sum runs over all data sets described above.

All simulations of the *in vivo* model were initialized with  $D_p = E_p = 0$ ,  $[K_{\text{in}}^+] = 250 \text{ mM}$ ,  $F = 0$ , and  $V = 2 \times 10^{-4}$ . The value of the volume fraction  $V$  was subsequently scaled by a factor 1150 to match the scale of  $\text{OD}_{600}$  measurements. To mimic the preparation of cells in overnight culture with abundant  $K^+$  then the model equations were evolved, but without depletion of extracellular

$K^+$  or population growth (i.e.  $\frac{d[K_{ex}^+]}{dt} = \frac{dV}{dt} = 0$ ), for 12 hours of simulated time in an environment with constant extracellular concentration  $[K_{ex}^+] = 10$  mM. After this time,  $[K_{ex}^+]$  was changed to the value of interest and the evolution of the extracellular concentration and population size were activated.

Multiple runs of the optimization procedure were again performed with different initial trial parameters. The best-fit set of parameters, used in Figure 2.1-8 and Figure 2.1-10, was as follows:  $\kappa_{auto} = 0.76 \text{ min}^{-1}$ ,  $K_{auto} = 0.18$ ,  $\kappa_{trans} = 1.1 \times 10^4 \mu\text{M}^{-1} \text{ min}^{-1}$ ,  $K_{trans} = 0.34$ ,  $\gamma = 0$  and  $\kappa_p = 32 \mu\text{M}^{-1} \text{ min}^{-1}$ ;  $v_{LA} = 2.3 \text{ mM min}^{-1}$ ,  $v_{HA} = 0.40 \mu\text{M min}^{-1}$ ;  $k_{tr} = 5400 \text{ min}^{-1}$ ,  $k_{deg,0} = 0.006 \text{ min}^{-1}$  and  $k_{deg,F} = 4.4 \times 10^{-7} \text{ min}^{-1}$ . Of these parameters, those governing the rate of transport of  $K^+$  were well constrained by the data, and produced consistent values across all realizations. Parameters describing *kdpFABC* expression and turnover were less restricted in their absolute values, although the ratios  $k_{tr}/k_{deg}$  lay in narrow range. Among the parameters describing KdpD/KdpE phosphorylation, it was found that the equilibrium constants  $K_{auto}$  and  $K_{trans}$  were precisely determined, as was  $\gamma$ . However, since the *in vitro* data provides no information about the phosphorylation dynamics per se, the kinetic rates of the various phosphorylation reactions were largely unconstrained by the data, and took a wide range of values in different realizations.

**Alternate regulation strategies.** To test different regulation strategies, the model equations were altered as follows. For the wild-type dual-sensing strategy (DUAL) the KdpD regulation functions were used described above. For the external regulation strategy (EX), the equilibrium constants of the switching model were set to  $K_1^{EX}([K_{ex}^+]) = K_1^{DUAL}([K_{ex}^+])$ ,  $K_2^{EX} = K_2^{DUAL}(46 \text{ mM})$ . For the internal regulation strategy (IN), the autokinase activity the equilibrium constants were  $K_1^{IN} = K_1^{DUAL}(2 \text{ mM})$ ,  $K_2^{IN}([K_{free}^+]) = K_2^{DUAL}([K_{free}^+])$ . The constant activity values were chosen such that the activity of the EX and IN variants coincide with the DUAL strategy for an environmental  $K^+$  concentration of 2 mM, which lies within the range of  $K^+$  levels at which induction of *kdpFABC* expression was observed (Figure 2.1-8C).

To study the steady state output of Kdp regulation, the model was again initialized with  $Dp = Ep = 0$ ,  $[K_{in}^+] = 250 \text{ mM}$ ,  $F = 0$ ,  $V = 2 \times 10^{-4}$ , but now with  $[K_{ex}^+]$  set to the indicated value. The dynamics were then simulated for each of the regulation strategies for a period of 120 hours without depletion of  $[K_{ex}^+]$  or growth ( $\frac{d[K_{ex}^+]}{dt} = \frac{dV}{dt} = 0$ ).

To simulate the competition between different regulation strategies, simulations were set up consisting of a copy of the variables  $\{Dp_s, Ep_s, F_s, [K_{in}^+]_s, V_s\}$  together with their associated dynamics for each of the three strategies,  $s \in \{\text{DUAL}, \text{EX}, \text{IN}\}$ , and a single shared environment

$[K_{ex}^+]$ . Simulations were initialized with  $\{Dp_s=Ep_s=0, [K_{in}^+]_s=250 \text{ mM}, F_s=0, V_s=(2/3)\times 10^{-4}\}$  for all strategies in an environment  $[K_{ex}^+]=5 \text{ mM}$  and again run for 12 hours with  $\frac{d[K_{ex}^+]}{dt} = \frac{dV_s}{dt} = 0$ . Subsequently growth and depletion of environmental  $[K_{ex}^+]$  was re-enabled and the simulation was switched to random environments. A random new  $[K_{ex}^+]$  value was selected from an exponential distribution with parameter  $\lambda=(2/\ln(2)) \text{ mM}$  chosen such that the median concentration equals the point at which the three strategies show matching activities. A new maximal growth rate parameter  $\mu_{max}$  (common to all strategies) was selected from a uniform distribution over the range  $0.25\text{-}2 \text{ h}^{-1}$ . The duration of this environment was chosen from an exponential distribution with mean  $\tau=90 \text{ min}$ . After this amount of simulation time had elapsed a new environment described by a set of  $[K_{ex}^+]$ ,  $\mu_{max}$  and  $\tau$  were selected. In addition, in order to keep the cell density manageable, each time that a new environment was generated the total population was re-diluted back to the initial density but maintaining the relative abundance of cells with each strategy,  $V_s \rightarrow \left(\frac{V_s}{\sum_s V_s}\right)\times 2\times 10^{-4}$  for each strategy  $s$ .

## 5 References

- Ahnert, F., R. Schmid, K. Altendorf & J.C. Greie, (2006) ATP binding properties of the soluble part of the KdpC subunit from the *Escherichia coli* K<sup>+</sup>-transporting KdpFABC P-type ATPase. *Biochemistry* **45**: 11038-11046.
- Alves, R. & M.A. Savageau, (2003) Comparative analysis of prototype two-component systems with either bifunctional or monofunctional sensors: differences in molecular structure and physiological function. *Mol Microbiol* **48**: 25-51.
- Amemura, M., K. Makino, H. Shinagawa, A. Kobayashi & A. Nakata, (1985) Nucleotide sequence of the genes involved in phosphate transport and regulation of the phosphate regulon in *Escherichia coli*. *J Mol Biol* **184**: 241-250.
- Anantharaman, V., S. Balaji & L. Aravind, (2006) The signaling helix: a common functional theme in diverse signaling proteins. *Biol Direct* **1**: 25.
- Aravind, L. & C.P. Ponting, (1997) The GAF domain: an evolutionary link between diverse phototransducing proteins. *Trends Biochem Sci* **22**: 458-459.
- Asha, H. & J. Gowrishankar, (1993) Regulation of *kdp* operon expression in *Escherichia coli*: evidence against turgor as signal for transcriptional control. *J Bacteriol* **175**: 4528-4537.
- Baba, T., T. Ara, M. Hasegawa, Y. Takai, Y. Okumura, M. Baba, K.A. Datsenko, M. Tomita, B.L. Wanner & H. Mori, (2006) Construction of *Escherichia coli* K-12 in-frame, single-gene knockout mutants: the Keio collection. *Mol Syst Biol* **2**: 2006 0008.
- Bai, Y., J. Yang, T.M. Zarrella, Y. Zhang, D.W. Metzger & G. Bai, (2014) Cyclic di-AMP impairs potassium uptake mediated by a cyclic di-AMP binding protein in *Streptococcus pneumoniae*. *J Bacteriol* **196**: 614-623.
- Banerjee, A., R.S. Adolph, J. Gopalakrishnapai, S. Kleinboelting, C. Emmerich, C. Steegborn & S.S. Visweswariah, (2015) A Universal Stress Protein (USP) in Mycobacteria Binds cAMP. *J Biol Chem* **290**: 12731-12743.
- Batchelor, E. & M. Goulian, (2003) Robustness and the cycle of phosphorylation and dephosphorylation in a two-component regulatory system. *Proc Natl Acad Sci U S A* **100**: 691-696.
- Beier, D. & R. Gross, (2006) Regulation of bacterial virulence by two-component systems. *Curr Opin Microbiol* **9**: 143-152.
- Bhate, M.P., K.S. Molnar, M. Goulian & W.F. DeGrado, (2015) Signal transduction in histidine kinases: insights from new structures. *Structure* **23**: 981-994.
- Blattner, F.R., G. Plunkett, 3rd, C.A. Bloch, N.T. Perna, V. Burland, M. Riley, J. Collado-Vides, J.D. Glasner, C.K. Rode, G.F. Mayhew, J. Gregor, N.W. Davis, H.A. Kirkpatrick, M.A. Goeden, D.J. Rose, B. Mau & Y. Shao, (1997) The complete genome sequence of *Escherichia coli* K-12. *Science* **277**: 1453-1462.
- Booth, I.R., (1985) Regulation of cytoplasmic pH in bacteria. *Microbiol Rev* **49**: 359-378.
- Bossemeyer, D., A. Borchard, D.C. Dosch, G.C. Helmer, W. Epstein, I.R. Booth & E.P. Bakker, (1989) K<sup>+</sup>-transport protein TrkA of *Escherichia coli* is a peripheral membrane protein that requires other *trk* gene products for attachment to the cytoplasmic membrane. *J Biol Chem* **264**: 16403-16410.
- Bramkamp, M., K. Altendorf & J.C. Greie, (2007) Common patterns and unique features of P-type ATPases: a comparative view on the KdpFABC complex from *Escherichia coli* (Review). *Mol Membr Biol* **24**: 375-386.
- Brandon, L., S. Dorus, W. Epstein, K. Altendorf & K. Jung, (2000) Modulation of KdpD phosphatase implicated in the physiological expression of the Kdp ATPase of *Escherichia coli*. *Mol Microbiol* **38**: 1086-1092.

## References

- Bren, A., Y. Hart, E. Dekel, D. Koster & U. Alon, (2013) The last generation of bacterial growth in limiting nutrient. *BMC Syst Biol* **7**: 27.
- Calva, E. & R. Oropeza, (2006) Two-component signal transduction systems, environmental signals, and virulence. *Microb Ecol* **51**: 166-176.
- Cann, M., (2007a) A subset of GAF domains are evolutionarily conserved sodium sensors. *Mol Microbiol* **64**: 461-472.
- Cann, M.J., (2007b) Sodium regulation of GAF domain function. *Biochem Soc Trans* **35**: 1032-1034.
- Corrigan, R.M., J.C. Abbott, H. Burhenne, V. Kaefer & A. Gründling, (2011) c-di-AMP is a new second messenger in *Staphylococcus aureus* with a role in controlling cell size and envelope stress. *PLoS Pathog* **7**: e1002217.
- Corrigan, R.M., L. Bowman, A.R. Willis, V. Kaefer & A. Gründling, (2015) Cross-talk between two nucleotide-signaling pathways in *Staphylococcus aureus*. *J Biol Chem* **290**: 5826-5839.
- Corrigan, R.M., I. Campeotto, T. Jeganathan, K.G. Roelofs, V.T. Lee & A. Gründling, (2013) Systematic identification of conserved bacterial c-di-AMP receptor proteins. *Proc Natl Acad Sci U S A* **110**: 9084-9089.
- Corrigan, R.M. & A. Gründling, (2013) Cyclic di-AMP: another second messenger enters the fray. *Nat Rev Microbiol* **11**: 513-524.
- Crépin, S., S.M. Chekabab, G. Le Bihan, N. Bertrand, C.M. Dozois & J. Harel, (2011) The Pho regulon and the pathogenesis of *Escherichia coli*. *Vet Microbiol* **153**: 82-88.
- Cromie, M.J., Y. Shi, T. Latifi & E.A. Groisman, (2006) An RNA sensor for intracellular  $Mg^{2+}$ . *Cell* **125**: 71-84.
- Datsenko, K.A. & B.L. Wanner, (2000) One-step inactivation of chromosomal genes in *Escherichia coli* K-12 using PCR products. *Proc Natl Acad Sci U S A* **97**: 6640-6645.
- Durell, S.R., E.P. Bakker & H.R. Guy, (2000) Does the KdpA subunit from the high affinity  $K^{+}$ -translocating P-type KDP-ATPase have a structure similar to that of  $K^{+}$  channels? *Biophys J* **78**: 188-199.
- Dutta, R., L. Qin & M. Inouye, (1999) Histidine kinases: diversity of domain organization. *Mol Microbiol* **34**: 633-640.
- Epstein, W., (2003) The roles and regulation of potassium in bacteria. *Prog Nucleic Acid Re* **75**: 293-320.
- Epstein, W. & B.S. Kim, (1971) Potassium transport loci in *Escherichia coli* K-12. *J Bacteriol* **108**: 639-644.
- Epstein, W. & S.G. Schultz, (1965) Cation Transport in *Escherichia coli*: V. Regulation of cation content. *J Gen Physiol* **49**: 221-234.
- Ferris, H.U., M. Coles, A.N. Lupas & M.D. Hartmann, (2014) Crystallographic snapshot of the *Escherichia coli* EnvZ histidine kinase in an active conformation. *J Struct Biol* **186**: 376-379.
- Ferris, H.U., S. Dunin-Horkawicz, N. Hornig, M. Hulko, J. Martin, J.E. Schultz, K. Zeth, A.N. Lupas & M. Coles, (2012) Mechanism of regulation of receptor histidine kinases. *Structure* **20**: 56-66.
- Filippou, P.S., L.D. Kasemian, C.A. Panagiotidis & D.A. Kyriakidis, (2008) Functional characterization of the histidine kinase of the *E. coli* two-component signal transduction system AtoS-AtoC. *Biochim Biophys Acta* **1780**: 1023-1031.
- Finn, R.D., A. Bateman, J. Clements, P. Coggill, R.Y. Eberhardt, S.R. Eddy, A. Heger, K. Hetherington, L. Holm, J. Mistry, E.L. Sonnhammer, J. Tate & M. Punta, (2014) Pfam: the protein families database. *Nucleic Acids Res* **42**: D222-230.
- Fisher, S.L., W. Jiang, B.L. Wanner & C.T. Walsh, (1995) Cross-talk between the histidine protein kinase VanS and the response regulator PhoB. Characterization and

## References

- identification of a VanS domain that inhibits activation of PhoB. *J Biol Chem* **270**: 23143-23149.
- Fohrmann, A., (2001) Bedeutung der Transmembrandomänen für die Reizaufnahme durch die Sensorkinase KdpD aus *Escherichia coli*. Diplomarbeit, Universität Osnabrück
- Fried, L., J. Lassak & K. Jung, (2012) A comprehensive toolbox for the rapid construction of *lacZ* fusion reporters. *J Microbiol Meth* **91**: 537-543.
- Gao, R. & A.M. Stock, (2009) Biological insights from structures of two-component proteins. *Annu Rev Microbiol* **63**: 133-154.
- Gao, R. & A.M. Stock, (2015) Temporal hierarchy of gene expression mediated by transcription factor binding affinity and activation dynamics. *MBio* **6**: e00686-00615.
- Garcia Vescovi, E., F.C. Soncini & E.A. Groisman, (1996) Mg<sup>2+</sup> as an extracellular signal: environmental regulation of *Salmonella* virulence. *Cell* **84**: 165-174.
- Gardner, S.G., K.D. Johns, R. Tanner & W.R. McCleary, (2014) The PhoU protein from *Escherichia coli* interacts with PhoR, PstB, and metals to form a phosphate-signaling complex at the membrane. *J Bacteriol* **196**: 1741-1752.
- Gaßel, M. & K. Altendorf, (2001) Analysis of KdpC of the K<sup>+</sup>-transporting KdpFABC complex of *Escherichia coli*. *Eur J Biochem* **268**: 1772-1781.
- Gaßel, M., T. Mollenkamp, W. Puppe & K. Altendorf, (1999) The KdpF subunit is part of the K<sup>+</sup>-translocating Kdp complex of *Escherichia coli* and is responsible for stabilization of the complex *in vitro*. *J Biol Chem* **274**: 37901-37907.
- Greie, J.C. & K. Altendorf, (2007) The K<sup>+</sup>-translocating KdpFABC complex from *Escherichia coli*: a P-type ATPase with unique features. *J Bioenerg Biomembr* **39**: 397-402.
- Guzman, L.M., D. Belin, M.J. Carson & J. Beckwith, (1995) Tight regulation, modulation, and high-level expression by vectors containing the arabinose P<sub>BAD</sub> promoter. *J Bacteriol* **177**: 4121-4130.
- Haldimann, A., S.L. Fisher, L.L. Daniels, C.T. Walsh & B.L. Wanner, (1997) Transcriptional regulation of the *Enterococcus faecium* BM4147 vancomycin resistance gene cluster by the VanS-VanR two-component regulatory system in *Escherichia coli* K-12. *J Bacteriol* **179**: 5903-5913.
- Hamann, K., P. Zimmann & K. Altendorf, (2008) Reduction of turgor is not the stimulus for the sensor kinase KdpD of *Escherichia coli*. *J Bacteriol* **190**: 2360-2367.
- Heermann, R., K. Altendorf & K. Jung, (1998) The turgor sensor KdpD of *Escherichia coli* is a homodimer. *Biochim Biophys Acta* **1415**: 114-124.
- Heermann, R., K. Altendorf & K. Jung, (2000) The hydrophilic N-terminal domain complements the membrane-anchored C-terminal domain of the sensor kinase KdpD of *Escherichia coli*. *J Biol Chem* **275**: 17080-17085.
- Heermann, R., K. Altendorf & K. Jung, (2003a) The N-terminal input domain of the sensor kinase KdpD of *Escherichia coli* stabilizes the interaction between the cognate response regulator KdpE and the corresponding DNA-binding site. *J Biol Chem* **278**: 51277-51284.
- Heermann, R., A. Fohrmann, K. Altendorf & K. Jung, (2003b) The transmembrane domains of the sensor kinase KdpD of *Escherichia coli* are not essential for sensing K<sup>+</sup> limitation. *Mol Microbiol* **47**: 839-848.
- Heermann, R. & K. Jung, (2009) Stimulus perception and signaling in histidine kinases. In: Bacterial Signaling. R. Krämer (ed). Weinheim, Germany: Wiley-VCH Verlag GmbH & Co. KGaA, pp. 135-162
- Heermann, R. & K. Jung, (2010) The complexity of the 'simple' two-component system KdpD/KdpE in *Escherichia coli*. *FEMS Microbiol Lett* **304**: 97-106.
- Heermann, R. & K. Jung, (2012) K<sup>+</sup> supply, osmotic stress and the KdpD/KdpE two-component system. In: Two-component systems in bacteria. R. Gross & D. Beier (eds). Norwich, UK: Caister Academic Press., pp. 181-198.

## References

- Heermann, R., M.L. Lippert & K. Jung, (2009a) Domain swapping reveals that the N-terminal domain of the sensor kinase KdpD in *Escherichia coli* is important for signaling. *BMC Microbiol* **9**: 133.
- Heermann, R., A. Weber, B. Mayer, M. Ott, E. Hauser, G. Gabriel, T. Pirch & K. Jung, (2009b) The universal stress protein UspC scaffolds the KdpD/KdpE signaling cascade of *Escherichia coli* under salt stress. *J Mol Biol* **386**: 134-148.
- Heermann, R., T. Zeppenfeld & K. Jung, (2008) Simple generation of site-directed point mutations in the *Escherichia coli* chromosome using Red®/ET® Recombination. *Microb Cell Fact* **7**: 14.
- Heermann, R., K. Zigann, S. Gayer, M. Rodriguez-Fernandez, J.R. Banga, A. Kremling & K. Jung, (2014) Dynamics of an interactive network composed of a bacterial two-component system, a transporter and K<sup>+</sup> as mediator. *PLoS One* **9**: e89671.
- Heikaus, C.C., J. Pandit & R.E. Klevit, (2009) Cyclic nucleotide binding GAF domains from phosphodiesterases: structural and mechanistic insights. *Structure* **17**: 1551-1557.
- Heitkamp, T., R. Kalinowski, B. Böttcher, M. Börsch, K. Altendorf & J.C. Greie, (2008) K<sup>+</sup>-translocating KdpFABC P-type ATPase from *Escherichia coli* acts as a functional and structural dimer. *Biochemistry* **47**: 3564-3575.
- Ho, Y.S., L.M. Burden & J.H. Hurley, (2000) Structure of the GAF domain, a ubiquitous signaling motif and a new class of cyclic GMP receptor. *EMBO J* **19**: 5288-5299.
- Hsieh, Y.J. & B.L. Wanner, (2010) Global regulation by the seven-component P<sub>i</sub> signaling system. *Curr Opin Microbiol* **13**: 198-203.
- Hsing, W. & T.J. Silhavy, (1997) Function of conserved histidine-243 in phosphatase activity of EnvZ, the sensor for porin osmoregulation in *Escherichia coli*. *J Bacteriol* **179**: 3729-3735.
- Huynh, T.N. & V. Stewart, (2011) Negative control in two-component signal transduction by transmitter phosphatase activity. *Mol Microbiol* **82**: 275-286.
- Jung, K. & K. Altendorf, (1998a) Individual substitutions of clustered arginine residues of the sensor kinase KdpD of *Escherichia coli* modulate the ratio of kinase to phosphatase activity. *J Biol Chem* **273**: 26415-26420.
- Jung, K. & K. Altendorf, (1998b) Truncation of amino acids 12-128 causes deregulation of the phosphatase activity of the sensor kinase KdpD of *Escherichia coli*. *J Biol Chem* **273**: 17406-17410.
- Jung, K., L. Fried, S. Behr & R. Heermann, (2012) Histidine kinases and response regulators in networks. *Curr Opin Microbiol* **15**: 118-124.
- Jung, K., R. Heermann, M. Meyer & K. Altendorf, (1998) Effect of cysteine replacements on the properties of the turgor sensor KdpD of *Escherichia coli*. *Biochim Biophys Acta* **1372**: 311-322.
- Jung, K., M. Krabusch & K. Altendorf, (2001) Cs<sup>+</sup> induces the *kdp* operon of *Escherichia coli* by lowering the intracellular K<sup>+</sup> concentration. *J Bacteriol* **183**: 3800-3803.
- Jung, K., B. Tjaden & K. Altendorf, (1997) Purification, reconstitution, and characterization of KdpD, the turgor sensor of *Escherichia coli*. *J Biol Chem* **272**: 10847-10852.
- Jung, K., M. Veen & K. Altendorf, (2000) K<sup>+</sup> and ionic strength directly influence the autophosphorylation activity of the putative turgor sensor KdpD of *Escherichia coli*. *J Biol Chem* **275**: 40142-40147.
- Karimova, G. & D. Ladant, (2005) A bacterial two-hybrid system based on a cyclic AMP signaling cascade. In: Protein-protein interactions. G. E (ed). NY: Cold Spring Harbor Laboratory Press, pp. 499-515.
- Karimova, G., J. Pidoux, A. Ullmann & D. Ladant, (1998) A bacterial two-hybrid system based on a reconstituted signal transduction pathway. *Proc. Natl. Acad. Sci. U S A* **95**: 5752-5756.

## References

- Kelley, L.A. & M.J. Sternberg, (2009) Protein structure prediction on the Web: a case study using the Phyre server. *Nat Protoc* **4**: 363-371.
- Kilian, C.T., (2005) *Modern control technology* p. xii, 648 p. Delmar Thomson Learning, Novato, CA.
- Kollmann, R. & K. Altendorf, (1993) ATP-driven potassium transport in right-side-out membrane vesicles via the Kdp system of *Escherichia coli*. *Biochim Biophys Acta* **1143**: 62-66.
- Laermann, V., (2014) Untersuchungen zur Stimulus-Wahrnehmung und Regulation des Zweikomponenten-Systems KdpD/KdpE aus *Escherichia coli*. Dissertation, Universität Osnabrück
- Laermann, V., E. Cudic, K. Kipschull, P. Zimmann & K. Altendorf, (2013) The sensor kinase KdpD of *Escherichia coli* senses external K<sup>+</sup>. *Mol Microbiol* **88**: 1194-1204.
- Laimins, L.A., D.B. Rhoads & W. Epstein, (1981) Osmotic control of *kdp* operon expression in *Escherichia coli*. *Proc Natl Acad Sci U S A* **78**: 464-468.
- Leder, P., D. Tiemeier & L. Enquist, (1977) EK2 derivatives of bacteriophage lambda useful in the cloning of DNA from higher organisms: the lambda<sub>dag</sub>WES system. *Science* **196**: 175-177.
- Levdikov, V.M., E. Blagova, V.L. Colledge, A.A. Lebedev, D.C. Williamson, A.L. Sonenshein & A.J. Wilkinson, (2009) Structural rearrangement accompanying ligand binding in the GAF domain of CodY from *Bacillus subtilis*. *J Mol Biol* **390**: 1007-1018.
- Lipmann, F. & L. Tuttle, (1945) A specific micromethod for the determination of acyl phosphates. *J Biol Chem* **193**: 265-275.
- Liu, J., A. Prindle, J. Humphries, M. Gabalda-Sagarra, M. Asally, D.Y. Lee, S. Ly, J. Garcia-Ojalvo & G.M. Süel, (2015) Metabolic co-dependence gives rise to collective oscillations within biofilms. *Nature* **523**: 550-554.
- Lowe, E.C., A. Basle, M. Czjzek, S.J. Firbank & D.N. Bolam, (2012) A scissor blade-like closing mechanism implicated in transmembrane signaling in a *Bacteroides* hybrid two-component system. *Proc Natl Acad Sci U S A* **109**: 7298-7303.
- Lowry, O.H., N.J. Rosebrough, A.L. Farr & R.J. Randall, (1951) Protein measurement with the Folin phenol reagent. *J Biol Chem* **193**: 265-275.
- Lüttmann, D., Y. Göpel & B. Görke, (2012) The phosphotransferase protein EIIA(Ntr) modulates the phosphate starvation response through interaction with histidine kinase PhoR in *Escherichia coli*. *Mol Microbiol* **86**: 96-110.
- Lüttmann, D., R. Heermann, B. Zimmer, A. Hillmann, I.S. Rampp, K. Jung & B. Görke, (2009) Stimulation of the potassium sensor KdpD kinase activity by interaction with the phosphotransferase protein IIA(Ntr) in *Escherichia coli*. *Mol Microbiol* **72**: 978-994.
- Maier, K.S., S. Hubich, H. Liebhart, S. Krauss, A. Kuhn & S.J. Facey, (2008) An amphiphilic region in the cytoplasmic domain of KdpD is recognized by the signal recognition particle and targeted to the *Escherichia coli* membrane. *Mol Microbiol* **68**: 1471-1484.
- Marina, A., C.D. Waldburger & W.A. Hendrickson, (2005) Structure of the entire cytoplasmic portion of a sensor histidine-kinase protein. *EMBO J.* **24**: 4247-4259.
- Martinez, S.E., J.A. Beavo & W.G. Hol, (2002) GAF domains: two-billion-year-old molecular switches that bind cyclic nucleotides. *Mol Interv* **2**: 317-323.
- Mascher, T., J.D. Helmann & G. Unden, (2006) Stimulus perception in bacterial signal-transducing histidine kinases. *Microbiol Mol Biol R* **70**: 910-938.
- Maslennikov, I., C. Klammt, E. Hwang, G. Kefala, M. Okamura, L. Esquivies, K. Mors, C. Glaubitz, W. Kwiatkowski, Y.H. Jeon & S. Choe, (2010) Membrane domain structures of three classes of histidine kinase receptors by cell-free expression and rapid NMR analysis. *Proc Natl Acad Sci U S A* **107**: 10902-10907.

## References

- McLaggan, D., J. Naprstek, E.T. Buurman & W. Epstein, (1994) Interdependence of K<sup>+</sup> and glutamate accumulation during osmotic adaptation of *Escherichia coli*. *J Biol Chem* **269**: 1911-1917.
- Mével-Ninio, M. & T. Yamamoto, (1974) Conversion of active transport vesicles of *Escherichia coli* into oxidative phosphorylation vesicles. *Biochim Biophys Acta* **357**: 63-66.
- Miller, J.H., (1972) Experiments in Molecular Genetics. In.: Cold Spring Harbor Laboratory Press, Cold Spring Harbor, NY, 1972, pp. 221-222 and 263-274.
- Miller, J.H., (1992) A short course in bacterial genetics : a laboratory manual and handbook for *Escherichia coli* and related bacteria. Cold Spring Harbor Laboratory Press, Plainview, N.Y.
- Møller, J.V., B. Juul & M. le Maire, (1996) Structural organization, ion transport, and energy transduction of P-type ATPases. *Biochim Biophys Acta* **1286**: 1-51.
- Monzel, C. & G. Unden, (2015) Transmembrane signaling in the sensor kinase DcuS of *Escherichia coli*: A long-range piston-type displacement of transmembrane helix 2. *Proc Natl Acad Sci U S A* **112**: 11042-11047.
- Moscoso, J.A., H. Schramke, Y. Zhang, T. Tosi, A. Dehbi, K. Jung & A. Gründling, (2015) Binding of c-di-AMP to the *Staphylococcus aureus* sensor kinase KdpD occurs via the USP domain and down-regulates the expression of the Kdp potassium transporter. *J Bacteriol* **198**: 98-110.
- Münch, A., L. Stingl, K. Jung & R. Heermann, (2008) *Photobacterium luminescens* genes induced upon insect infection. *BMC Genomics* **9**: 229.
- Nakashima, K., A. Sugiura, K. Kanamaru & T. Mizuno, (1993) Signal transduction between the two regulatory components involved in the regulation of the *kdpABC* operon in *Escherichia coli*: phosphorylation-dependent functioning of the positive regulator, KdpE. *Mol Microbiol* **7**: 109-116.
- Narayanan, A., S. Kumar, A.N. Evrard, L.N. Paul & D.A. Yernool, (2014) An asymmetric heterodomain interface stabilizes a response regulator-DNA complex. *Nat Commun* **5**: 3282.
- Narayanan, A., L.N. Paul, S. Tomar, D.N. Patil, P. Kumar & D.A. Yernool, (2012) Structure-function studies of DNA binding domain of response regulator KdpE reveals equal affinity interactions at DNA half-sites. *PLoS One* **7**: e30102.
- Neiditch, M.B., M.J. Federle, A.J. Pompeani, R.C. Kelly, D.L. Swem, P.D. Jeffrey, B.L. Bassler & F.M. Hughson, (2006) Ligand-induced asymmetry in histidine sensor kinase complex regulates quorum sensing. *Cell* **126**: 1095-1108.
- Nissen, P., J. Hansen, N. Ban, P.B. Moore & T.A. Steitz, (2000) The structural basis of ribosome activity in peptide bond synthesis. *Science* **289**: 920-930.
- Ochrombel, I., L. Ott, R. Krämer, A. Burkovski & K. Marin, (2011) Impact of improved potassium accumulation on pH homeostasis, membrane potential adjustment and survival of *Corynebacterium glutamicum*. *Biochim Biophys Acta* **1807**: 444-450.
- Ohwada, T. & S. Sagisaka, (1987) An immediate and steep increase in ATP concentration in response to reduced turgor pressure in *Escherichia coli* B. *Arch Biochem Biophys* **259**: 157-163.
- Ottmann, K.M., W. Xiao, Y.K. Shin & D.E. Koshland, Jr., (1999) A piston model for transmembrane signaling of the aspartate receptor. *Science* **285**: 1751-1754.
- Parkinson, J.S. & E.C. Kofoid, (1992) Communication modules in bacterial signaling proteins. *Annu Rev Genet* **26**: 71-112.
- Peterson, G.L., (1977) A simplification of the protein assay method of Lowry *et al.* which is more generally applicable. *Anal Biochem* **83**: 346-356.

## References

- Pettersen, E.F., T.D. Goddard, C.C. Huang, G.S. Couch, D.M. Greenblatt, E.C. Meng & T.E. Ferrin, (2004) UCSF Chimera--a visualization system for exploratory research and analysis. *J Comput Chem* **25**: 1605-1612.
- Podgornaia, A.I. & M.T. Laub, (2013) Determinants of specificity in two-component signal transduction. *Curr Opin Microbiol* **16**: 156-162.
- Podust, L.M., A. Ioanoviciu & P.R. Ortiz de Montellano, (2008) 2.3 Å X-ray structure of the heme-bound GAF domain of sensory histidine kinase DosT of *Mycobacterium tuberculosis*. *Biochemistry* **47**: 12523-12531.
- Polarek, J.W., G. Williams & W. Epstein, (1992) The products of the *kdpDE* operon are required for expression of the Kdp ATPase of *Escherichia coli*. *J Bacteriol* **174**: 2145-2151.
- Price-Whelan, A., C.K. Poon, M.A. Benson, T.T. Eidem, C.M. Roux, J.M. Boyd, P.M. Dunman, V.J. Torres & T.A. Krulwich, (2013) Transcriptional profiling of *Staphylococcus aureus* during growth in 2 M NaCl leads to clarification of physiological roles for Kdp and Ktr K<sup>+</sup> uptake systems. *MBio* **4**: e00407-13.
- Prindle, A., J. Liu, M. Asally, S. Ly, J. Garcia-Ojalvo & G.M. Süel, (2015) Ion channels enable electrical communication in bacterial communities. *Nature* **527**: 59-63.
- Rao, N.N., M.F. Roberts, A. Torriani & J. Yashphe, (1993) Effect of *glpT* and *glpD* mutations on expression of the *phoA* gene in *Escherichia coli*. *J Bacteriol* **175**: 74-79.
- Record, M.T., Jr., E.S. Courtenay, D.S. Cayley & H.J. Guttman, (1998) Responses of *E. coli* to osmotic stress: large changes in amounts of cytoplasmic solutes and water. *Trends in Biochemical Sciences* **23**: 143-148.
- Rees, D.C., E. Johnson & O. Lewinson, (2009) ABC transporters: the power to change. *Nat Rev Mol Cell Biol* **10**: 218-227.
- Rhoads, D.B., F.B. Waters & W. Epstein, (1976) Cation transport in *Escherichia coli*. VIII. Potassium transport mutants. *J Gen Physiol* **67**: 325-341.
- Roe, A.J., D. McLaggan, C.P. O'Byrne & I.R. Booth, (2000) Rapid inactivation of the *Escherichia coli* Kdp K<sup>+</sup> uptake system by high potassium concentrations. *Mol Microbiol* **35**: 1235-1243.
- Roelofs, K.G., J. Wang, H.O. Sintim & V.T. Lee, (2011) Differential radial capillary action of ligand assay for high-throughput detection of protein-metabolite interactions. *Proc Natl Acad Sci U S A* **108**: 15528-15533.
- Römmling, U., (2008) Great times for small molecules: c-di-AMP, a second messenger candidate in Bacteria and Archaea. *Sci Signal* **1**: pe39.
- Rothenbücher, M.C., S.J. Facey, D. Kiefer, M. Kossmann & A. Kuhn, (2006) The cytoplasmic C-terminal domain of the *Escherichia coli* KdpD protein functions as a K<sup>+</sup> sensor. *J Bacteriol* **188**: 1950-1958.
- Santos-Beneit, F., (2015) The Pho regulon: a huge regulatory network in bacteria. *Front Microbiol* **6**: 402.
- Scaramozzino, F., A. White, M. Perego & J.A. Hoch, (2009) A unique GTP-dependent sporulation sensor histidine kinase in *Bacillus anthracis*. *J Bacteriol* **191**: 687-692.
- Schlösser, A., A. Hamann, D. Bossemeyer, E. Schneider & E.P. Bakker, (1993) NAD<sup>+</sup> binding to the *Escherichia coli* K<sup>+</sup>-uptake protein TrkA and sequence similarity between TrkA and domains of a family of dehydrogenases suggest a role for NAD<sup>+</sup> in bacterial transport. *Mol Microbiol* **9**: 533-543.
- Schlösser, A., M. Meldorf, S. Stumpe, E.P. Bakker & W. Epstein, (1995) TrkH and its homolog, TrkG, determine the specificity and kinetics of cation transport by the Trk system of *Escherichia coli*. *J Bacteriol* **177**: 1908-1910.
- Schramke, H., (2011) Funktionelle und strukturelle Charakterisierung der GAF-Domäne der Sensorkinase KdpD in *Escherichia coli*. Diplomarbeit, Ludwig-Maximilians Universität München

## References

- Searcy, D.G., (1976) *Thermoplasma acidophilum*: intracellular pH and potassium concentration. *Biochim Biophys Acta* **451**: 278-286.
- Shinar, G., R. Milo, M.R. Martinez & U. Alon, (2007) Input output robustness in simple bacterial signaling systems. *Proc Natl Acad Sci U S A* **104**: 19931-19935.
- Shulman, R.G., T.R. Brown, K. Ugurbil, S. Ogawa, S.M. Cohen & J.A. den Hollander, (1979) Cellular applications of <sup>31</sup>P and <sup>13</sup>C nuclear magnetic resonance. *Science* **205**: 160-166.
- Sievers, F., A. Wilm, D. Dineen, T.J. Gibson, K. Karplus, W. Li, R. Lopez, H. McWilliam, M. Remmert, J. Soding, J.D. Thompson & D.G. Higgins, (2011) Fast, scalable generation of high-quality protein multiple sequence alignments using Clustal Omega. *Mol Syst Biol* **7**: 539.
- Silva, J.C., A. Haldimann, M.K. Prahalad, C.T. Walsh & B.L. Wanner, (1998) In vivo characterization of the type A and B vancomycin-resistant enterococci (VRE) VanRS two-component systems in *Escherichia coli*: a nonpathogenic model for studying the VRE signal transduction pathways. *Proc Natl Acad Sci U S A* **95**: 11951-11956.
- Siryaporn, A. & M. Goulian, (2008) Cross-talk suppression between the CpxA-CpxR and EnvZ-OmpR two-component systems in *E. coli*. *Mol Microbiol* **70**: 494-506.
- Skerker, J.M., M.S. Prasol, B.S. Perchuk, E.G. Biondi & M.T. Laub, (2005) Two-component signal transduction pathways regulating growth and cell cycle progression in a bacterium: a system-level analysis. *PLoS Biol* **3**: e334.
- Söding, J., A. Biegert & A.N. Lupas, (2005) The HHpred interactive server for protein homology detection and structure prediction. *Nucleic Acids Res* **33**: W244-248.
- Stadtman, E., (1957) Preparation and assay of acetyl phosphate. *Methods Enzymol* **3**: 228-231.
- Stewart, L.M., E.P. Bakker & I.R. Booth, (1985) Energy coupling to K<sup>+</sup> uptake via the Trk system in *Escherichia coli*: the role of ATP. *J Gen Microbiol* **131**: 77-85.
- Stock, A.M., V.L. Robinson & P.N. Goudreau, (2000) Two-component signal transduction. *Ann Rev Biochem* **69**: 183-215.
- Studier, F.W. & B.A. Moffatt, (1986) Use of bacteriophage T7 RNA polymerase to direct selective high-level expression of cloned genes. *J Mol Biol* **189**: 113-130.
- Suelter, C.H., (1970) Enzymes activated by monovalent cations. *Science* **168**: 789-795.
- Sugiura, A., K. Hirokawa, K. Nakashima & T. Mizuno, (1994) Signal-sensing mechanisms of the putative osmosensor KdpD in *Escherichia coli*. *Mol Microbiol* **14**: 929-938.
- Sugiura, A., K. Nakashima, K. Tanaka & T. Mizuno, (1992) Clarification of the structural and functional features of the osmoregulated *kdp* operon of *Escherichia coli*. *Mol Microbiol* **6**: 1769-1776.
- Surmann, K., V. Laermann, P. Zimmann, K. Altendorf & E. Hammer, (2014) Absolute quantification of the Kdp subunits of *Escherichia coli* by multiple reaction monitoring. *Proteomics* **14**: 1630-1638.
- Swanson, R.V., L.A. Alex & M.I. Simon, (1994) Histidine and aspartate phosphorylation: two-component systems and the limits of homology. *Trends Biochem Sci* **19**: 485-490.
- Tkaczuk, K.L., A.S. I, M. Chruszcz, E. Evdokimova, A. Savchenko & W. Minor, (2013) Structural and functional insight into the universal stress protein family. *Evol Appl* **6**: 434-449.
- Ugurbil, K., H. Rottenberg, P. Glynn & R.G. Shulman, (1978) <sup>31</sup>P nuclear magnetic resonance studies of bioenergetics and glycolysis in anaerobic *Escherichia coli* cells. *Proc Natl Acad Sci U S A* **75**: 2244-2248.
- Ugurbil, K., H. Rottenberg, P. Glynn & R.G. Shulman, (1982) Phosphorus-31 nuclear magnetic resonance studies of bioenergetics in wild-type and adenosinetriphosphatase<sup>-</sup> *Escherichia coli* cells. *Biochemistry* **21**: 1068-1075.
- Van der Laan, M., M. Gabel & K. Altendorf, (2002) Characterization of amino acid substitutions in KdpA, the K<sup>+</sup>-binding and -translocating subunit of the KdpFABC complex of *Escherichia coli*. *J Bacteriol* **184**: 5491-5494.

## References

- Voelkner, P., W. Puppe & K. Altendorf, (1993) Characterization of the KdpD protein, the sensor kinase of the K<sup>+</sup>-translocating Kdp system of *Escherichia coli*. *Eur J Biochem* **217**: 1019-1026.
- Walderhaug, M.O., D.C. Dosch & W. Epstein, (1987) Potassium transport in bacteria. In: Ion transport in prokaryotes. B.P. Rosen (ed). New York: Academic press, pp. 84-130.
- Walderhaug, M.O., J.W. Polarek, P. Voelkner, J.M. Daniel, J.E. Hesse, K. Altendorf & W. Epstein, (1992) KdpD and KdpE, proteins that control expression of the *kdpABC* operon, are members of the two-component sensor-effector class of regulators. *J Bacteriol* **174**: 2152-2159.
- Webb, D.C., H. Rosenberg & G.B. Cox, (1992) Mutational analysis of the *Escherichia coli* phosphate-specific transport system, a member of the traffic ATPase (or ABC) family of membrane transporters. A role for proline residues in transmembrane helices. *J Biol Chem* **267**: 24661-24668.
- Weiden, P.L., W. Epstein & S.G. Schultz, (1967) Cation transport in *Escherichia coli*. VII. Potassium requirement for phosphate uptake. *J Gen Physiol* **50**: 1641-1661.
- Willett, J.W. & J.R. Kirby, (2012) Genetic and biochemical dissection of a HisKA domain identifies residues required exclusively for kinase and phosphatase activities. *PLoS Genet* **8**: e1003084.
- Wilson, D.S. & A.D. Keefe, (2001) Random mutagenesis by PCR. *Curr Protoc Mol Biol* Chapter 8: Unit8 3.
- Winkler, K., A. Schultz & J.E. Schultz, (2012) The S-helix determines the signal in a Tsr receptor/adenylyl cyclase reporter. *J Biol Chem* **287**: 15479-15488.
- Wood, J.M., (2006) Osmosensing by bacteria. *Sci STKE* **2006**: pe43.
- Wood, J.M., (2011) Bacterial osmoregulation: a paradigm for the study of cellular homeostasis. *Annu Rev Microbiol* **65**: 215-238.
- Wood, J.M., (2015) Bacterial responses to osmotic challenges. *J Gen Physiol* **145**: 381-388.
- Xavier, K.B., M. Kossmann, H. Santos & W. Boos, (1995) Kinetic analysis by in vivo <sup>31</sup>P nuclear magnetic resonance of internal Pi during the uptake of sn-glycerol-3-phosphate by the *pho* regulon-dependent Ugp system and the *glp* regulon-dependent GlpT system. *J Bacteriol* **177**: 699-704.
- Zeng, Y., X. Han & R.W. Gross, (1998) Phospholipid subclass specific alterations in the passive ion permeability of membrane bilayers: separation of enthalpic and entropic contributions to transbilayer ion flux. *Biochemistry* **37**: 2346-2355.
- Zhou, L., Grégori, G., Blackman J.M., Robinson, P., Wanner, B.L., (2005) Stochastic activation of the response regulator PhoB by noncognate histidine kinases. *J Integr Bioinform* **2**: 11-24.
- Zimmann, P., W. Puppe & K. Altendorf, (1995) Membrane topology analysis of the sensor kinase KdpD of *Escherichia coli*. *J Biol Chem* **270**: 28282-28288.
- Zimmann, P., A. Steinbrugge, M. Schniederberend, K. Jung & K. Altendorf, (2007) The extension of the fourth transmembrane helix of the sensor kinase KdpD of *Escherichia coli* is involved in sensing. *J Bacteriol* **189**: 7326-7334.

## 6 Supplemental Material

### 6.1 Supplemental Figures

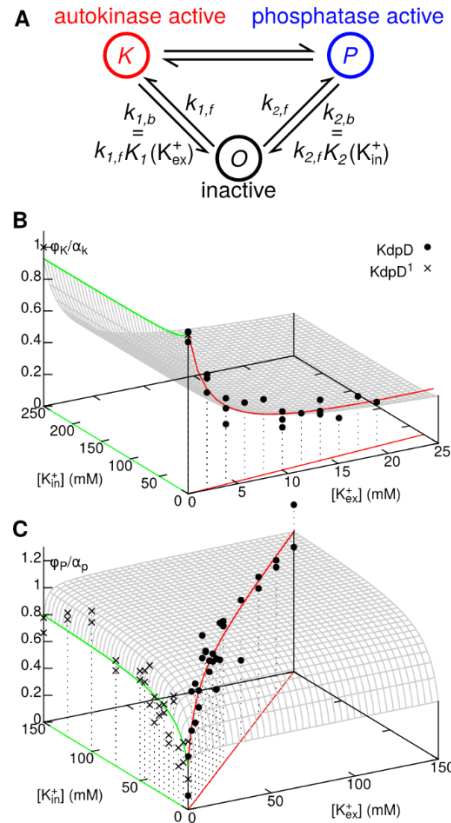


**Figure S1: Fitting of KdpD state-switching model.** (A) KdpD switching model, showing the definition of the equilibrium constants  $K_1$  and  $K_2$ . Parameters of the KdpD state-switching were determined by fitting to the autokinase (B) and phosphatase (C) activities measured *in vitro* for KdpD and KdpD<sup>1</sup> (data points), which lie along lines in the two-dimensional input space. The resulting parameters define an activity response surface as a function of internal and external  $K^+$ . The figure was created by Filipe Tostevin.

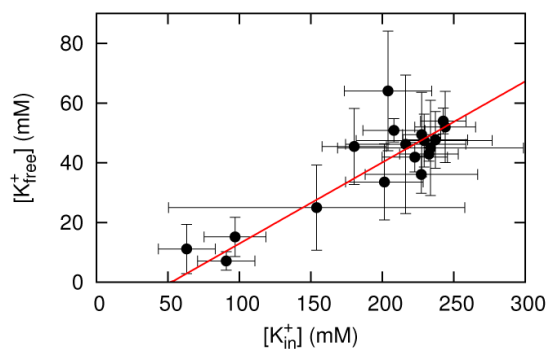


**Figure S2: Intracellular free  $K^+$ .** Wild-type cells were grown in minimal medium containing 10 mM  $K^+$  and then shifted to minimal medium containing different  $K^+$  concentrations. After 2 hours samples were taken and the intracellular  $K^+$  concentration was determined. Measured intracellular free  $K^+$  is plotted against total intracellular  $K^+$ . The full line shows the best linear fit,  $[K^+]_{\text{free}} = 0.27[K^+]_{\text{in}} - 14$  mM. The figure was created by Filipe Tostevin.

## 6.2 Supplemental tables

Table S1: Strains used in this study.

Name	Genotype	Reference
<b>Commonly used strains</b>		
DH5 $\alpha$	F <sup>-</sup> $\Phi$ 80 <i>lacZ</i> $\Delta$ M15 $\Delta$ ( <i>lacZYA-argF</i> ) U169 <i>recA1 endA1 hsdR17</i> ( $r_K^-$ , $m_K^+$ ) <i>phoA supE44</i> $\lambda^- thi-1 gyrA96 relA1$	Promega
MG1655	<i>E. coli</i> K-12 reference strain	(Blattner <i>et al.</i> , 1997)
BL21 (DE3/pLysS)	F <sup>-</sup> <i>ompT hsdSB</i> ( $r_B m_B^-$ ) <i>dcm gal</i> (DE3) pLysS (Cm <sup>R</sup> )	(Studier & Moffatt, 1986)
TKR2000	$\Delta$ <i>kdpFABCDE trkA405 trkD1 atp706</i>	(Kollmann & Altendorf, 1993)
HAK006	CSH26 $\Delta$ <i>kdpABCD::neo</i> $\lambda$ <i>attB::kdpFA'-lacZ</i> $\Delta$ ( <i>lac-pro</i> ) <i>ara thi</i>	(Nakashima <i>et al.</i> , 1993)
LF3	MG1655 <i>rpsL150 P<sub>kdp</sub>::lacZ</i> ; Kan <sup>s</sup> Strp <sup>r</sup>	(Fried <i>et al.</i> , 2012)
BTH101	F <sup>-</sup> <i>cyaA-99 araD139 galE15 galK16 rpsL1 hsdR2 mcrA1 mcrB1</i>	(Karimova <i>et al.</i> , 1998)
ArcticExpress (DE3) RIL	F <sup>-</sup> <i>ompT hsdS</i> ( $r_B m_B^-$ ) <i>dcm</i> <sup>+</sup> Tet <sup>r</sup> <i>gal</i> $\lambda$ (DE3) <i>endA Hte</i> [ <i>cpn 10 cpn60 Gent</i> <sup>r</sup> ] [ <i>argU ileY leuW Str</i> <sup>r</sup> ]	Agilent Technologies
<b>Strains used in chapter 2.1</b>		
HS1	MG1655 <i>rpsL150 P<sub>kdp</sub>::lacZ</i> ; <i>kdpD::rpsL-neo</i> , Kan <sup>r</sup> Str <sup>s</sup>	this study
HS2	MG1655 <i>rpsL150 P<sub>kdp</sub>::lacZ</i> ; <i>kdpD</i> <sup>Pro466Ala,Thr469Ala,Leu470Ala,Val472Ala</sup> , Kan <sup>s</sup> Str <sup>r</sup>	this study
HS3	MG1655 <i>rpsL150 P<sub>kdp</sub>::lacZ</i> ; <i>kdpD</i> <sup>Thr677Ala</sup> , Kan <sup>s</sup> Str <sup>r</sup>	this study
HS4	MG1655 <i>rpsL150 P<sub>kdp</sub>::lacZ</i> ; <i>kdpD</i> <sup>Pro466Ala,Thr469Ala,Leu470Ala,Val472Ala,Thr677Ala</sup> , Kan <sup>s</sup> Str <sup>r</sup>	this study
<b>Strains used in chapter 2.3</b>		
LB2240	<i>thi metE rpsL gal rha kup1 AtrkA</i>	P. Zimmann, Universität Osnabrück, unpublished
TKV2209	$\Delta$ <i>kdpD</i> <sup>128-894</sup> $\Delta$ <i>kdpE trkA405 trkD1 nagA thi rha lacZ</i>	(Zimmann <i>et al.</i> , 1995)
JW3705	BW25113 <i>pstC::npt</i>	(Baba <i>et al.</i> , 2006)
JW0390	BW25113 <i>phoR::npt</i>	(Baba <i>et al.</i> , 2006)
JW3702	BW25113 <i>phoU::npt</i>	(Baba <i>et al.</i> , 2006)
LB2240 $\Delta$ <i>kdpD</i>	$\Delta$ <i>kdpD thi metE rpsL150 gal rha kup1 AtrkA</i>	(Laermann, 2014)
LB2240 $\Delta$ <i>kdpD,kdpE</i> <sup>D52N</sup>	$\Delta$ <i>kdpDkdpED52N thi metE rpsL150 gal rha kup1 AtrkA</i>	(Laermann, 2014)
LB2240 $\Delta$ <i>kdpD</i> $\Delta$ <i>pta</i> $\Delta$ <i>ackA</i>	$\Delta$ <i>kdpD(pta ackA)::rpsL-kan thi metE rpsL150 gal rha kup1 AtrkA</i>	(Laermann, 2014)
LB2240 $\Delta$ <i>pstC</i>	LB2240 <i>pstC::npt</i>	This work
LB2240 $\Delta$ <i>kdpD</i> $\Delta$ <i>pstC</i>	LB2240 $\Delta$ <i>kdpD pstC::npt</i>	This work
LF3 $\Delta$ <i>kdpD</i>	MG1655 <i>rpsL150 P<sub>kdp</sub>::lacZ</i> $\Delta$ <i>kdpD</i>	This work
LF3 $\Delta$ <i>pstC</i>	LF3 <i>pstC::npt</i>	This work
LF3 $\Delta$ <i>kdpD</i> $\Delta$ <i>pstC</i>	MG1655 <i>rpsL150 P<sub>kdp</sub>::lacZ</i> $\Delta$ <i>kdpD pstC::npt</i>	This work

Supplemental Material

LF3 $\Delta$ kdpD $\Delta$ pstC $\Delta$ phoR	MG1655 <i>rpsL150 P<sub>kdp</sub>::lacZ <math>\Delta</math>kdpD<math>\Delta</math>pstC phoR::npt</i>	This work
LF3 $\Delta$ kdpD $\Delta$ phoU	MG1655 <i>rpsL150 P<sub>kdp</sub>::lacZ <math>\Delta</math>kdpD phoU::npt</i>	This work
LF3 $\Delta$ kdpD $\Delta$ phoR	MG1655 <i>rpsL150 P<sub>kdp</sub>::lacZ <math>\Delta</math>kdpD phoR::npt</i>	This work
LF3 $\Delta$ kdpD $\Delta$ phoU $\Delta$ phoR	MG1655 <i>rpsL150 P<sub>kdp</sub>::lacZ <math>\Delta</math>kdpD<math>\Delta</math>phoU phoR::npt</i>	This work
LF3 $\Delta$ kdpD $\Delta$ phoU $\Delta$ phoR	MG1655 <i>rpsL150 P<sub>kdp</sub>::lacZ <math>\Delta</math>kdpD<math>\Delta</math>phoU phoR::npt</i>	This work
<b>Strains used in chapter 2.4</b>		
ArcticExpress (DE3) RIL $\Delta$ atpIBEFHA	F <sup>-</sup> <i>ompT hsdS (r<sub>B</sub> m<sub>B</sub>) dcm<sup>+</sup> Tet<sup>r</sup> gal<math>\lambda</math>(DE3) endA Hte [<i>cpn 10 cpn60</i> Gent<sup>r</sup>] [<i>argU ileY leuW</i> Str<sup>r</sup>] <math>\Delta</math>atpIBEFHA</i>	This work

**Table S2: Plasmids used in this study.**

Name	Relevant genotype or description	Reference
<b>Commonly used plasmids</b>		
pET16B	Amp <sup>r</sup> -cassette, T7-promoter, pBR322 origin, 5'-His-tag coding sequence, <i>lacI</i> -coding sequence, <i>lac</i> operator	Novagen
pBAD18	Amp <sup>r</sup> -cassette, pBR322 origin	(Guzman <i>et al.</i> , 1995)
pBD5-3	<i>kdpD</i> in pBAD18, Amp <sup>r</sup>	(Jung <i>et al.</i> , 1998)
pPV5-3	<i>kdpD</i> 6His in pKK223-3	(Jung & Altendorf, 1998a)
pPV5-3/NheI	zusätzliche NheI Schnittstelle	Günther Gabriel, plasmid collection AG K. Jung
pEE	10His- <i>kdpE</i> in pET16B, Amp <sup>r</sup>	(Heermann <i>et al.</i> , 2003a)
pBD5-9	<i>kdpD</i> in pBAD18	(Zimmann <i>et al.</i> , 2007)
pBD/C-less	Cysteine free <i>kdpD</i> in pBAD18, Amp <sup>r</sup>	(Jung <i>et al.</i> , 1998)
pRED/ET	$\lambda$ -RED recombinase in pBAD24, Amp <sup>r</sup>	Gene Bridges
pCP20	Helper plasmid, Cm <sup>R</sup>	(Datsenko & Wanner, 2000)
pBR-Cherry		(Münch <i>et al.</i> , 2008)
<b>Plasmids used for BACTH</b>		
pUT18	Expression vector, Ap <sup>R</sup>	(Karimova & Ladant, 2005)
pUT18C	Expression vector, Ap <sup>R</sup>	(Karimova & Ladant, 2005)
pKT25	Expression vector, Km <sup>R</sup>	(Karimova & Ladant, 2005)
pUT18C-zip	Control plasmid, N-terminal CyaA-T18-yeast leucine zipper fusion, Ap <sup>R</sup>	(Karimova & Ladant, 2005)
pKT25-zip	Control plasmid, N-terminal CyaA-T25-yeast leucine zipper fusion, Km <sup>R</sup>	(Karimova & Ladant, 2005)
pUT18-gene	Gene of interest cloned in PstI and BamHI sites of pUT18, resulting in C-terminal CyaA-T18-protein fusions (T18-gene)	This work
pUT18C-gene	Gene of interest cloned in PstI and BamHI sites of pUT18, resulting in N-terminal CyaA-T18-protein fusions (gene-T18)	This work
pKT25-gene	Gene of interest cloned in PstI and BamHI/EcoRI sites of pKT25, resulting in N-terminal CyaA-T25-protein fusions (gene-T25)	This work

## Supplemental Material

<b>Plasmids used in chapter 2.1</b>		
pBD/6-92	<i>kdpD</i> <sup>A12-395</sup> in pBAD18	(Jung & Altendorf, 1998b)
pET16b/C3	<i>kdpD</i> <sup>A2-498</sup> in pET/16b	this study
pPV5-3/ΔTM1-4	<i>kdpD</i> <sup>AG401-V498</sup> in pPV/5-3	(Fohrmann, 2001)
pBD/ΔTM1-4/10Gly	<i>kdpD</i> <sup>AG401-V498,V397G,Q501R,A502S□I399-Y400,R499-Y500,10Gly</sup> in pBAD18	(Fohrmann, 2001)
pBD/ΔTM1-4/5(Gly,Ala)	<i>kdpD</i> <sup>AG401-V498,V397G,Q501R,A502S□I399-Y400,R499-Y500 5(Gly,Ala)</sup> in pBAD18	(Fohrmann, 2001)
pBD/ΔTM1-4/loop3	<i>kdpD</i> <sup>AF391-F462, ΔD474-R500</sup> in pBAD18	This study
pBD/F463A	<i>kdpD</i> <sup>P463A</sup> in pBD	this study
pBD/I464A	<i>kdpD</i> <sup>I464A</sup> in pBD	this study
pBD/P466A	<i>kdpD</i> <sup>P466A</sup> in pBD	this study
pBD/R467A	<i>kdpD</i> <sup>A467A</sup> in pBD	this study
pBD/T469A	<i>kdpD</i> <sup>T469A</sup> in pBD	this study
pBD/L470A	<i>kdpD</i> <sup>L470A</sup> in pBD	this study
pBD/V472A	<i>kdpD</i> <sup>V472A</sup> in pBD	this study
pBD/S473A	<i>kdpD</i> <sup>S473A</sup> in pBD	this study
pBD/#3	<i>kdpD</i> <sup>P466A, T469A, L470A, V472A</sup> in pBD	this study
pBD/T677A	<i>kdpD</i> <sup>T677A</sup> in pBD	this study
pBD/#4	<i>kdpD</i> <sup>P466A, T469A, L470A, V472A, T677A</sup> in pBD	this study
<b>Plasmids used in chapter 2.2</b>		
pBD/Q548A,L550A, V613A,E615A	<i>kdpD</i> <sup>Q548A,L550A,V613A,E615A</sup> in pBD	Günther Gabriel, plasmid collection AG K. Jung
pBD/Q548N,L550Y, V613N,E615N	<i>kdpD</i> <sup>Q548N,L550Y,V613N,E615N</sup> in pBD	Günther Gabriel, plasmid collection AG K. Jung
pBD/GAF3E0Y	<i>kdpD-GAF3E0Y</i> in pBD	(Schramke, 2011)
pBD/S.a.GAF	<i>kdpD-GAF S. aureus</i> in pBD	Verena Pfaffinger, plasmid collection AG K. Jung
pBD/V.c.GAF	<i>kdpD-GAF V. cholerae</i> in pBD	Verena Pfaffinger, plasmid collection AG K. Jung
pBD/P.m.GAF	<i>kdpD-GAF P. mirabilis</i> in pBD	Verena Pfaffinger, plasmid collection AG K. Jung
pBD/NarX S-helix	<i>kdpD-NarX S-helix</i> in pBD	this study
pBD/Tsr S-helix	<i>kdpD-Tsr S-helix</i> in pBD	this study
pBD/KdpD S-helix	<i>kdpD-KdpD S-helix</i> in pBD	this study
pBD/all088 S-helix	<i>kdpD-all088 S-helix</i> in pBD	this study
pBD/Δ625-632	<i>kdpD</i> <sup>Δ625-632</sup> in pBD	this study
pBD/Δ633-640	<i>kdpD</i> <sup>Δ633-640</sup> in pBD	this study
pBD/Δ641-648	<i>kdpD</i> <sup>Δ641-648</sup> in pBD	this study
pBD/L636A,L637A, V638A	<i>kdpD</i> <sup>L636A,L637A,V638A</sup> in pBD	this study

Supplemental Material

pBD/L645A,L647A	<i>kdpD</i> <sup>L645A,L647A</sup> in pBD	this study
pBD/L630A,L631A	<i>kdpD</i> <sup>L630A,L631A</sup> in pBD	this study
pBD/R508E	<i>kdpD</i> <sup>R508E</sup> in pBD	(Schramke, 2011)
pBD/E626R	<i>kdpD</i> <sup>E626R</sup> in pBD	Günther Gabriel
pBD/R629E	<i>kdpD</i> <sup>R629E</sup> in pBD	(Schramke, 2011)
pBD/R508E,E626R	<i>kdpD</i> <sup>R508E,E626R</sup> in pBD	(Schramke, 2011)
pBD/R508E,R629E	<i>kdpD</i> <sup>R508E,R629E</sup> in pBD	(Schramke, 2011)
pBD/C-less R508C,E626C	<i>kdpD</i> <sup>C-less, R508C,E626C</sup> in pBD	this study
pBD/C-less R508C,E626C,C852, C874	<i>kdpD</i> <sup>C-less, R508C,E626C,C852,C874</sup> in pBD	this study
<b>Plasmids used in chapter 2.3</b>		
pPV-2/D52N	<i>kdpE</i> <sup>D52N</sup> in pPV-2	Ralf Heermann, plasmid collection AG K. Jung
pDL39	<i>phoB</i> -His <sub>10</sub> under <i>P</i> <sub>tac</sub> control in pKES170	(Lüttmann <i>et al.</i> , 2012)
pDL40	<i>phoR</i> (codon52-431)-His <sub>10</sub> under <i>P</i> <sub>tac</sub> control in pKES170	(Lüttmann <i>et al.</i> , 2012)
pBR-Cherry pPstS	<i>P</i> <sub>pstS</sub> promoter region in pBR-Cherry	This work
<b>Plasmids used in chapter 2.4</b>		
pET28b-KdpD	<i>S. aureus kdpD</i> in pET28b	(Corrigan <i>et al.</i> , 2013)

**Table S3: Oligonucleotides used in this study.**

Name	Sequence (5'-3')
<b>General primers</b>	
XmaI_s	acccggggatccgctgcacctgcaggctc
NotI_s	gtggttgccggcgcgttatgcgcc
HindIII_as	aaaacagccaagctttgtcacatc
<b>Primers for insertion of kanamycine cassettes</b>	
KdpD_up	gtggcgctattttatgacgctggccttcagtggttgccaccgtcattaaggcctggtgatgatggcgggat cg
KdpD_low	gggcgtgggggtgatccttcgctgccagatcgagcgtaagattctgcctcagaagaactgcaagaag gcg
<b>Primers for construction of deletion strains</b>	
delta KdpD_up	tcttcagcgtaaccacttttctcaaataaagccgcccggactgaataattaaccctcactaaaggcg
delta KdpD_down	actcaatctggcgctgataaaactgatgaataacgaacccttacgtccctaatacactcactatagggct c
50bp <i>kdpD</i> _rpsL- kan_sense	ccagccggttgcaacattgtgaactcaatctggcgctcgacaacttgacaataaggcctggtgatgat ggcgggatcgttg
50bp <i>kdpD</i> _rpsL- kan_antisense	gcgcaagaagcgacgaatagcctgttcattcaacaatcagaactttgtcagaagaactgcaagaag gcatag
$\Delta$ <i>kdpD</i> _sense	gacgaataacaaactgttattgattggaagatg
$\Delta$ <i>kdpD</i> _antisense	cagaactgttattctgcaagttgtcagcggccagattgag

Supplemental Material

kdpCDforI_sense	cgcaagcggcggcctggc
kdpE_antisense	ccggtgaatcacgcgggcggc
50bpkdpE_rpsL- kan sense	ctcgcacggcgcctggaggcgcacgggatgcgcgtctttaggcccgaacggcctggatgatggcggg
50bpkdpE_rpsL/ kan_antisense	tttaccagcggatcgggcgcgggtggggcagagtgccggcgtaatgcgactcagaagaactgtcaagaag
kdpE_sense	ccggtgaatcacgcgggcggc
kdpE_antisense	ccggagcggatgattatctg
50bpackApta_rpsL-kan_sense	taacgataacgccggtgatgttgggttttggcaccgccgaagctgtggcctggatgatggcggg
50bpackApta_rpsL-kan_sense	ggcctaagtagtacatattcattgagtcgtaaatcatatacatattgctcagaagaactgtcaagaag
delta ATP (IBEFHA)_up	ttgcggcctgccctaaggcaagcccgacgttaccaggattgggttgcaattaaccctactaaaggcgc
delta ATP (IBEFHA)_down	acacgcggcatacctgaaggagcaggagtgaaaacgtgatgtctgtgtaaacgactactataggctc
<b>Check primers deletion strains</b>	
check kdpD_s	atcaccggcaccgcctccactggcgc
check kdpD_as	gttccggttgaactggtgacggcatcg
check pstC_s	cgttcggcagaccaccacttcc
check pstC_as	ctgaaattcttcgactggcgctac
check phoR_s	ccgcacggtcgcgatgccacattc
check phoR_as	cagtatgacagcacctgaagcgc
check phoU_s	caccgtggtgatgctcacc
check phoU_as	gttatgacaggtttgcctgcga
check ATP_up	ccaatcactttgcgcgatggttctgc
check ATP_down	gctttaccaggtgtttacgcgttatt
<b>Primers for insertion of point mutations</b>	
F463A_s	cgatctctttgctatcgccccacgc
F463A_as	gcgtggggcgatagcaagagatcg
I464A_s	cgatctctttttgcccggcggc
I464A_as	gcgtggggcgcaaaaaagagatcg
P466A_s	tttatcggccgcacgcggtacc
P466A_as	ggtaccgcgtgcggcgataaa
R467A_s	atgccccagccggtaccctcgccgtc
R467A_as	gacggcgcagggtaccggctggggcgat
T469A_s	cggtgccctcgccgtctctgatg
T469A_as	catcagagacggcgcaggaccg
L470A_s	cggtaccggcggcgtctctgatg
L470A_as	catcagagacggcgcgggtaccg
V472A_s	cggtaccctcgccgctctgatg
V472A_as	catcagagggcggcgcagggtaccg
S473A_s	ctcggcgtcgtgatgtgcaatc
S473A_as	gatattgcacatcagcgacggcgag
T677A_s	atg att tac gcg cgc cgc tta cg
T677A_as	cgt aag cgg cgc gcg taa atc at
P466A,V472A, L470A_s	ttatcggccgcacgcggtaccgcagcccatctgatg
P466A, V472A, L470A_as	catcagatgcggctgcgggtaccgcgtgcggcgataa
P466A, T469A,V472A, L470A_s	gcacgcgggtgccgcagccgcatc
P466A, T469A,V472A, L470A_as	gatgcggctgcggcaccgcgtgc
L630A,L631A_s	cagcagcggcggcggagacgtttac

Supplemental Material

L630A,L631A_as	gtaaacgtctccgccgcgctgctg
L636A,L637A,V638A_s	acgtttacggcggcagccgccaatgcc
L636A,L637A,V638A_as	ggcattggcggctgccgtaaacgt
L645A,L647A_s	tgagcgggacggcaaccgccag
L645A,L647A_as	ctggcggttgccctgcccgtca
R508C_s	gtagcccgtactgcgagcaacgcacg
R508C_as	cgtgcggtgctgcagtaacgggctac
C874_s	aaggtggtgctgtttcgtgttacac
C874_as	gtgtaacacgaaaacaggcaccacctt
C852_s	gactggcaattgtcgggcgatag
C852_as	ctatgcccgacaaattgccagtc
<b>Primers for construction of truncated <i>kdpD</i> variants</b>	
499_NdeI_s	ggc gca tat gcg tta tca ggc gcg g
499+505_BamHI_as	agc tcg gat cct cac ata tcc tca tg
delta TM4_as	ccg cgc ctg ata aga gac ggc gag g
delta TM1-3_s	gat aac cgc tct ttt atc gcc cca c
delta TM1-3_as	gtg ggg cga taa aag agc ggt tat c
deltaP625-E632_s	gccagttgatgatcacgtttacgctg
deltaP625-E632_as	cagcgtaaacgtgatcatcaactggc
deltaT633-N640_s	gcccctgctggaggcccttgagcggc
deltaT633-N640_as	gcccgtcaagggcctccagcagcgcg
deltaA641-T648_s	gttagtcgccaatgccagcgaagaacag
deltaA641-T648_as	ctgtttctcgtggcattggcgactaac
<b>Primers for construction of BACTH plasmids</b>	
KdpD_PstI_s_pUT18C	ttggctgcagcatgaataacgaacccttacg
KdpD_BamHI_as_pUT18C	gacggatcctcacatattcctcatgaaattcttc
KdpE_PstI_s_pKT25	ttggctgcagcagtgacaaacgttctgattgttg
KdpE_EcoRI_as_pUT18C+pKT25	gacgaattcgtcaaagcataaacggatagccaat
PhoR_PstI_s_pUT18+C	ttggctgcagcgtgctggaacggctgctggtg
PhoR_BamHI_as_pUT18C + pKT25	gatcggatccttaacgctgtttttggc
PhoR_PstI_s_pKT25	ttggctgcagcagtgctggaacggctgctggtg
PhoU_PstI_s_pUT18+C	ttggctgcagcatggacagctcaatcttaata
PhoU_BamHI_as_pUT18	gacggatccgatttgcgtatctttccccg
PhoU_PstI_s_pKT25	ttggctgcagcaatggacagctcaatcttaata
PhoU_BamHI_as_pUT18C+pKT25	gatcggatccttatttgcgtatctttcc
PhoB_PstI_s_pUT18+C	ttggctgcagcatggcgagacgtattctggtcg
PhoB_BamHI_as_pUT18	gacggatccgaaaagcgggtgaaaaacgatat
PhoB_PstI_s_pKT25	ttggctgcagcaatggcgagacgtattctg
PhoB_BamHI_as_pUT18C+pKT25	gatcggatccttaaaaagcgggtgaaaaac
<b>qRT-PCR primers</b>	
KdpAfor2	gccgccagcgggattgcgg
KdpArev2	cttcaacgggtattcacagcctg
KdpDfor	cgccgccatgctggaagggc
KdpDrev	gcttcagcagttctcgcgatc
GapAfor1	ctccactcagccggttctg

## Supplemental Material

GapArev1	cttcgcaccagcggatgatgtg
<b>Primers for reporter plasmid construction</b>	
pPstS_BamHI_s	gatcggatcctcttcgccgatcaggatgcg
pPstS_XmaI_as	gatccccgggaatgtctcctgggagattc

**Table S4: KdpD variants identified by random mutagenesis**

<b>KdpD variant</b>
KdpD/L583Q, E643A, T677A
KdpD/V524A, L630P, E643A
KdpD/Y561C, E643A
KdpD/E643A, R664H
KdpD/E643A, L671P
KdpD/E643A, E661G
KdpD/delta 514-655
KdpD/P528L+L592stop
KdpD/S541P, E643A
KdpD/S519P, E643A
KdpD/G588D, E643A
KdpD/S527G, E643A

## **Danksagung**

Zunächst möchte ich mich bei Frau Prof. Dr. Kirsten Jung für die Aufnahme in die Arbeitsgruppe sowie für die gute Betreuung und Unterstützung während meiner Doktorarbeit bedanken. Ich habe in den Jahren sehr viel gelernt und die Arbeit an dem Projekt hat mir immer sehr viel Spaß gemacht.

Weiterhin möchte ich mich bei meinem Prüfungskomitee insbesondere bei Prof. Dr. Marc Bramkamp bedanken, der sich als Zweitgutachter für meine Arbeit zur Verfügung gestellt hat.

CiPSMwomen danke ich für die finanzielle Unterstützung bei projektspezifischen Sachmitteln und für Reisekostenzuschüsse bei der Teilnahme an Konferenzen.

Darüber hinaus bedanke ich mich bei unseren Kollaboratoren Dr. Filipe Tostevin, Prof. Dr. Ulrich Gerland, Dr. Vera Laermann, Prof. Dr. Karlheinz Altendorf, Dr. Joana Moscoso und Prof. Dr. Angelika Gründling für die gute und erfolgreiche Zusammenarbeit.

Bei allen aktuellen und ehemaligen Mitgliedern der AG K. Jung, AG H. Jung und AK R. Heermann insbesondere bei Nicola Lorenz, Dr. Laure Plener, Angela Glaeser, Jannis Brehm, Verena Pfaffinger, Dr. Jürgen Lassak, Dr. Luitpold Fried und PD Dr. Ralf Heermann möchte ich mich für wissenschaftlichen Input, die großartige Arbeitsatmosphäre und die schöne Zeit bedanken, die wir auch außerhalb der Arbeitszeit verbracht haben. Ich werde euch alle sehr vermissen!

Weiterhin möchte ich mich bei Kurbelkatz Paddy (Patrick) Kopp (Team „Schere, Stein, Vampir“), Hirschi (Jiri) Nitschke, Raimund Seidl, Oli Faro und allen anderen Tischfußballstüchtigen aus Flex, Substanz und Co für die zahlreichen (meist viel zu langen) Kickerabende bedanken, die für mich ein Ausgleich zu der arbeitsintensiven Zeit während der Doktorarbeit waren.

Die weltbesten Bürokollegen aus dem „Deo-Büro“: Schnieki aka Schlori (Nicola Lorenz), Geli Gläser aka Angelika Glaser aka Frangi (Angela Glaeser) und Jannibär aka Jannis-Pannis (Jannis Brehm). Vielen Dank für die lustige Zeit und das Miteinander in guten wie in schlechten Zeiten.

Mein allergrößter und tiefster Dank gilt meiner Mama Fanny Schramke, meiner Schwester Susanne Schramke, Holger Welter, meinem Papa Hans Schramke und meiner Oma Annelore Wasner. Vielen Dank, dass ihr immer für mich da wart und seid und mich in allem unterstützt, was ich tue!

## Curriculum vitae

### Personal Data

Name	Hannah Schramke
Address	Netzegastr. 1, 81377 Munich (Germany)
Telephone number	+49 (0) 176 30363429
E-Mail	<a href="mailto:hannah.schramke@gmx.de">hannah.schramke@gmx.de</a>
Current institution	Center for integrated Protein Science Munich (CiPSM) at the Ludwig-Maximilians-Universität, Munich, Department of Biology I, Microbiology
Date of Birth	10.12.1985
Place of Birth	Munich
Nationality	German
Marital Status	single

### Education

Since 08/2011	PhD student in the lab of Prof. Dr. Kirsten Jung at the Ludwig-Maximilians-Universität, Munich  Topic: Stimulus perception and signal transduction within the histidine kinase KdpD in <i>Escherichia coli</i>
09/2006 – 07/2011	Diploma in Biology (Grade: 1.3), Ludwig-Maximilians-Universität, Munich
09/2010 – 07/2011	Thesis in the lab of Prof. Dr. Kirsten Jung at the Ludwig-Maximilians-Universität, Munich  Topic: Funktionelle und strukturelle Charakterisierung der GAF Domäne der Sensorkinase KdpD in <i>Escherichia coli</i> (Grade 1.0)
1996 – 2005	Erasmus-Grasser-Gymnasium, Munich Graduation: Abitur (Grade 2.0)
1992 – 1996	Grundschule an der Gilmstraße, Munich

## Conferences

- March 2016 Annual conference of the VAAM (Association of general and applied Microbiology) 2016 in Jena, Germany  
**Talk:** Cross-talk between the Kdp and Pho two-component systems interconnects  $K^+$  and  $PO_4^{3-}$  homeostasis in *Escherichia coli*.
- May 2015 Bacterial Networks Conference in San Feliu de Guixols, Spain  
**Poster:** Dual  $K^+$ -sensing controls the kinase/phosphatase switch of the bifunctional receptor KdpD.
- March 2015 Annual conference of the VAAM (Association of general and applied Microbiology) 2015 in Marburg, Germany  
**Talk:** IN and OUT, ON and OFF – An efficient concept of stimulus perception by a histidine kinase.
- October 2014 "Mechanisms of Gene Regulation 2014" in Jülich, Germany  
**Talk:** IN and OUT, ON and OFF – An efficient model of stimulus detection in bacterial two-component systems.
- February 2014 CIPSM-Conference in Wildbad-Kreuth, Germany  
**Poster:** The bifunctional histidine kinase KdpD of *Escherichia coli* senses external and internal  $K^+$ .
- January 2014 Gordon Research Conference "Sensory Transduction in Microorganisms" in Ventura, United States of America  
**Poster:** The bifunctional histidine kinase KdpD of *Escherichia coli* senses external and internal  $K^+$ .
- March 2013 Bacterial Networks Conference in Pultusk, Poland  
**Poster:** Dual perception of the  $K^+$ -stimulus by the histidine kinase KdpD.
- October 2012 29<sup>th</sup> Symposium "Mechanisms of Gene Regulation" in Herrsching, Germany  
**Talk:** Elucidation of a  $K^+$ -binding site within the histidine kinase KdpD in *Escherichia coli*.
- March 2012 Annual conference of the VAAM (Association of general and applied Microbiology) 2012 in Tübingen, Germany  
**Poster:** The importance of the GAF domain for  $K^+$ -sensing in the sensor kinase KdpD in *Escherichia coli*.

## Publications

1. Schramke H, Wang Y, Heermann R, Jung K: **Stimulus perception by histidine kinases.** In de Bruijn, F.J. (Editor) Stress and environmental control of gene expression in bacteria, Wiley-Blackwell Publishers. (accepted)
2. Moscoso JA, Schramke H, Zhang Y, Tosi T, Debhi A, Jung K, Gründling A: **Binding of c-di-AMP to the *Staphylococcus aureus* sensor kinase KdpD occurs via the USP domain and down-regulates the expression of the Kdp potassium transporter.** *J. Bacteriol.* 2015 Jul 20. pii: JB.00480-15.
3. Schramke H, Tostevin F, Heermann R, Gerland U, Jung K: **A dual-sensing receptor confers robust cellular homeostasis.** (Cell Reports, under review)
4. Schramke H, Gabriel G, Wang Y, Pfaffinger V, Heermann R, Jung K: **Functional analysis of the GAF domain within the histidine kinase KdpD of *Escherichia coli*.** (In preparation)
5. Schramke H, Laermann V, Tegetmeyer H, Brachmann A, Jung K, Altendorf K: **Cross-talk between the Kdp and Pho two-component systems interconnects K<sup>+</sup> and PO<sub>4</sub><sup>3-</sup> homeostasis in *Escherichia coli*.** (In preparation)

## Grants

1. **Travel grants:** CiPSMwomen travel grants in 2013, 2014 and 2015. Total funding: 2554.42€
2. **Research grants:** CiPSMwomen grants for project specific material expenses in 2012, 2014 and 2015. Total funding: 4580.91€